MONSOONAL CLIMATE CHANGE DURING THE HOLOCENE: SPELEOTHEM EVIDENCE FROM SOUTHWESTERN CHINA, NORTHERN INDIA, AND THE SOUTHEASTERN USA

by

FUYUAN LIANG

(Under the Direction of GEORGE A. BROOK)

ABSTRACT

Variations in $\delta^{18}O$ and $\delta^{13}C$ values, luminescence, gray color, and mineralogy along the growth direction of speleothems from Southwestern China, Northern India and the Southeastern USA provide high-resolution and absolute-dated records of Asian and Southeast USA monsoonal climate change through the Holocene. Stalagmite records from Southwestern China document a gradual weakening in the Asian summer monsoon from the mid-Holocene in response to declining Northern Hemisphere summer solar radiation. This brought wetter conditions during the mid-Holocene when the stronger Asian summer monsoon brought more intense and more total precipitation to the Yangtze River Valley. The Asian summer monsoon weakened during the late-Holocene and retreat of the monsoonal front to the further south resulted in less rainfall to the Shangdong Cave area.

Stalagmite evidence from Northern India suggests a wetter Little Ice Age resulting in calcite deposition from AD 1480-1900 and aragonite deposited before and after these dates.

Climate changes in Northern India from AD 1250-1800 were of low magnitude but after AD 1800 climate fluctuated significantly.

A transition from calcite to aragonite deposition at 6 ka B.P. in a column collected from DeSoto Caverns in Alabama, USA, suggests a wetter early Holocene followed by a drier mid-Holocene. There is no clear trend in $\delta^{18}O$ and $\delta^{13}C$ values in records for the last 4400 years obtained from vertical stalagmite cores drilled from two stalagmites in DeSoto Caverns. Instead, the climate record is characterized by alternating wetter and drier periods, with wetter conditions centered at 4300, 3400, 2500, 1400, 770, 420, and 120 years B.P. and drier conditions at ~3900, 3000, 2700, 530, and 130 years ago. The data indicate a wetter Medieval Warm Period and a drier Little Ice Age in the Southeastern USA.

INDEX WORDS: Speleothems, Asian monsoon, Southeastern USA, Northern India, paleoenvironments, Holocene, Little Ice Age, Medieval Warm Period

MONSOONAL CLIMATE CHANGE DURING THE HOLOCENE: SPELEOTHEM EVIDENCE FROM SOUTHWESTERN CHINA, NORTHERN INDIA, AND THE SOUTHEASTERN USA

by

FUYUAN LIANG

BE, Changchun University of Science and Technology, R.R. China, 1997

MS, Institute of Geographic Sciences and Natural Resources Research, Chinese Academy of Sciences, P.R. China, 2000

A Dissertation Submitted to the Graduate Faculty of The University of Georgia in Partial Fulfillment of the Requirements for the Degree

DOCTOR OF PHILOSOPHY

ATHENS, GEORGIA

2008

MONSOONAL CLIMATE CHANGE DURING THE HOLOCENE: SPELEOTHEM EVIDENCE FROM SOUTHWESTERN CHINA, NORTHERN INDIA, AND THE SOUTHEASTERN USA

by

FUYUAN LIANG

Major Professor:	George A. Brook
Committee:	Bruce Railsback David S. Leigh Marguerite Madden

Electronic Version Approved:

Maureen Grasso
Dean of the Graduate School
The University of Georgia
December 2008

ACKNOWLEDGEMENTS

I would like to express my sincere gratitude to many people. Without their considerable support, my dissertation research would not have been accomplished. I am deeply indebted to my major advisor, George A. Brook for his guidance, encouragement, and support to my doctoral study and research. Thanks also are due to the my committee, Bruce Railsback, David Leigh, Marguerite Madden, and Chor-Pang Lo, for their timely assistance and advice. Special thanks particularly go to Bruce Railsback for his petrographic expertise. Dr. Chor-Pang Lo will always remain in my heart. It is so sad to lose such a great mentor, advisor, and teacher.

My appreciations also go to Allen W. Mathis for his permission to sample speleothem from DeSoto Caverns; to Bianshen Wu, Yuruo Shi, and Huabin Chen for their support to my field trip in China; to Ben Hardt, Xianfeng Wang, Hai Cheng, and Edwards Larry at the University of Minnesota for their help in dating my samples. I would also like to thanks Julia Cox and Chris Romanek in the Geology Department at the University of Georgia, and Xinggong Kong in the Department of Geography at Nanjing Normal University for their help in processing my stable isotopes samples.

I would also like to acknowledge Audrey Hwakins, Kate Blane, Jodie Guy, Emily Duggar, Loretta Scott, Robert Phares, Donna Johnson, and Emily Coffee for their great help to my 5-year doctoral study in the Department of Geography, University of Georgia. I would also like to thank my fellow graduate students and friends, Bo Xu, Liang Zou, Linna Li, Yanfeng Le, Qingfang Wang, Yanbing Tang, Qingming Meng, Zhiyong Hu, Minho Kim, and Hwahwan Kim for their support and friendship in the last five years.

My sincere thanks also go to the Department of Geography, Graduate School of the University of Georgia, and the National Science Foundation Dissertation Improvement Grant for the financial support to my doctoral study and dissertation research. Finally I am grateful to my parents and my family for their patience, understanding, and support.

TABLE OF CONTENTS

CHAPTER 1

INTRODUCTION AND STATEMENT OF PURPOSE

Introduction

Monsoon climates develop over low-latitude continental regions in response to seasonal changes in the thermal contrast between the continent and adjacent oceans (Ramage, 1971; Hastenrath, 1994). Monsoon circulation exhibits an onshore flow of air during the summer and offshore flow during the winter. As a result, areas influenced by a monsoon climate usually receive abundant rainfall during the summer and much less precipitation during the winter. Monsoons are important because they bring precipitation that affects the lives of billions of people. Unexpected strong monsoons or monsoons that fail can generate devastating floods or extreme droughts that significantly influence agricultural and economic activities in the monsoon areas. For example, a famine in 1877 and 1878 caused by a significant drought due to the failure of the summer monsoon killed more than eight million people in India (Srivastava, 1968). Therefore, to mitigate potential impacts of monsoon climate change on human society, it is critical for us to understand and be able to forecast future climate changes.

To predict future monsoon intensity, knowing about the past history of monsoon climates is important. This is because the history documents monsoon variability under different conditions that may provide insights about the natural and regional impacts of future climate change (An et al., 2000). Of the major monsoon systems, the Asian monsoon is perhaps the best understood. Records of past Asian monsoon characteristics have been derived from marine sediments (e.g. Wang, 1999; Gupta et al., 2003), ice cores (e.g. Thompson et al., 1989, 2000), stalagmites (Neff et al., 2001; Fleitmann et al., 2003; Wanget al., 2001, 2005; Yuan et al., 2004, Wang et al., 2008), lake sediments (e.g. Enzel., et al., 1999; Chen et al., 1999; Hodell et al., 1999), and loess sequences (e.g. Sun et al., 1998). Proxy data from these studies document dramatic changes in Asian monsoon strength during the Holocene, which resulted in significant changes in paleoenvironmental conditions over east and south Asia, particularly in China. However, a common misconception is that a strong East Asian monsoon brings more rainfall to all areas of China. In fact, we now know that in the past a strong Asian monsoon brought more rainfall to Northern China but less to the Yangtze valley and Southern China. This is because a strong monsoonal front moves rapidly northwards depositing less rainfall in the southern part of the country and more in the north. By contrast, a weak monsoon stagnates in the Yangtze valley and Southern China bringing more rainfall to these regions while Northern China is much drier than normal (Tao and Chen, 1987; Shi and Zhu, 1996). As a result, peak summer monsoon precipitation was asynchronous in different areas of China during the Holocene, occurring at ca. 10-8 ka B.P. in Northern China, 7-5 ka ago in the middle and lower reaches of the Yangtze River, and 3 ka ago in Southern China (An et al., 2000).

During the Holocene, the southwest Asian monsoon behaved in a similar fashion to the East Asian monsoon (e.g. Neff et al., 2001; Fleitmann et al., 2003; Gupta et al., 2003). However, due to lack of high-resolution data for South Asia, it is not yet clear if spatial variations in rainfall over the Indian landmass were similar to China (i.e. did the zone of maximum rainfall move southwards as the monsoon weakened towards the end of the Holocene). Paleoenvironmental conditions in Northern India and Nepal are particularly interesting due to their location in the southern foothills of the Himalayas. Orographic uplift of moist air from the Indian Ocean as it moved into the Himalayas would have enhanced precipitation in this region. However, so far there is insufficient data to say how monsoon rainfall in this region would have been affected by periods of stronger or weaker monsoon.

Compared to the major monsoon systems of Africa, India and Asia, much less is known about the less marked monsoon systems such as that originating in the Gulf of Mexico and affecting the climate of the Southeastern USA. Climate in this region is described as being influenced by a "temperate monsoon" (Budel, 1982; Hardy et al., 1982). Fossil pollen evidence from the Southeastern USA is ambiguous with many sites in Florida and Southern Georgia indicating drier conditions than present during the Early Holocene (e.g. Watts, 1969, 1971, 1975; Rich, 1984), and sites further north indicating wetter conditions (e.g. Seielstad, 1994; Brook, 1996; LaMoreaux, 1999; Goman and Leigh, 2004). The geomorphic evidence is equally unhelpful. Large paleomeanders along the Ogeechee River of Georgia dating to 10-4.5 ka indicate at least a doubling of present discharge, a 10-30% increase in precipitation, and

pronounced precipitation seasonality (Leigh and Feeney, 1995). By contrast, there is OSL- and TL-dated evidence of enhanced aeolian activity indicating drier conditions at the same time (10.5-8.5 and 6.8-5.7 ka) along the Gulf Coast (Otvos and Price, 2001; Otvos, 2004).

Records of variations in the Asian monsoon are in sufficient detail to suggest a direct link between monsoon strength and summer solar radiation in the northern hemisphere (Wang et al., 2005). However, it is clear that conditions in the world's oceans and ice masses have also impacted the monsoon in ways not yet fully understood. Links have been noted between monsoon intensity and Heinrich and Dansgaard-Oeschger events, and Bond cycles (e.g. Wang et al., 2001, 2008; Yuan et al., 2005), but the mechanisms linking these events are not clear. Much less is known about the Southeastern USA monsoon as its history is complicated by the persistence of the Laurentide Ice Sheet, which lasted much longer than either the Scandinavian or Siberian Ice Sheets. As the Laurentide Ice Sheet did not fully melt until the mid- to late-Holocene, maximum monsoon activity in the Southeastern USA is not coincident with maximum northern hemisphere summer solar radiation as it is with the Asian monsoon.

As much remains to be learned about the Asian and Southeast USA monsoons, this dissertation examines these monsoons by studying records preserved in cave speleothems in Southwest China, Northern India, and the Southeast USA. Speleothem records from caves in these areas will not only help us understand past monsoonal climate during the Holocene, but will also provide new insights into the possible mechanisms that drive past climate changes.

High-resolution Paleoenvironmental Data from Stalagmites

Cave speleothems are an extremely valuable source of paleoenvironmental data because they occur in all climate regions and are deposited slowly over time. Furthermore, they can be dated precisely by the ICP-MS U-series technique back to ca. 500 ka, and are currently being used to refine the chronologies of events documented in ice cores and deep-ocean cores. Multi-proxy variables, including growth rate and variations in gray color, UV-stimulated luminescence, and oxygen and carbon stable isotope values, can provide a wealth of climatic information for the region near the cave.

At higher latitudes an increase in speleothem growth may signal a change from a glacial to an interglacial period, while it may tell of a transition from wet to dry conditions in a subtropical or tropical environment (Gascoyne, 1992). In arid or semi-arid regions, speleothem deposition on its own may indicate increased humidity (Brook et al., 1990, 1999b). In coastal areas, speleothems below sea level record periods of lower sea level during glacial intervals (Li et al., 1989; Gascoyne, 1992; Richards et al., 1994), while submerged speleothems well above sea level suggest lower ground water tables in the past and, thus, likely much drier conditions (Brook et al., 1996, 1997). Pollen grains and spores preserved in cave speleothems are able to provide a wealth of palaeoenvironmental information about the general composition of the vegetation and hence the climate near a cave at the time of speleothem deposition (Brook, et al., 1990). This is particularly useful in arid and semi-arid regions where pollen-bearing lake sediments are relatively scarce (Brook et al., 1990; Burney et al., 1994). Trace elements in speleothems may

record annual or even seasonal variations in temperature, changes in groundwater residence time, and availability of precipitation (Roberts et al., 1998; Huang et al., 2001; Treble et al., 2003). Variations in color are associated with changes in annual temperature and moisture, with darker color reflecting a warmer, wetter environment (Holmgren et al., 1999; Qin et al., 2000). Although the thickness of annual laminations is controlled by many environmental factors, spectral analysis suggests that in some areas it is related to annual precipitation (Chen, 1992; Sheen, 1996; Holmgren et al., 1999), surface temperature (Frisia et al., 2003; Tan et al., 2003), or both temperature and rainfall together (Qin et al., 2000). Stalagmite annual layer thickness in an area affected by ENSO may also record the frequency of El Niño events (Brook et al., 1999a).

Variations in $\delta^{18}O$ and $\delta^{13}C$ values of speleothem carbonate are an important source of paleoenvironmental information (Hendy, 1971; Gascoyne, 1992). Although there is no definite relationship between $\delta^{18}O$ and temperature, variations in speleothem carbonate $\delta^{18}O$ along the growth axis often define special climatic events. In fact, many recent stable isotope studies of speleothems have attempted to provide precise estimates for the timing and duration of major oxygen isotope-defined climatic events. This is because speleothems can be accurately dated, whereas ocean and ice cores cannot. So, speleothems are being used to formulate chronologies for Dansgaard-Oeschger events (Spötl and Mangini, 2002; Genty et al., 2003; Burn et al., 2003), Heinrich events (Bar-Matthews, et al., 1999; Wang et al., 2001), the 8200-year cool interval (Wang et al., 2005), and Terminations, particularly Termination II (Winograd et al., 1992).

The amplitude of fluctuations in $\delta^{18}O$ of speleothem carbonate recovered from areas influenced by monsoon climate is usually too large to be completely explained by equilibrium fractionation caused by a change in the temperature of deposition (Wang et al., 2001; Neff et al., 2001; Fleitmann et al., 2003; Yuan et al., 2004). Rather, periods with lower $\delta^{18}O$ values in speleothems from South Asia are believed to indicate a strong summer monsoon, which brings more intense rainfall with lower $\delta^{18}O$ values. By contrast, less negative (higher) values suggest a weaker monsoon, indicative of less intense rainfall, which has more positive $\delta^{18}O$ values.

This research making up this dissertation attempts to use the great potential of cave stalagmites in Southern China, Northern India, and the Southeastern USA to extract high-resolution paleoenvironmental data. Variations in oxygen and carbon isotopes, as well as stalagmite color, luminescence, and petrographic characteristics are used to reconstruct past monsoon climate change, as well as the resulting paleoenvironmental conditions over Southern China, Northern India, and the Southeastern USA.

Aims and Objectives

The overall aim of this research is to develop high-resolution and absolute-dated Holocene paleoenvironmental records, which document monsoonal climate change over Southern China, Northern India, and the Southeastern USA. Records from these different monsoonal systems will be compared to try to identify potential factors that have influenced past monsoon activity. To achieve these aims, a series of more specific objectives were established.

1) Develop proxy records of late Pleistocene and Holocene monsoon activity in Southern China, Northern India, and the Southeastern USA by examining variations in growth rate, color, luminescence, petrography, $\delta^{18}O$, and $\delta^{13}C$ along the central growth axes of stalagmites collected from China, India, and the United States. A chronological framework for the proxy information will be developed using ICP-MS U-series ages of speleothem carbonate.

2) Integrate data from the stalagmites to produce records of climate change for three regions under study and compare the records with other published paleoclimate data for the respective regions. Refine the interpretations as appropriate.

3) Compare the records of monsoon variation in Southern China and the Southeastern USA during the Holocene with solar radiation, ice core and ocean core data. Specifically examine whether different monsoon systems respond synchronously to external forces. If possible, assess whether events in the North Atlantic, Western Pacific, and Southern Ocean influenced monsoon strength, and also determine the role of sea ice around the Antarctic (Hodell et al., 2001), ENSO intensity, Heinrich and Dansgaard-Oeschger events, and Bond cycles (e.g. see Wang et al., 2005).

Scientific Contribution

This research is significant because it will provide high-resolution and absolute dated records of climate change in three areas of the world. These records will be compared to

determine the impact of the slow melting of the Laurentide Ice Sheet on the Holocene climate of the Southeastern USA compared to Southern China, and they will also be compared with appropriate ocean core and ice core records to determine if and how ice events such as Heinrich events, or Dansgaard-Oeschger events affected monsoon activity in the two areas. At the present time there is insufficient data to make these comparisons with any certainty.

This research contributes to current paleoclimatic research on speleothems by broadening the typical scope of stalagmite studies and by employing a new sampling method that can be used to extract data from very large stalagmites. Most published records from cave stalagmites are based largely on variations in carbonate oxygen isotope values. By contrast, this dissertation research studies changes in color, luminescence, and petrography of the stalagmites as well. These variables are particularly important in understanding past variations in the Asian summer monsoon that so far are based almost exclusively on variations in oxygen isotopes. As a result, published stalagmite data reveals little about changes in total rainfall across China because other data, such as carbon isotope values, luminescence, gray color, and petrography, have not been evaluated in most cases.

In addition, in this research a vertical coring system is used to drill vertical cores from large stalagmites and to derive proxy paleoenvironmental data from these cores. The sampling approach allows study of stalagmites that are too big to cut and remove from a cave for study. In the future, the method could be used to derive long records from large stalagmites in other karst

areas of the world and enable us to extend climate records further back in time without inflicting significant damage to caves.

Also, this research attempts to derive records from columns in caves rather than the more popular stalagmite. Columns have been little used in the past to obtain paleoclimate records. Unlike stalagmites that grow upwards, columns simply get bigger by deposition all along the height to the formation. So carbonate is added to the outside and the column in many ways grows horizontally outwards from a central core area. This study will examine whether or what kind of information can be obtained along the horizontal growth direction of columns in caves. Finally, this research also attempts to derive paleoclimatic records from dirty speleothem formations. Most previous studies have specifically targeted clean and pure stalagmites as these give more reliable U-series ages and more accurate stable isotope data. However, detrital sediment in speleothems can provide information on past dust accumulation event or floods that washed sediment in with the dripwater (e.g. Webster et al., 2006). This study will attempt to use dirty speleothems to derive paleoclimatic information and will document the additional data that can be obtained beyond the usual stable isotope values.

Dissertation Outline

Chapter 2 of this dissertation provides a detailed description of the methodologies employed in this study, including sample preparation, dating, and gray scale, luminescence and isotope analysis. Chapter 3 examines a stalagmite record from Guizhou Province in China covering the

period from 5.1-1.6 ka B.P. This record documents a gradual weakening of the East Asian monsoon in response to declining solar radiation over the Northern Hemisphere. A 750-year record from a stalagmite in Northern India is discussed in Chapter 4. Deposition of calcite in this stalagmite from ca. A.D.1500-1900 suggests a wetter Little Ice Age in the foothills of the Himalayas. Chapter 5 presents a record reconstructed from vertical cores drilled from two stalagmites in DeSoto Caverns, Alabama. The records obtained document a transition from wetter to drier regimes in the Southeastern USA during the last 4400 years. This monsoon record is extended to ca. 37 ka B.P. (with a hiatus in data from 30-13 ka B.P.) by examining a horizontal slab cut from a collapsed column near the entrance of the cave. The information obtained from analysis of this slab is discussed in Chapter 6. The last chapter, Chapter 7, compares the records obtained from China, India and the U.S.A. and summarizes the important similarities and differences observed.

References

An, Z., Porter, S. C., Kutzbach, J. E., Wu, X., Wang, X., Liu, X., Li, W. and Zhou, W., 2000. Asynchronous Holocene optimum of the East Asian monsoon. *Quaternary Science Reviews* 19, 743-762.

Bar-Matthews, M., Ayalon, A., Matthews, A., Sass, E. and Halicz, L., 1996. Carbon and oxygen isotope study of the active water-carbonate system in a karstic Mediterranean Cave: Implications for palaeoclimate research in semiarid regions. *Geochimica et CosmochimicaActa* 60, 337-347.

Brook, F. Z., 1996. A late-Quaternary pollen record from the middle Ogeechee River Valley, southeastern Coastal Plain, Georgia. Master Thesis, University of Georgia, Athens, GA.

Brook, G. A., Burney, D. A. and Cowart, J. B., 1990. Desert paleoenvironmental data from cave speleothems with examples from the Chihuahuan, Somali-Chalbi, and Kalahari deserts. P*alaeogeography, Palaeoclimatology, Palaeoecology* 76, 311-329.

Brook, G. A., Cowart, J. B., Brandt, S. A. and Scott, L., 1997. Quaternary climatic change in southern and eastern Africa during the last 300 ka: the evidence from caves in Somalia and the Transvaal region of South Africa. *Zeitschrift für Geomorphologie*, N.F. Suppl.-Bd. 108, 15-48.

Brook, G. A., Cowart, J. B., and Marais, E., 1996. Wet and dry periods in the southern African summer rainfall zone during the last 300 kyr from speleothem, tufa, and sand dune age data. *Palaeoecology of Africa* 24, 147-158.

Brook, G. A., Ellwood, B. B., Railsback, L. B. and Cowart, J. B., 2006. A 164 ka Record of Environmental Change in the American Southwest from a Carlsbad Cavern Speleothem. *Palaeogeography, Palaeoclimatology, Palaeoecology* 237, 483-507.

Brook, G. A., Rafter, M. A., Railsback, B. L., Sheen, S. W. and Lundberg, J., 1999a. A high-resolution proxy record of rainfall and ENSO since AD 1550 from layering in stalagmites from Anjohibe Cave, Madagascar. *Holocene* 9, 695-705.

Brook, G. A., 1999b. Arid Zone Paleoenvironmental Records from Cave Speleothems. Chapter 8, In: Palaeoenvironmental Reconstruction in Arid Lands (eds. A. K. Singhvi and E. Derbyshire), Oxford and IBH Publishing Co. Pvt. LTD., New Delhi, India, p. 217-262.

Budel, J., 1982. Climatic geomorphology. Princeton, N.J., Princeton University Press, 443p.

Burney, D. A., Brook, G. A. and Cowart, J. B., 1994. A Holocene pollen record for the Kalahari Desert of Botswana from a U-series dated speleothem. *The Holocene* 4, 225-232.

Burns, S. J., Fleitmann, D., Matter, A., Kramers, J. and Al-Subbary, A. A., 2003. Indian Ocean climate and an absolute chronology over Dansgaard/Oeschger events 9 to 13. *Science* 301, 1365-1367.

Chen, F. H., Bloemenda, J., Zhang, P. Z. and Lin, Y.S., 1999. An 800 ky proxy record of climate from lake sediments of the Zoige Basin, eastern Tibetan Plateau. *Palaeogeography, Palaeoclimatology, Palaeoecology* 151, 307–320.

Chen, J., 1992. Climate variation in Botswanna over the last 600 years: Evidence from annual growth layers in a stalagmite from Drotsky's Cave, Ngamiland, Botswanna. M.A.Thesis, Department of Geography, University of Georgia, Athens, Georgia,125pp.

Enzel, Y., Ely, L. L., Mishra, S., Ramesh, R., Amit, R., Lazar, B., Rajaguru, S. N., Baker, V. R. and Sandler, A., 1999. High-resolution Holocene Environmental changes in the Thar Desert, Northwestern India. *Science* 284, 125-128.

Fleitmann, D., Bruns, S. J., Mudelsee, M., Neff, U., Kramers, J., Mangini, A. and Matter, A., 2003. Holocene forcing of the Indian monsoon recorded in a stalagmite from Southern Oman. *Science* 300, 1737-1739.

Frisia, S., Borsato, A, Preto, N. and McDermott, F., 2003. Late Holocene annual growth in three Alpine stalagmites records the influence of solar activity and the North Atlantic Oscillation on winter climate. *Earth and Planetary Science Letters* 216, 411-424.

Gascoyne, M., 1992. Paleoclimate determination from cave calcite deposits. *Quaternary Science Reviews* 11, 609–632.

Genty, D., Blamart, D., Ouahdi, R., Gilmour, M, Baker, A., Jouzel, J. and Van-Exter, S., 2003. Precise dating of Dansgaard–Oeschger climatic oscillations in western Europe from stalagmite data. *Nature* 421, 833–837.

Goman, M., and Leigh, D. S., 2004. Wet early to middle Holocene conditions on the upper Coastal Plain of North Carolina, USA. *Quaternary Research* 61, 256-264.

Gupta, A. K., Anderson, D. M. and Overpeck, J. T., 2003. Abrupt changes in the Asian southwest monsoon during the Holocene and their links to the North Atlantic Ocean. *Science* 421, 354-357.

Hardy, R., 1982. The Weather Book. Boston, Little-Brown, 224 p.

Hastenrath, S., 1994. Climate dynamics of the tropics. Kluwer Academic Publishers. 488pp.

Hays, J. D, Imbrie, J. and Shackleton, N. J., 1976. Variations in the Earth's orbit: pacemaker of the ice ages. *Science* 194, 1121-1131.

Hendy, C. H., 1971. The isotopic geochemistry of speleothems, 1. The calculation of the effects of different modes of formation on the isotopic composition of speleothems and their applicability as paleoclimatic indicators. *Geochimica et Cosmochimica Acta* 35, 801-824.

Hodell, D. A., Brenner, M. and Kanfoush, S. L., 1999. Paleoclimate of Southwestern China for the past 50,000 yr inferred from lake sediment records. *Quaternary Research* 52, 369-380.

Hodell, D. A., Kanfoush, S. L., Shemesh, A., Crosta, X., Charles, C. D. and Guilderson, T. P., 2001. Abrupt cooling of Antarctic surface waters and sea ice expansion in the South Atlantic sector of the Southern Ocean at 5000 cal yr B.P. *Quaternary Research* 56, 191-198.

Holmgren, K., Karlén, W., Lauritzen, S. E., Lee-Thorp, J. A., Partridge, T. C., Piketh, S., Repinski, P., Stevenson, Svanered, C. O. and Tyson, P. D., 1999. A 3000-year high-resolution stalagmite-based record of palaeoclimate for northeastern South Africa. *The Holocene* 9, 295–309.

Huang, Y., Fairchild, I. J., Borsato, A., Frisia, S., Cassidy, N. J., Mcdermott, F. and Andhawkesworth, C. J., 2001. Seasonal variations in Sr, Mg and P in modern speleothems (Grotta di Ernesto, Italy). *Chemical Geology* 175, 429-448.

LaMoreaux, H. K., 1999. Human-environmental relationships in the coastal plain of Georgia based on high-resolution paleoenvironmental records from three peat deposits. Ph.D. Dissertation, University of Georgia, Athens, GA.

Leigh, D. S. and Feeney, T. P., 1995. Paleochannels indicating wet climate and lack of response to lower sea level, Southeast Georgia. *Geology* 23, 687-690.

Li, W. X., Lundberg, J., Dickin, A. P., Ford, D. C., Schwarcz, H. P., McNutt,R. and Williams, D., 1989. High-precision mass-spectrometric uranium-series dating of cave deposits and implications for palaeoclimate studies. *Nature* 339, 534-536.

Neff, U., Burns, S. J., Mangini, A., Mudelsee, M., Fleitmann, D. and Matter, A., 2001. Strong coherence between solar variability and the monsoon in Oman between 9 and 6 kyr ago. *Science* 411, 290-293.

Otvos, E. G., 2004. Prospects for interregional correlations using Wisconsin and Holocene aridity episodes, northern Gulf of Mexico coastal plain. *Quaternary Research* 61, 105-118.

Otvos, E. G. and Price, D. M., 2001. Late Quaternary inland dunes of southern Louisiana and arid climate phases in the Gulf Coast region. *Quaternary Research* 55, 150-158.

Qin, X., Tan, M, Liu, D. S, Wang, X. F., Li, T. Y. and Lü, J. P., 2000. Characteristics of annual laminae gray level variations in a stalagmite from Shihua Cave, Beijing and its climatic significance (II).*Science in China(Series D)* 43, 521-533.

Ramage, C. S., 1971. Monsoon meteorology. Academic Press. New York, 296 pp.

Rich, F. J., 1984. An ancient flora of the eastern Okefenokee swamp as determined by palynology. In: The Okefenokee Swamp: Its Natural History, Geology, and Geochemistry. Cohen, A.J., Casagrande, D.J., Andrejko, M.J., Best, G.R., (eds) Wetland Surveys, Los Alamos, NM.

Richards, D. A., Smart, P. L. and Edwards, R. L., 1994. Maximum sea levels for the last glacial period from U-series ages of submerged speleothems. *Nature* 367, 357-360.

Roberts, M. S., Smart, P. L. and Baker, A., 1998. Annual trace element variations in a Holocene speleothem. *Earth and Planetary Science Letters* 154, 237-246.

Seielstad, C. A., 1994. Holocene environmental history at Chatterton Springs on the southern coastal plain of Georgia. Unpublished Master Thesis. Department of Geography, University of Georgia. Athens. 153pp.

Sheen, S.-W., 1996. Cyclic variations in southern African rainfall and water surplus, the Southern Oscillation, and annual layers in a Botswana speleothem. M.A. Thesis, Department of Geography, University of Georgia. Athens, 219pp.

Shi, Y. F. and Zhu, Q. G., 1996. An abrupt change in the intensity of the East Asian summer monsoon index and its relationship with temperature and precipitation over east China. International *Journal of Climatology* 16, 757-764.

Spötl, C. and Mangini, A., 2002. Stalagmite from the Austrian Alps reveals Dansgaard–Oeschger events during isotope stage 3: implications for the absolute chronology of Greenland ice cores. *Earth and Planetary Science Letters* 203, 507–518.

Srivastava, H.S., 1968. The history of Indian famines 1858-1918 and development of famine policy. Agra: Sri Ram Mehra and Co., 417 pp.

Sun, D. H., Shaw, J., An, Z. S., Cheng, M.Y. and Yue, L. P., 1998. Magnetostratigraphy and paleoclimatic interpretation of a continuous 7.2 Ma Late Cenozoic eolian sediments from the Chinese Loess Plateau. *Geophysical Research Letters* 25, 85-88.

Tan, M., Liu, T., Hou, J., Zhang, H. C. and Li, T. Y., 2003. Cyclic rapid warming on centennial-scale revealed by a 2650-year stalagmite record of warm season temperature, *Geophysical Research Letters* 30, 1617-1620.

Tao, S. Y., and Chen, L. X., 1987. A review of recent research on the East Asian summer monsoon in China. In Monsoon Meteorology, ed. C.P. Chang and T.N. Krishnamurti, 60-92. New York: Oxford University Press.

Thompson, L. G., Mosley-Thompson, E., Davis, M. E., Bolzan, J., Dai, J., Gunderstrup, N., Yao, T., Wu, X. and Xie, Z., 1989. Holocene-Late Pleistocene climatic ice core records from Qinghai-Tibetan Plateau. *Science* 246, 474-477.

Thompson, L. G., Yao, T., Mosley-Thompson, E., Davis, M. E., Henderson, K. A. and Lin, P., 2000. A high-resolution millennial record of the south Asian monsoon from Himalayan ice cores. *Science* 289, 1916-1919.

Treble P., Shelley, J. M. G. and Chappell, J., 2003. Comparison of high resolution sub-annual records of trace elements in a modern (1911-1992) speleothem with instrumental climate data from southwest Australia. *Earth and Planetary Science Letters* 216, 141-153.

Wang, P. X., 1999. Response of Western Pacific marginal seas to glacial cycles: paleoceanographic and sedimentological features. *Marine Geology* 156, 5-39.

Wang, S., Gong, D. and Zhu, J., 2001. Twentieth-century climatic warming in China in the context of the Holocene. *The Holocene* 11, 313-321.

Wang, Y. J., Cheng, H., Edwards, R. L., An, Z. S., Wu, J. Y., Shen, C. C. and Dorale, J. A., 2001. A high-resolution absolute-dated late Pleistocene monsoon record from Hulu cave, China. *Science* 294, 2345-2348.

Wang, Y. J., Cheng, H., Edwards, R. L., He, Y. Q., Kong, X. G., An, Z. S., Wu, J. Y., Kelly, M. J., Dykoski, C. A. and Li, X. D., 2005. The Holocene Asian Monsoon: links to solar changes and North Atlantic climate. *Science* 308, 854-857.

Wang, Y., Cheng, H., Edwards, R. L., Kong, X., Shao, X., Chen, S., Wu, J., Jiang, X., Wang, X. and An, Z., 2008. Millennial- and orbital-scale changes in the East Asian monsoon over the past 224,000 years. *Nature* 451, 1090-1093.

Watts, W. A., 1969. A pollen diagram from Mud Lake, Marion County, north-central Florida. *Geological Society of America Bulletin* 80, 631-642.

Watts, W. A., 1971. Postglacial and interglacial vegetation history of Southern Georgia and central Florida. *Ecology* 52,676-690.

Watts, W. A., 1975. A late-Quaternary record of vegetation from Lake Annie, South-central Florida. *Geology* 3, 344-346.

Webster, J. W., Brook, G. A., Railsback, L. B., Cheng, H., Edwards, R. L., Alexander, C. and Reeder, P. P. 2007. Stalagmite Evidence from Belize Indicating Significant Droughts at the Time of Preclassic Abandonment, the Maya Hiatus, and the Classic Maya Collapse. *Palaeogeography, Palaeoclimatology, Palaeoecology* 250, 1-17.

Winograd, I. J., Coplen T. B., Landwehr, J. M., Riggs, A. C., Ludwig, K .R., Szabo, B.J., Kolesar, P. T., and Revesz, K. M., 1992. Continuous 500,000-year climate record from vein calcite in Devils Hole, Nevada. *Science* 258, 255–260.

Yuan, D. X., Cheng, H., Edwards, R. L., Dykoski, C. A., Kelly, M. J., Zhang, M. L., Qin, J. M., Lin, Y. S., Wang, Y .J., Wu, J. Y., Dorale, J .A., An, Z. S. and Cai, Y. J., 2004. Timing, Duration, and Transitions of the last interglacial Asian monsoon. *Science* 304, 575-578.

CHAPTER 2

RESEARCH METHODS

Sample Collection

This research involved analysis of four stalagmites and one column. Two small stalagmites were removed from caves in China and India and parts of a broken column from a cave in the USA. In addition, cores were drilled from large stalagmites in DeSoto Caverns so as to preserve the stalagmites themselves (Fig. 2.1).

A 25 cm long stalagmite (Shangdong-A) was collected by Honglin Xiao in 2000 from Shangdong Cave (26°24′N 106°29′E), 30 km southwest of Guiyang, the capital of Guizhou Province in Southern China. Stalagmite PGH-1 was collected by Bahadur Kotlia in 2005 from Panigarh Cave (29°33′10″N; 80°07′31″E; 1520 m above mean sea level), which is located 300 km northeast of New Delhi and 20 km west of the western boundary of Nepal.

Vertical cores were drilled (by Liang and Brook) from two large, active stalagmites in DeSoto Caverns (33°18′24″N, 86°16′39″W, 160 m above mean sea level) in Alabama, USA, with the permission of the owner Allen W. Mathis III. One is 80 cm high and up to 50 cm in diameter; the other is 120 cm high, and part of a group of several stalagmites. The coring approach was preferred over complete removal of the stalagmites first because they are large formations and would have been difficult to remove, and secondly because the stalagmites are quite impressive and part of the regular tourist route in DeSoto Caverns.

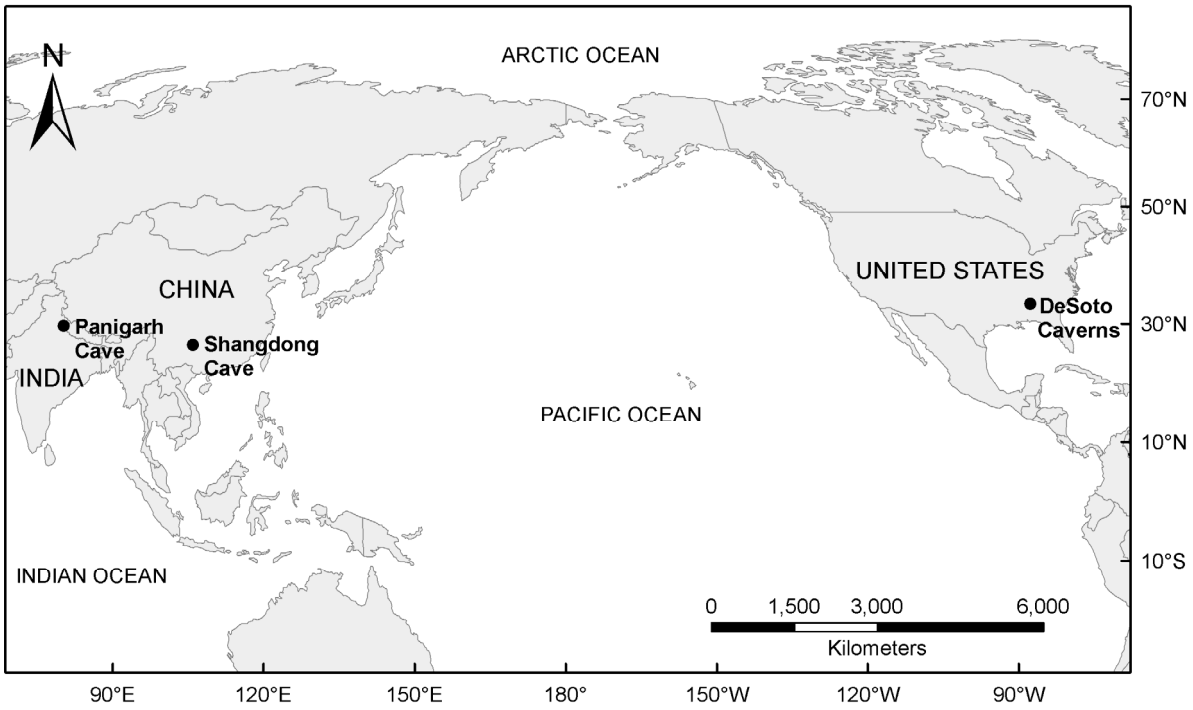

Figure 2.1. Location map showing the three study sites.

Cores were obtained from the two stalagmites in DeSoto Caverns using a modified electric drilling system manufactured by Milwaukee Electric Tool Corporation. The system is similar to that used previously to obtain 3 m long horizontal cores from two stalagmites in Carlsbad Caverns, New Mexico (Brook et al., 2006). The drill stem consisted of a series of threaded steel extension pipes (ca. 30 cm long and 5.5 cm in diameter), one of which is impregnated with industrial diamonds and serves as the drill bit (Fig. 2.2).

A wooden platform was built around the stalagmites and the drill was attached to the platform to assure drilling along the stalagmite growth axis (Fig. 2.3). During the drilling process, the drill stem and abrading surface were cooled and lubricated with water flushed down the center of the drill barrel and out around the cutting surface. Drilling was stopped when the core broke or extension pipes were added. Core sections were removed from the drill hole and drilling direction and position in sequence were carefully marked.

In the mid 1990s, the natural entrance to DeSoto Caverns was enlarged to accommodate a small vehicle. In the process one or more speleothem columns were removed. Large sections of two of these were transported to the University of Georgia in 1995 by Heidi LaMoreaux and put in storage. A slab cut from one of the two broken columns was analyzed here and a record of paleoclimate changes obtained (see Chapter 6).

Laboratory Analysis

Petrographic Analysis

Whole stalagmites were cut into two halves along the central growth axis and cores were cut parallel with the drilling direction. Chips about 0.6 cm thick were cut from one half of

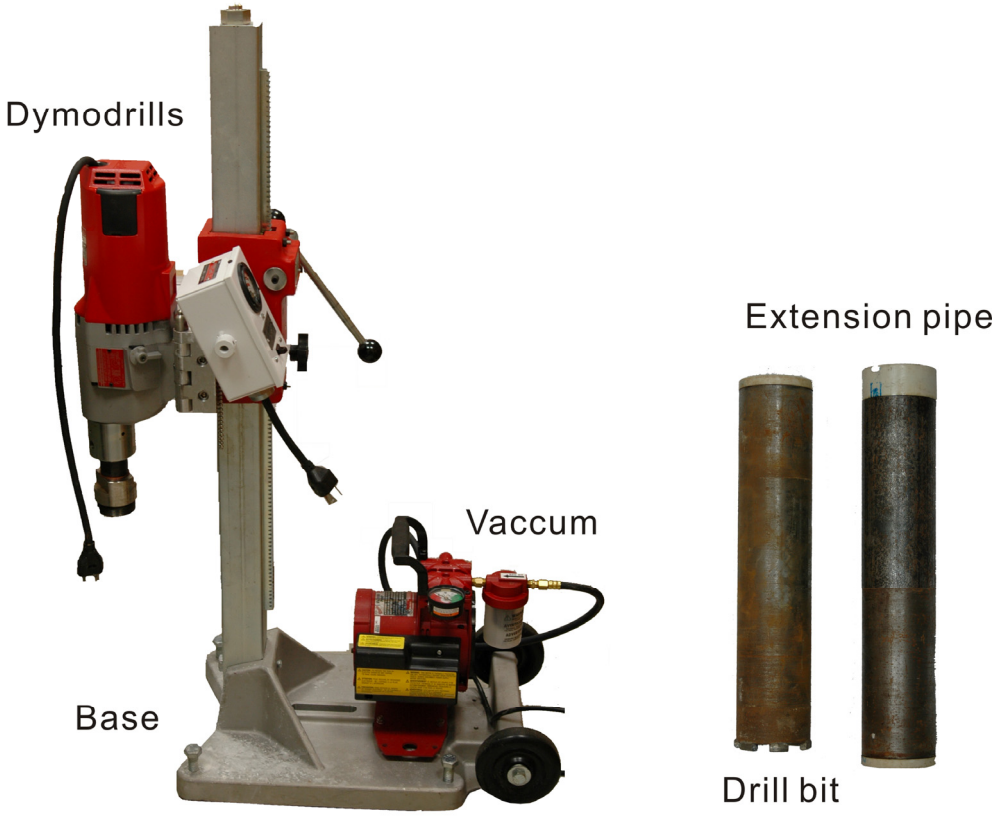

Figure 2.2. Drilling rig and extension pipes.

Figure 2.3. Platform built for drilling stalagmites at DeSoto Caverns (photograph by George A. Brook).

the speleothems/cores and 5x7.5 cm thin sections were prepared (Quality Thin Sections, Tucson, Arizona). Speleothem carbonate microfabrics, including mineralogy, and crystal shape, size, and layering were studied by examining the thin sections using a Leica petrographic microscope.

Detrital materials in the speleothem carbonate were examined following procedures proposed in Railsback (1993). Samples cut from the speleothems were broken into small pieces and then powdered. The powder was treated with 0.5M acetic acid-sodium hydroxide buffer solution until pH values of the solution reached around 5 to dissolve carbonates. Residues were collected by centrifuging and then mounted on glass slides. After air drying the insoluble material was analyzed by X-Ray diffraction (XRD).

Gray Level and Luminescence

Digital images of the speleothems studied in this research were obtained by scanning polished surfaces on a standard flat-bed scanner at a resolution of 300 dpi and 8-bit gray level resolution. Variations in gray level were then measured using Erdas Imagine along a linear transect parallel with the growth axis.

UV-induced luminescence of speleothem carbonate was measured by illuminating a polished surface with ultraviolet lights (320 to 420 nm) manufactured by Macken Instruments Incorporation in a dark room. The speleothem was placed on a dark cloth, which does not emit any luminescence, and the polished surface made horizontal. The resulting luminescence was recorded by a six mega-pixel digital camera (Nikon D70) fitted with a Kodak Wratten Gelatin Filter #2E to prevent transmission of the UV excitation energy band. An f-stop of 4.5 was used. A series of shutter speeds, usually from 0.5 second to 4 seconds, was used to record the

luminescence, only the best image being used. Variations in luminescence were then measured using Erdas Imagine along a linear transect parallel with the growth axis or growth direction.

U-series dating

Samples (ca. 100 mg) were drilled from the speleothems and dated by inductively coupled plasma mass spectrometry (ICP-MS) in the Stable Isotope Laboratory at the University of Minnesota following procedures outlined by Edwards et al., (1987) and Shen et al., (2002). Preliminary chronologies were established using ages obtained by Hai Cheng, Benjamin Hardt, and Xianfeng Wang of the University of Minnesota. Additional samples were then dated (by Liang) in December, 2007 and January, 2008.

Samples for dating were dissolved into 7N HNO_3 until fizzing stopped and no residue was left in the beaker. The carbonate was spiked with a mixed ^{229}Th-^{233}U-^{236}U tracer (Cheng et al., 2000). Two spikes can be used: the speleothem spike and the coral spike. The coral spike was added to samples drilled from the PGH-1 stalagmite due to the higher concentration of ^{238}U (greater than 1ppm). Samples from DeSoto Caverns were traced by adding the speleothem spike due to the relatively low concentration of ^{238}U. Approximately 4 drops of $HClO_4$ were added to the solution to remove any organic matter. Uranium and thorium in the solution were then co-precipitated with ~0.3 to 0.6 mg $FeCl_3$. Deposits were rinsed three times by adding super-clean water and then extracted from the solution by centrifuging. Uranium and thorium were then separated to produce clean Fe-free uranium and thorium fractions using an anion exchanges resin (BioRad 1-X8, 100-200 mesh, 0.6-1.0 ml column volume). ICP-MS analysis of the isotopic compositions of uranium and thorium was performed on a Finnigan MAT Element

mass spectrometer. Finally the results were calculated using half-lives determined in Cheng et al., (2000) and reported with analytical errors of 2σ of the mean.

Stable Isotope Measurements

Once preliminary chronologies had been developed for the speleothems, a sampling interval and sampling procedures were selected based on the speleothem growth rate and the desired temporal resolution of the isotope data. Samples were obtained from the Shangdong (61 samples), PGH-1 (36 samples), and DeSoto (286 samples) stalagmites at an interval of 0.5 cm using a hand-held dental drill. Ages for the DeSoto column indicated a much slower growth rate in the horizontal direction and so samples were obtained by micromilling, which was performed on a New Wave micro sampling system (Fig. 2.4) in the Department of Geology at the University of Georgia. The part of the slab from 120-70 mm depth was sampled at an interval of 0.6 mm, and the outer 70 mm at an interval of 3 mm. In total 109 samples were obtained.

The New Wave micro sampling system consists of a stereo microscope and color CCD video camera for sample viewing, a fine resolution automated stage, and a high torque DC milling carbide tipped drill. A polished, ca. 0.5 cm thick slab was prepared and fixed to the sample stage with double-sided tape. After calibrating the drill tip position in relation to the slab thickness and sample surface, parameters in the software were adjusted and samples were milled from the slab at a designated location, depth and length. Powder milled from the slab was collected by two thin blades and transferred to 1 dram vials. The surface of the slab and drill bit were carefully air cleaned before each sample run.

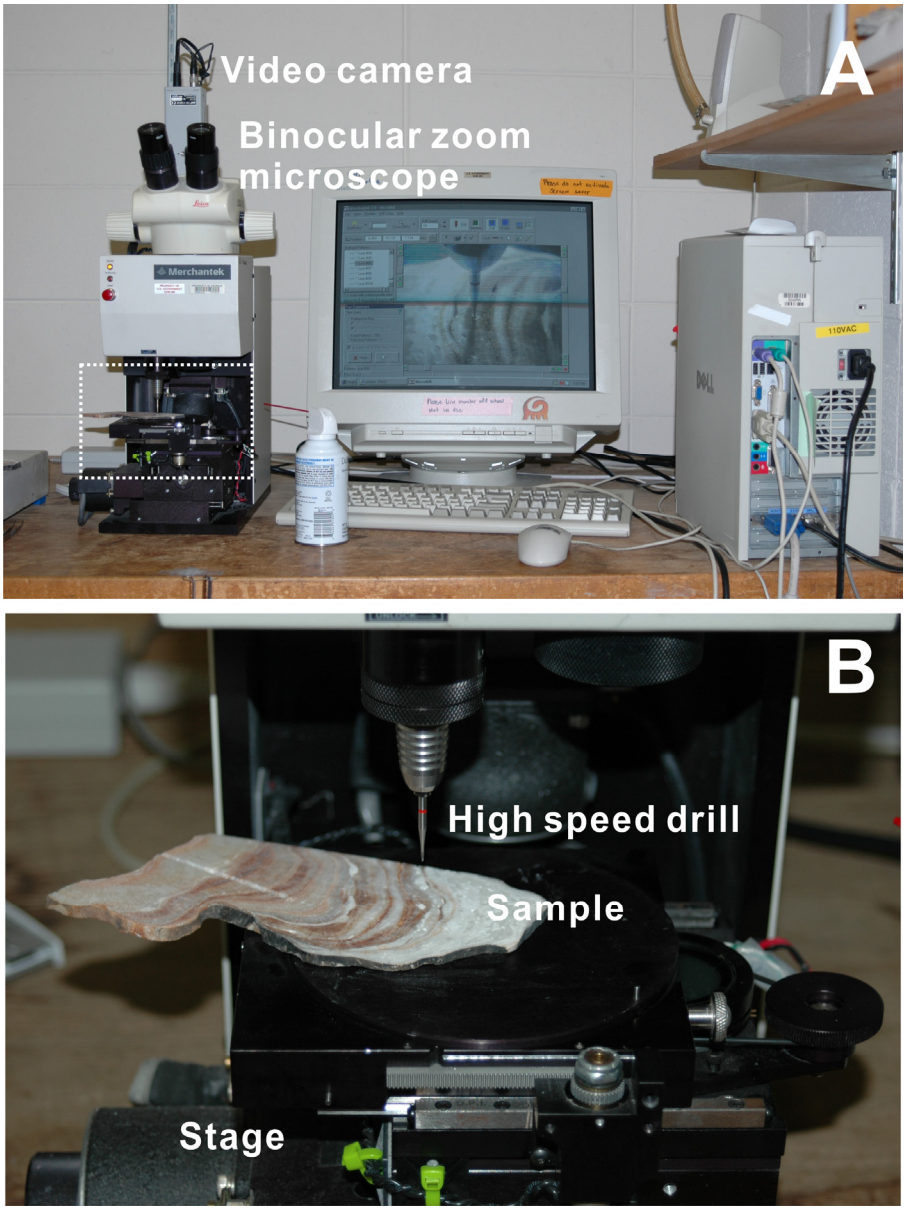

Figure 2.4. Micromill sampling system and sampling stage. (B) shows the area in A delimited by a rectangle.

Three different systems were used to measure stable isotopic compositions. Samples drilled from the Shangdong stalagmite were processed following procedures in McCrea (1950) and Al-Aasm et al. (1990). Approximately 5 mg of carbonate powder was reacted in an evacuated vessel with 100% outgassed orthophosphoric acid in a thermostated water bath at 25°C for 12 hours. Conventional cryogenic methods were used to collect the evolved CO_2 for analysis on a Finnegan-MAT 252 mass spectrometer in the Stable Isotope Laboratory in the University of Georgia Department of Geology. Carbonate powder drilled from PGH-1 and milled from the DeSoto column slab was processed in the Savannah River Ecology Laboratory, University of Georgia following procedures outlined by Jimenez-Lopez and Romanek (2004). Approximately 150 μg of carbonate powder was loaded into 10 ml vacutainers™ and flushed with helium gas. Concentrated phosphoric acid was injected into the vacutainers to dissolve carbonate and samples were left to react overnight. Stable isotope measurement was performed on a Finnigan DeltaplusXL isotope ratio mass spectrometer operated in continuous flow mode (CF-IRMS) using the Gasbench II peripheral device. Replicates were run for every tenth sample and standards were run for every five samples. The analytical precision (1σ) was ±0.14‰ for $\delta^{13}C$ and ±0.23‰ for $\delta^{18}O$, respectively, based on the repeated measurement of the NBS-19 standard. Samples from the DeSoto cores were analyzed in the Isotope Laboratory at Nanjing Normal University, China. Samples were prepared with an on-line and automated carbonate preparation system (Kiel III) and analyzed by a Finnigan MAT-253 gas source mass spectrometer. Reliability was checked by running standards (NBS-19) every nine samples, with calculated standard deviation of 0.06‰ for $\delta^{18}O$ and 0.03‰ for $\delta^{13}C$ values. All isotope measurements are reported in ‰ units versus the V-PDB standard using conventional delta (δ) notation (Craig, 1957).

Data Processing

Variations in stable isotopes, gray color, luminescence, as well as petrographic information from each speleothem were integrated to produce records of past environmental conditions for each cave site. These records were compared with published data from the same general area. Records for the Asian and Southeastern USA monsoon were compared to determine how the slow melting of the Laurentide Ice Sheet may have affected the climate of eastern North America during the Holocene. Records were further compared with appropriate records from ocean cores, ice cores, lake cores, and loess deposits to examine the influence of external factors. Results are presented in Chapters 3-6 and are summarized in Chapter 7.

References

Al-Aasm, I. S., Taylor, B. E. and South, B., 1990. Stable isotope analysis of multiple carbonate samples using selective acid extraction. *Chemical Geology* 80, 119–125.

Brook, G. A., Ellwood, B. B., Railsback, L. B. and Cowart, J. B., 2006. A 164 ka record of environmental change in the American southwest from a Carlsbad Cavern speleothem. *Palaeogeography, Palaeoclimatology, Palaeoecology* 237, 483-507.

Cheng, H., Edwards, R. L., Hoff, J., Gallup, C. D., Richards, D. A. and Asmerom, Y., 2000. The half-lives of uranium-234 and thorium-230. *Chemical Geology* 169, 17-33.

Craig, H., 1957. Isotopic standards for carbon and oxygen and correction factors for mass-spectrometric analysis of carbon dioxide. *Geochimica et Cosmochimica Acta* 12, 133-149.

Edwards, R. L, Chen, H. and Wasserburg, G. J., 1987. ^{238}U–^{234}U–^{230}Th–^{232}Th Systematics and the precise measurement of time over the past 500,000 years. *Earth and Planetary Science Letters* 81,175–192.

Jimenez-Lopez, C. and Romanek, C. S., 2004. Precipitation kinetics and carbon isotope partitioning of inorganic siderite at 25°C and 1 atm. *Geochimica et Cosmochimica Acta* 68, 557-571.

McCrea, J. M., 1950. On the isotopic chemistry of carbonates and a paleotemperature scale. *Journal of Chemical Physics* 18, 849-857.

Railsback, L. B., 1993. Effect of acidic buffers on clay minerals recovered from calcareous soils: an X-ray diffraction study. *Soil Science* 155, 206-210.

Shen, C.-C., Edwards, R. L., Cheng, H., Dorale, J. A., Thomas, R. B., Moran, S. B., Weinstein, S. and Edmonds, H. N., 2002. Uranium and thorium isotopic and concentration measurements by magnetic sector inductively coupled plasma mass spectrometry, *Chemical Geology* 185, 165–178.

CHAPTER 3

VARIATIONS IN THE STRENGTH OF THE ASIAN SUMMER MONSOON DURING THE MIDDLE AND LATE HOLOCENE: STALAGMITE EVIDENCE FROM SHANGDONG CAVE, SOUTHWESTERN CHINA*

*Fuyuan Liang, George A. Brook, L. Bruce Railsback, to be submitted to *The Holocene*.

Abstract

Paleoenvironmental changes in Southwestern China from ca. 5.1-1.6 ka were determined by examining variations in mineralogy, $\delta^{18}O$, $\delta^{13}C$, gray color, and luminescence along the growth axis of a 25 cm long stalagmite from Shangdong Cave in Guizhou Province, China. The stalagmite is enriched in ^{18}O and depleted in ^{13}C over time in response to a gradual decline in summer solar radiation over the Asian continent at 40ºN. Lower $\delta^{18}O$ and higher $\delta^{13}C$ values from 5.1-3.5 ka suggest a stronger monsoon bringing intense rains and more total precipitation to the Yangtze Valley. A gradual increase in $\delta^{18}O$ and a decrease in $\delta^{13}C$ values from ca. 3.5-1.6 ka records a weakening monsoon and drier conditions when the monsoon front retreated further south, bringing less rainfall to the Shangdong Cave area. A marked increase in $\delta^{18}O$ (~1.2‰) and a drop in $\delta^{13}C$ (~0.8‰) values around 3.5 ka appears to record the end of the Holocene Climatic Optimum near Shangdong Cave.

Key words: stalagmite; stable isotopes; Asian Monsoon; Holocene; Southwestern China.

Introduction

The Asian monsoon is an integral part of the global atmospheric circulation and plays a significant role in the current and past climate of regions in East Asia. The Asian monsoonal climate is perhaps the best understood of the major monsoon systems. Records of past monsoon variability have been derived from marine sediments, ice cores, stalagmites, lake sediments, and loess sequences (see Wang et al., 2005a), indicating that variations in Asian monsoon strength significantly affected climates in East Asia during the late Pleistocene and Holocene. Syntheses of published proxy data and numerical modeling suggest significant spatial variations in climate across China during the Holocene (An et al., 2000), indicating maximum precipitation in North China at ca. 10,000-7000 yr B.P., in the middle and lower reaches of the Yangtze River ca.7000-5000 yr B.P., and in Southern China around 3000 yr BP.

Previous research on stalagmites suggests that a strong summer Asian monsoon in the early Holocene began to weaken gradually from the middle Holocene (e.g., Cai et al., 2001; Wang et al., 2005; Dykoski et al., 2005b). However, only variations in $\delta^{18}O$ of speleothem carbonate are examined in these studies. Other climate proxy evidence, such as petrography, and variations in $\delta^{13}C$ values, luminescence, and gray color along the growth axis of the stalagmites examined were in most cases not evaluated. Here, we report a multi-proxy record from a stalagmite from Guizhou Province, Southwestern China, a region strongly influenced by the Asian monsoon. Variations in $\delta^{18}O$ provide information on past climates, while variations in $\delta^{13}C$ values, luminescence, and gray color appear to document transitions from wetter to drier conditions near the cave resulting from variations in the strength of the Asian summer monsoon.

Shangdong Cave

A 25cm long stalagmite (Shangdong-A) was collected from Shangdong Cave (26°24' N 106°29'E), 30km southwest of Guiyang, the capital of Guizhou Province in China (Fig. 3.1). Shangdong Cave is located in a small karst hill about 10 m above Yangzhipo Cave. A stalagmite from Yangzhipo Cave has provided information on Holocene climate change in this area, but the record in incomplete (Xiao et al., manuscript in prep.). The region in which both caves are located has a subtropical monsoon climate with a mean annual temperature of 15.4°C with an average annual precipitation of 1753 mm. About 75% of precipitation falls from late April to August when the Asian summer monsoon front passes over the area.

Methodology

The Shangdong-A stalagmite was cut along the central growth axis and one exposed surface was polished. This surface was scanned at 300 dpi spatial resolution and 8 bit (256 increments) gray level resolution on a flatbed scanner. It was then illuminated by long-wave ultraviolet light (320 to 420 nm) from two Macken Instruments Model 22-UV lamps under darkroom conditions. Spatial variations in the resulting luminescence of the stalagmite were recorded using a Nikon D-70, 6-megapixel digital camera (speed 0.5 seconds; f-stop 5.6) fitted with a Kodak Wratten Gelatin Filter #2E to prevent transmission of the UV excitation energy band. Variations in gray color and luminescence were measured using image analysis software along a 5 pixel wide (0.4 mm) traverse down the central growth axis of the stalagmite. The gray-level (0=black; 255=white) and luminescence (0=black; 255=white) values have a spatial resolution of 0.08 mm (i.e., ~1.3 year per dot).

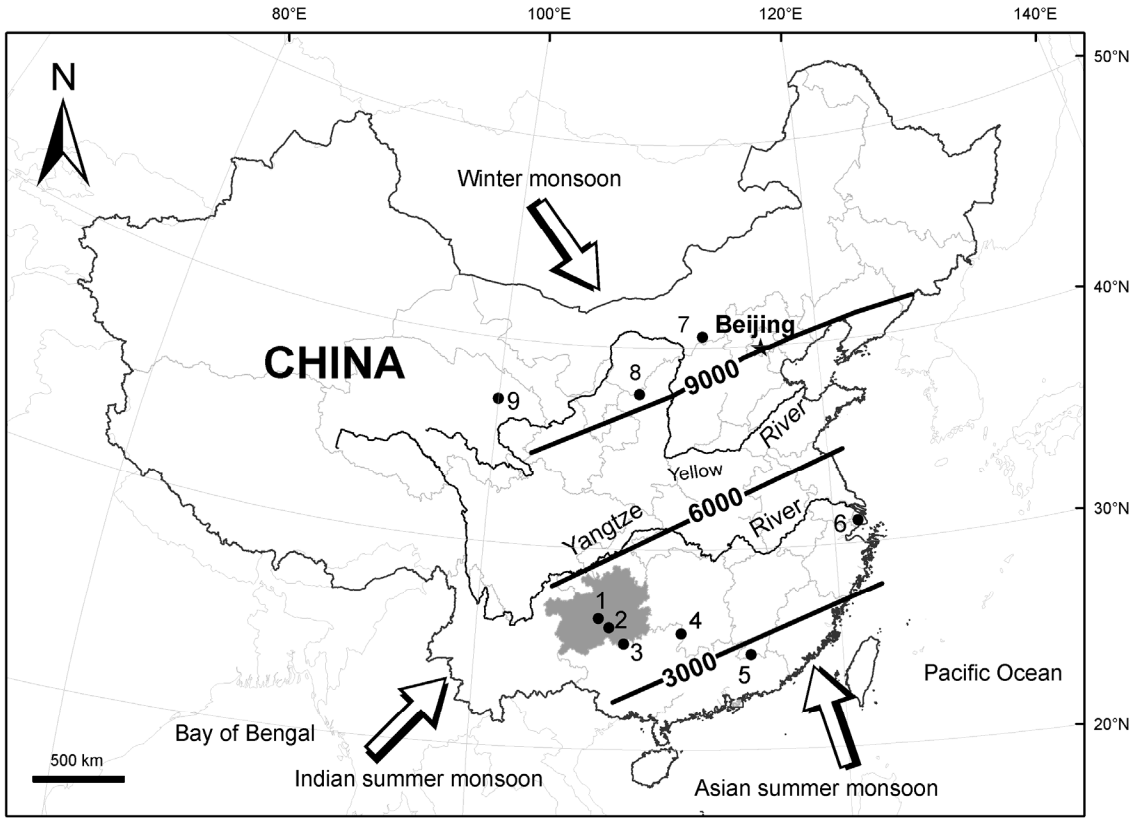

Figure 3.1. Map of China showing the Asian and Indian monsoons and the location of Shangdong Cave and other important sites discussed in the text. The dark gray shaded area is Guizhou Province. Numbered sites are: (1) Shangdong Cave (this study); (2) Qixing Cave (Cai et al., 2001); (3) Dongge Cave (Yuan et al., 2004; Dykoski et al., 2005; Wang et al., 2005); (4) Xiangshui Cave (Zhang et al., 1999); (5) Dahu Swamp (Zhou et al., 2004); (6) Yangtze River Delta (Yi et al., 2003); (7) Lake Daihai (An et al., 1991); (8) Midiwan Section (Li et al., 2003); (9) Lake Qinghai (Wang, 1992). Black thick lines labeled with "9000", "6000", and "3000" show that maximum precipitation occurred at 9000 years ago in Northern China, 6000 years ago in the middle and lower reaches of the Yangtze River, and 3000 years ago in Southern China (An et al., 2000).

Four large (51mm x 76 mm) thin sections were prepared for petrographic study. Samples of ~100 mg from 0.8, 15.2, and 25.0 cm from the top of the stalagmite were dated by AMS radiocarbon techniques. In addition, eleven samples of ~200 mg were drilled at points along the central growth axis for ICPMS U-series dating and fifty samples of ~5 mg were drilled every 0.5 cm for $\delta^{13}C$ and $\delta^{18}O$ analysis. An additional 12 samples for stable isotope analysis were taken at 0.5 cm intervals along two growth layers 4.2 and 20.5 cm from the top of the stalagmite to determine if carbonate deposition was in isotopic equilibrium with precipitating waters following the criteria of Hendy (1971). In stable isotope analysis, carbonate powders were reacted under vacuum with 100% orthophosphoric acid at 25°C following the procedures described in McCrea (1950) and Al-Aasm et al. (1990). Conventional cryogenic methods were used to collect the evolved CO_2 for analysis on a Finnegan-MAT 252 mass spectrometer in the Department of Geology Stable Isotope Laboratory at the University of Georgia.

Chronology and Growth Rates

Eleven ^{230}Th ages were obtained for the Shangdong-A stalagmite (Table 3.1.). With the exception of four samples at 1.5, 3.5, 4.5, and 5.6 cm from the top of the stalagmite, the ages are in correct stratigraphic order (Fig. 3.2). These four samples were not used in developing a chronology for Shangdong-A as they are significantly older than adjacent samples. Of importance is that the four samples have the lowest $^{230}Th/^{232}Th$ ratios of the eleven samples, suggesting significant contamination by ^{232}Th at the time of stalagmite deposition, mainly because these samples were drilled along or very close to layers with visible detritus (Table 3.1).

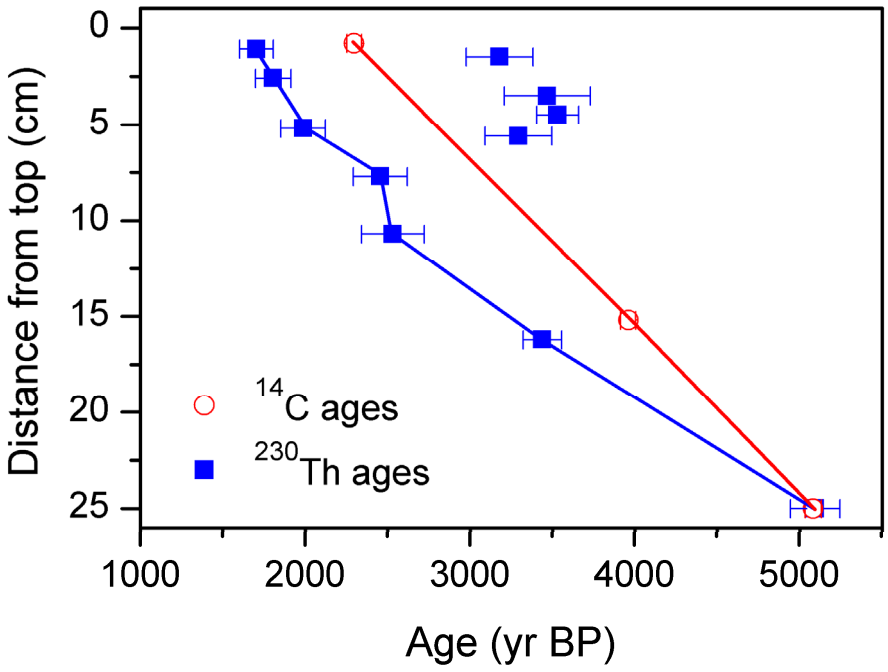

Figure 3.2. ICPMS U-series (solid squares) and radiocarbon ages (empty circles) for the Shangdong-A stalagmite. Four of the eleven U-series ages appear to contain detrital ^{232}Th and were not used in developing a chronology for the stalagmite. The radiocarbon ages are Libby ages corrected to -25‰ for isotopic fractionation and are in ^{14}C yr. B.P.

Three Libby radiocarbon ages for the stalagmite are in correct stratigraphic order with a typical age uncertainty of ~50 years. Comparison of ICP-MS U-series and ^{14}C ages for a Yangzhipo Cave stalagmite shows an average 8.5% old carbon in the stalagmite carbonate, with four matching sample pairs having 4, 6, 10 and 14% old carbon, respectively (Xiao et al., manuscript in prep.). Assuming similar conditions at Yangzhipo and Shangdong Cave, the Shandong-A radiocarbon ages were also corrected by assuming 8.5% old carbon and then calibrated using OxCal version 3.9 (Ramsey, 1995, 2001) and the calibration curve of Stuiver et al. (1998). This gave ages of 1600 ± 140, 3595 ± 95, and 5125 ± 215 calendar years (cal. yr), respectively (Table 3.2) that correspond quite well to the reliable ^{230}Th ages, particularly considering the uncertainty in estimating the old carbon content of the samples. The final chronology was developed using the seven U-series ages and indicates that the stalagmite grew from 5092 to 1628 yr (adding 76 years for the undated top 1.1 cm) or from about 5.1-1.6 ka before present. Estimated growth rates are 0.05 mm/yr from 25.0 to 16.2 cm depth, and 0.17 mm/yr from 16.2 to 0.8 cm depth, indicating more rapid growth after 2.5 ka than earlier (Fig. 3.2).

Petrography

The Shangdong-A stalagmite consists almost entirely of clear dense columnar calcite, except the basal 2.1 cm, which consists of columnar calcite with scattered and elongated macropores. Individual calcite crystals are up to 0.65 mm wide and many are up to 6 mm long. The lower ~ ⅔ rd of the stalagmite contains very little detrital material. In this region layers are defined only by rare surfaces along which scattered small calcite crystals nucleated, but were engulfed in columnar calcite that formed syntaxially with the calcite below.

Table 3.1. ICP-MS uranium-series age data for the Shangdong-A stalagmite.

Sample ID	Depth (cm)	^{238}U ppb	^{232}Th ppt	$d^{234}U$ measured	$[^{230}Th/^{238}U]$ activity	$[^{230}Th/^{232}Th]^{a}$ ppm	Age (yrs BP) (uncorrected)	Age (yrs BP)[b] (corrected)	$d^{234}U_{initial}$ (corrected)
SH-1.1	1.1	390.2±1.1	595±4	540.3±3.7	0.024267±0.00141	263±15	1733±101	1704±102	542.9±3.7
SH-1.5	1.5	332.1±0.9	4845±23	547.1±4.4	0.048231±0.00205	55±2	3452±149	3179±202	552.0±4.5
SH-2.6	2.6	389.8±1.1	585±4	528.6±3.8	0.025486±0.00149	280±17	1834±108	1806±109	531.4±3.9
SH-3.5	3.5	337.0±1.1	6574±33	534.6±5.5	0.05308±0.00250	45±2	3837±184	3467±261	539.8±5.6
SH-4.5	4.5	420.1±1.2	3046±13	558.2±4.1	0.05153±0.00149	117±3	3665±108	3531±127	563.7±4.2
SH-5.2	5.2	376.1±1.1	1317±7	509.8±4.7	0.02817±0.00177	133±8	2055±130	1987±135	512.7±4.8
SH-5.6	5.6	289.6±1.0	3951±20	535.2±5.2	0.049205±0.00213	60±3	3551±156	3293±203	540.2±5.3
SH-7.7	7.7	237.0±0.9	143±2	575.2±6.3	0.035221±0.00230	961±65	2466±163	2455±163	579.2±6.3
SH-10.7	10.7	261.3±0.9	76±3	584.4±5.8	0.036433±0.00270	2055±173	2537±190	2532±190	588.6±5.9
SH-16.2	16.2	214.2±0.5	171±2	562.9±4.5	0.048736±0.00162	1010±35	3453±117	3438±117	568.4±4.6
SH-25	25.0	284.0±0.7	868±5	501.5±3.6	0.069344±0.00193	375±11	5151±147	5092±150	508.8±3.7

Analytical errors are 2 of the mean. Decay constants are 9.1577 x 10^{-6} yr^{-1} for ^{230}Th, 2.8263 x 10^{-6} yr^{-1} for ^{234}U, and 1.55125 x 10^{-10} yr^{-1} for ^{238}U (Cheng et al., 2000). [a] The degree of detrital ^{230}Th contamination is indicated by the $[^{230}Th/^{232}Th]$ atomic ratio instead of the activity ratio. [b]Age corrections were calculated using an average crustal $^{230}Th/^{232}Th$ atomic ratio of 4.4 x 10^{-6} ± 2.2 x 10^{-6}. Those are the values for a material at secular equilibrium, with the crustal $^{232}Th/^{238}U$ value of 3.8. The errors are arbitrarily assumed to be 50%.

Table 3.2. AMS radiocarbon age data for the Shangdong Cave Stalagmite.

Sample ID	UGAMS ID	Depth (cm)	Percentage of modern carbon (± 1σ)	$\delta^{13}C$ (‰)	Libby Age (± 1σ)	Old Carbon (%)	Calibrated Age (±2σ)	Mean Cal. Years
Shang-0.8	R00805	0.8	75.1 ± 0.4	-10.1	2296 ± 45	8.5	260-540 AD	1600
Shang-15.2	R00857	15.2	61.08 ± 0.3	-8.5	3960 ± 40	8.5	1690-1500 BC	3595
Shang-25	R00811	25.0	53.1 ± 0.3	-7.8	5081 ± 50	8.5	3340-2910 BC	5125

The upper ~ ⅓ rd of the stalagmite contains layers of detrital material that are typically 0.04 mm thick, but locally up to 0.22 mm thick. Most detrital particles are not resolvable with a light microscope and so must be less than 0.001 mm in diameter. However, many particles exceed 0.02 mm and a few 0.14 mm making them fine sand on the Wentworth scale. The bases of detrital layers are commonly sharp and overlie euhedral crystal terminations, whereas upper boundaries are commonly gradational into columnar calcite.

The presence of detrital grains of very fine to fine sand size suggests that the detrital material was deposited by flowing water, not as an aerosol. Euhedral crystal faces below detrital layers further suggest a considerable flow of water across the speleothem to maintain a thick film of water into which growing tips of crystals could protrude. Detrital layers in euhedrally-tipped columnar calcite in the upper part of the stalagmite (corresponding with the period from 2.3 to 1.6 ka B.P.) suggest an increased water flow, either prolonged or episodic. Dense calcites in the lower part of Shangdong-A stalagmite deposited from 4.8 to 2.3 ka suggests considerable dripwater, as they are usually associated when water is abundant (Genty and Quinif, 1996; Mattey et al., 2008). By contrast, columnar calcite is deposited with scattered and elongated macropores due to low calcite-supersaturated precipitating water (Genty and Quinif, 1996; Mattey et al., 2008), suggesting more intense water flow brought by intense rainfall above the cave. In summary, the petrography of Shangdong-A stalagmite suggests that the area near the cave was wetter during the mid- to late-Holocene, but with more intense rainfall from 4.8 to 5.1 ka B.P.

Stable Isotopes

Equilibrium Tests

Samples along a growth layer 4.2 cm from the top of the stalagmite and another 20.5 cm from the top, have similar $\delta^{18}O$ (-8.67~-9.49‰) and $\delta^{13}C$ (-7.28~-8.17‰) values over a distance of 3 cm from the central growth axis (Figs 3.3A and C). There is no perceptible increase (actually there is a slight decrease) in these values along either growth layer as would be expected with significant kinetic fractionation. Also, although $\delta^{18}O$ and $\delta^{13}C$ in each layer are positively correlated (R^2 =0.73 for layer 1 and R^2 =0.66 for layer 2), the correlations are weak (Fig. 3.3 B and D). In fact the Hendy test (1971) is excellent in theory, but it is extremely difficult to implement in practice (Lauritzen and Lundberg, 1999) because it requires drilling several samples from one annual layer of a stalagmite with a drill bit whose diameter is invariably greater than the thickness of the annual layer. As a result, we feel that our results do not rule out the possibility that the Shangdong Cave stalagmite was deposited in isotopic equilibrium with precipitating waters.

Oxygen Isotopes

Along the growth axis, $\delta^{18}O$ values of Shangdong-A stalagmite vary from -10.0‰ to -7.7‰ (PDB) and exhibit a steady trend toward enrichment in ^{18}O from 5.1 ka to 1.5 ka (Fig. 3.4C). Remarkably similar variations in $\delta^{18}O$ over this time period (Fig. 3.5) in other stalagmites from Guizhou province (Yuan et al., 2004; Wang et al., 2005b) strongly suggest that this change is in response to a shift in regional climate and is not a response to a local change in stalagmite hydrology.

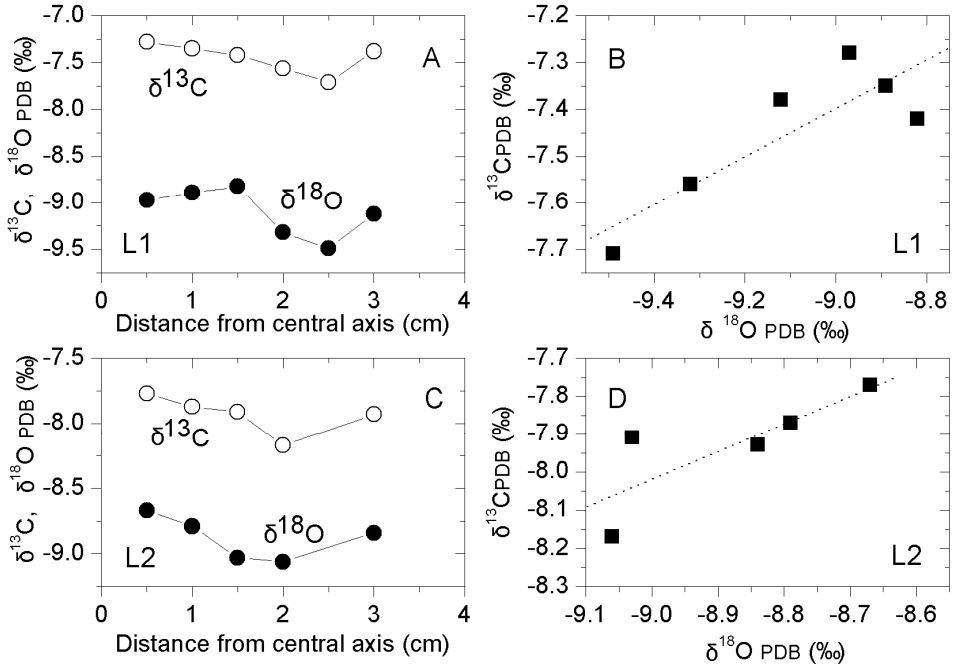

Figure 3.3. Variations in $\delta^{13}C$ and $\delta^{18}O$ values along single growth layers L1, L2, which are at 4.2 cm and 20.5 cm from the top of Shangdong Cave stalagmite. Variations in stable isotope composition from the stalagmite axis along L1 and L2 are shown in A and C, and correlations between $\delta^{13}C$ and $\delta^{18}O$ in B and D, respectively.

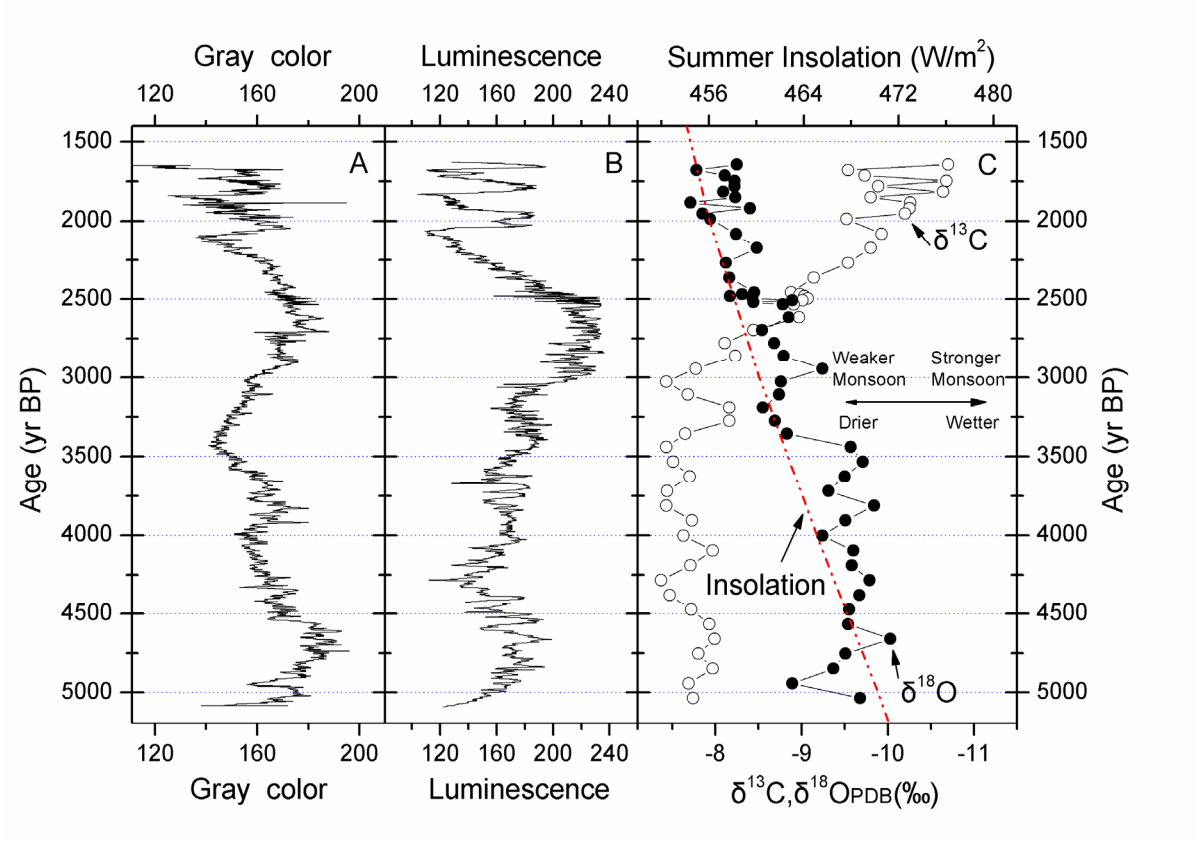

Figure 3.4. Variations in gray-scale color (A), luminescence intensity (B), and stable isotope composition (C) along the central growth axis of Shangdong-A stalagmite. The dashed line in (C) shows the gradual decline in average summer (June, July, August) insolation at 40^{o}N from the mid to late Holocene.

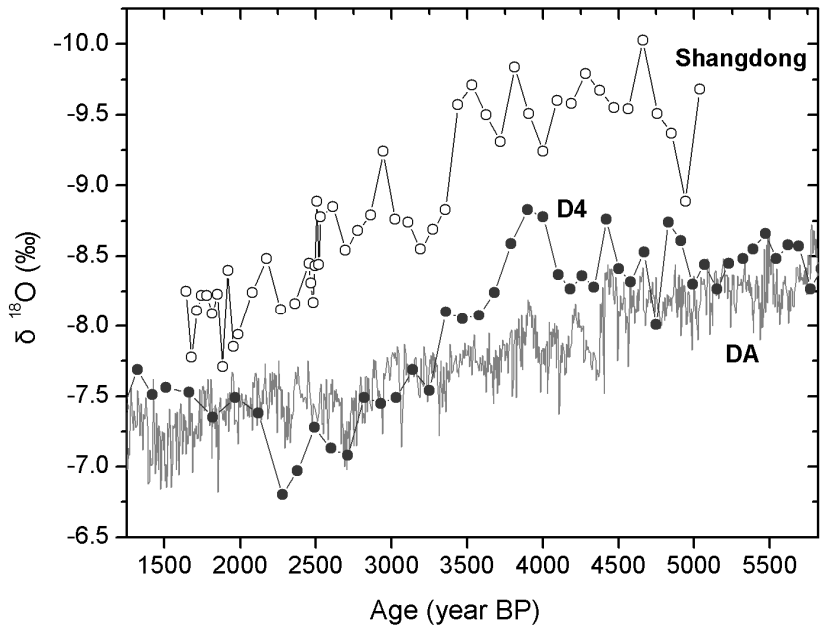

Figure 3.5. The Shangdong-A $\delta^{18}O$ record compared with the D4 and DA records from Dongge Cave 200 km southeast of Shangdong Cave in Guizhou Province (Yuan et al., 2004; Dykoskyi et al., 2005; Wang et al., 2005).

As mentioned previously, the Shangdong-A stalagmite may have been deposited in isotopic equilibrium with precipitating waters so that changes in $\delta^{18}O$ values may reflect variations in temperature and $\delta^{18}O$ of precipitating water over time (Hendy, 1971; Schwarcz et al., 1976; Gascoyne, 1992). However, the influence of temperature on $\delta^{18}O$ is slight (-0.23‰/^{o}C, Friedman and O'Neil, 1977) and temperature in Southwestern China varied by no more than 2^{o}C during the mid- and late-Holocene (Huang et al., 2000; Wang et al., 2001). As a result, we believe that the observed large variation in oxygen isotope ratios (2.3‰) was caused by variations in the $\delta^{18}O$ of precipitating waters, reflecting variations in the $\delta^{18}O$ of meteoric precipitation (Harmon, 1979; Yonge et al., 1985).

The present climate of Southwestern China is characterized by a cool, dry season during winter and a warm, wet season in summer. In winter, moisture is derived mainly from frontal rain associated with mid- to low-latitude weather systems; in summer it is brought by tropical weather systems associated with the Asian monsoon and typhoons. Summer rainfall is usually depleted in ^{18}O by preferential loss en route from the West Pacific Warm Pool to South China, and is isotopically more negative than winter frontal rainfall (Zhang et al., 2004a). Rainfall produced by strong storms is more depleted in ^{18}O than storms of modest intensity and duration (e.g., Ohsawa and Yusa, 2000; Lawrence and Gedzelman, 1996). Also, $\delta^{18}O$ of rainfall in China is significantly influenced by the "amount effect", with higher precipitation in summer having more negative $\delta^{18}O$ values, and the lower precipitation in winter more enriched in ^{18}O (Johnson et al., 2004). Hence, we believe that variations in $\delta^{18}O$ values along the growth axis of Shangdong-A record changes in both rainfall intensity and amount over time, with more negative values indicating more intense and higher rainfall, while more positive values indicate lower, and less intense rainfall. In fact, instrumental precipitation records across China suggest that higher

annual rainfall is directly associated with stronger precipitation intensity and vice versa (Domrös and Peng, 1998). Intense rainfall in Southwestern China is usually associated with a stronger summer Asian monsoon (Yuan et al., 2004; Wang et al., 2005b). As a result, variations in Shangdong-A $\delta^{18}O$ values can be used as a proxy for the strength of the summer Asian monsoon during the mid- to late-Holocene.

Carbon Isotopes

Values of $\delta^{13}C$ in Shangdong-A range from -10.7 to -7.4‰ with a general trend toward depletion in ^{13}C from the mid- to late-Holocene (Fig. 3.4C). Factors influencing stalagmite carbonate $\delta^{13}C$ include: (1) the $\delta^{13}C$ values of vegetation above the cave; (2) open- or closed-system conditions of limestone dissolution; and (3) kinetic fractionation of ^{13}C during carbonate deposition (e.g. McDermott, 2004; Quad, 2004; Brook et al., 2006). The Shandong Cave area has a temperate climate and is dominated by C_3 not C_4 vegetation. In addition, if deposition was in isotopic equilibrium as our data suggest, higher $\delta^{13}C$ values are unlikely to be the result of kinetic fractionation. As a result, we believe that observed variations in $\delta^{13}C$ values in the Shangdong stalagmite are a response to the degree to which limestone solution is an open or closed system. Under closed-system conditions, rainfall penetrates the limestone bedrock rapidly; there is little exchange of carbon dissolved from the bedrock (with $\delta^{13}C$ values of ~0‰) with soil CO_2 carbon (with $\delta^{13}C$ values of ~-26‰). As a result, carbonate deposited on the stalagmite has a higher $\delta^{13}C$ value (Hendy, 1971; Baker et al., 1997).

By contrast, more carbon from soil CO_2 will be dissolved in water draining into Shangdong Cave under more open-system conditions due to a slower percolation and therefore slower drip rate (probably because of less intense precipitation). Speleothem carbonate deposited

in this case would likely have relatively lower $\delta^{13}C$ values. As a result, elevated $\delta^{13}C$ values in the mid-Holocene are taken to indicate conditions of closed-system dissolution, mainly due to the intense rains. More negative $\delta^{13}C$ values in the late-Holocene may reflect a more open system dissolution process when there was prolonged rain but in reduced intensity.

Color and Luminescence

Gray color and luminescence range from 108-190 and 137-237 respectively (Figs 3.4A and B), with higher values indicating lighter reflective colors and stronger luminescence. Layers with detritus in the upper portion of the stalagmite are darker in color and have lower luminescence since detrital materials (mainly clay particles) are brown in color (while pure carbonate minerals are colorless) and do not luminesce. In contrast, the lower ~⅔ rd of the stalagmite has few detrital minerals so that the basal 2.1 cm of porous calcite is even lighter in color.

Increased luminescence usually indicates a higher content of organic acids in fluid inclusions in the spelean calcite (Lauritzen, 1986; Shopov et al., 1994; Ramseyer et al., 1997) due to enhanced productivity in the soil and vegetation above the cave. As the Shangdong area was relatively warm during the Holocene, plant growth was probably influenced mostly by changes in precipitation. Hence, variations in Shangdong-A luminescence are believed to record moisture availability as suggested by studies of cave drip waters (Baker et al., 1999; Tan et al., 2006). However, this relationship may be complicated by hydrological conditions. For example, organic acids may be diluted in during periods of intense rainfall even though there are abundant organic acids in the soil. This would result in reduced stalagmite luminescence despite high organic productivity above the cave. This may be why the basal 2.1 cm of the stalagmite has lower luminescence.

From 5.1 to 2.5 ka, the color of the Shangdong-A stalagmite becomes darker and luminescence increases, suggesting a gradual reduction in rainfall intensity, as porous calcite was replaced by dense calcite and the content of organic acids in dripwaters increased. Superimposed on these trends are high-frequency variations in both luminescence and gray color, with good correspondence between the two variables (Figs 3.4A and B). These high-frequency variations probably record short-term changes in moisture availability and soil productivity above the cave. During the last 900 years of the record (2.5 to 1.6ka), the Shangdong stalagmite becomes even darker in color and luminescence declines due to the presence of detrital materials washed into the cave during brief episodes of increased precipitation and water flow into the cave.

The Shangdong Paleoenvironmental Record

Marked variations in color, luminescence, $\delta^{18}O$, and $\delta^{13}C$ of the Shandong-A stalagmite indicate a gradual weakening of the Asian monsoon and a transition from wetter to drier conditions near the cave from the mid- to late-Holocene. The period from 5.1 to 3.5 ka BP was characterized by more negative $\delta^{18}O$ values (-8.9~-10.0‰; mean = -9.5‰) suggesting a stronger Asian summer monsoon with more intense rains and higher rainfall amounts. Higher $\delta^{13}C$ values (-8.0~-7.4‰), relatively low luminescence and brighter colors are a further indication of increased rainfall intensity during this period. The Asian monsoon weakened rapidly around 3.5 ka BP as evidenced by a sharp increase in $\delta^{18}O$ values (from -9.7 to -8.6‰) and a significant decrease in $\delta^{13}C$ (-8.2 to -7.4‰). During the following ~1000 years (3.5-2.5ka BP), the weaker monsoon brought less intense and lower precipitation to the Shangdong area allowing a more open system dissolution process. As a result, the content of organic acids in cave dripwaters and

speleothem carbonate increased as there was less dilution, and this produced carbonated with higher luminescence.

After 2.5 ka, the Asian summer monsoon continued to weaken and precipitation declined as indicated by higher $\delta^{18}O$ values in the carbonate deposited. At the same time, more negative values of $\delta^{13}C$ indicate a change to more open-system dissolution of the limestone bedrock due to a reduced water flow. Lower luminescence suggests drier conditions, while detrital materials indicate short periods of enhanced flow that washed soil particles into the cave. These short intervals of intense rainfall are also recorded by high frequency variations in $\delta^{18}O$ and $\delta^{13}C$ values after 2 ka BP (Fig. 3.4C). Together these changes indicate a slightly drier climate characterized by less intense rains and lower total precipitation.

Comparison with other Records

Records from the Shangdong Cave stalagmite document a gradual decline in Asian monsoon strength from the mid- to late-Holocene. Evidence of this change has also been obtained from stalagmites in Guizhou (Cai et al., 2001, Wang et al., 2005b, Dykoski et al., 2005) and Guangxi (Zhang et al., 2004b) in Southern China. In Southern Oman, which is also affected by a monsoon climate, the Q5 stalagmite records a decline in the intensity of the African monsoon with lower $\delta^{18}O$ values in the mid-Holocene indicating a stronger monsoon and higher values suggesting a weakening monsoon in the late-Holocene (Fleitmann et al., 2003).

Porous columnar calcite with lower luminescence and whiter color in the basal 2.1 cm of Shangdong-A suggests rapid and intense water flow from 5.25 to 4.8 ka B.P. This is consistent with the presence of a truncation surfaces shortly after 5.4 ka in the Yangzhipo stalagmite, in the

same hill as Shangdong Cave (Xiao et al., manuscript in prep.). The truncation surface was developed by the rapid input of undersaturated water into the cave probably caused by intense precipitation. Intense rains and wetter conditions lasted until 3.5 ka as suggested by more negative ^{18}O values in the Shangdong-A stalagmite, and also by deposition of calcite with lower $\delta^{13}C$ values in the Yangzhipo stalagmite above the truncation surface (Xiao et al., manuscript in prep.), probably because the monsoon front stagnated in the Yangtze River Valley during this period. An et al. (2000) examined published proxy data across the Chinese mainland and suggest that the Yangtze Valley received maximum precipitation during the Holocene around 6 ka and Southern China around 3 ka. As Shangdong Cave is located south of the Yangtze River Valley, it may have received maximum precipitation in the period 5-4.5 ka BP, which is consistent with evidence from the Shangdong stalagmite. In the Yangtze River Delta many trees were buried by boulders, gravel, and coarse sand before 4 ka B.P. (Fig. 3.6 F), further evidence that during the mid-Holocene Southern China received much more intense rainfall that produced massive Yangtze River floods that transported large amounts of sediment of very large size (Zhang et al., 2005). During the cooler "Holocene Event 3", at ~4 ka B.P., the middle and lower reaches of the Yangtze River experienced wetter conditions or even flooding (Wu and Liu, 2004) at a time when the Shangdong stalagmite shows evidence of a stronger summer monsoon.

The stronger summer monsoon around 5 ka B.P. appears to have penetrated further north and brought more precipitation to Northern China, as evidenced by higher levels of Lake Qinghai (Wang et al., 1992) and Daihai (An et al., 1991) (Fig. 3.6 A & C). Higher concentrations of pollen and total organic carbon (TOC) in the Midiwan peat section of the loess-desert transitional belt (Fig. 3.1), show that Northern China was wetter before cal. 4.5 ka (4000 ^{14}C years) than after (Li et al., 2003). Aquatic pollen is also present during this period. After 4.5 ka,

TOC and pollen concentration decline, indicating a shift to more arid climate conditions. An et al., (2006) synthesized multiple-proxy records derived from lake, peat, ice core, loess in north and northwest China and found that the climate of northwest China shifts to drier conditions around 4 ka B.P., although the onset of the drier conditions is spatially variable. As a result, we believe that the summer Asian monsoon weakened around 4 ka BP and the monsoon front retreated southwards and failed to reach Northern China. There was a significant reduction in monsoon intensity at 3.5 ka B.P. documented by an abrupt increase in $\delta^{18}O$ in Shangdong-A stalagmite.

After 3.5 ka BP, higher $\delta^{18}O$ values suggest a weaker monsoon that brought less precipitation to Guizhou Province, probably because the monsoon front retreated south of Nanling Mountain and brought maximum precipitation to Southern China around 3 ka BP (An et al., 2000). Wetter climatic conditions at this time in Southern China are documented by lower total organic carbon in the Dahu Swamp after cal. 4.2 ka (3800 ^{14}C years) (Figs. 3.1 and 3.6F) (Zhou et al., 2004). By contrast, higher TOC values show a much drier period from 6.0 to 3.8 cal. yr B.P., although a brief wetter period from ~4.45 to 4.0 cal. ka B.P.) is suggested by a sharp drop in TOC (Zhou et al., 2004).

The general weakening of the Asian monsoon parallels the decline in northern hemisphere summer solar radiation from the mid- to late-Holocene (Fig. 3.5C), suggesting that the broad trends in the strength of the Asian monsoon are due to changes in solar energy. When northern hemisphere summer solar radiation was higher in the mid-Holocene, there was a pronounced thermal contrast between the Asian landmass and adjacent oceans resulting in a strong Asian

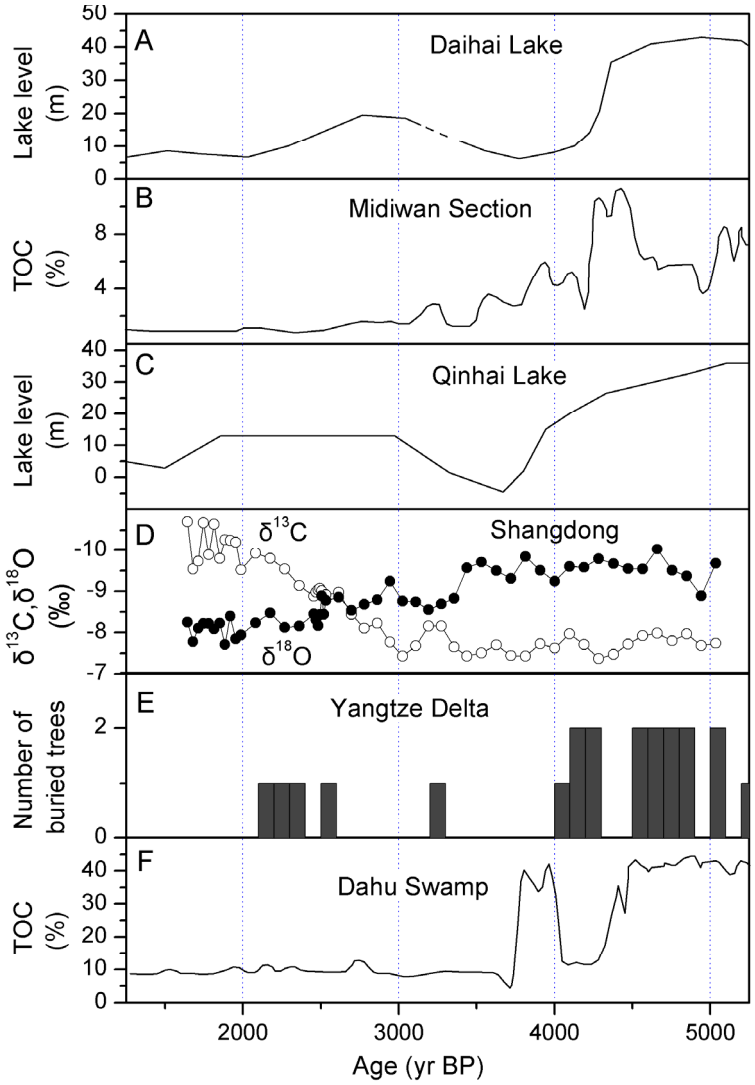

Figure 3.6. Comparison of the Shangdong-A stalagmite with other records showing that Northern China was wetter in the mid-Holocene but drier in the late-Holocene, while Southern China was drier in the mid-Holocene but wetter in the late-Holocene. (A) Daihai Lake level, Inner Mongolia (An et al., 1991); (B) Midiwan section, loess/desert boundary (Li et al., 2003); (C) Qinhai Lake level, Qinhai-Tibetan Plateau (Wang, 1992); (D) Shangdong-A stalagmite record, Southwestern China (This study); (E) Dahu Swamp, Southern China (Zhou et al., 2004); (F) Yangzi Delta, Southern China (Zhang et al., 2005).

monsoon. The monsoon front probably moved to the Yangtze River Valley and possibly much further north, bringing more and more intense precipitation to Northern China and the Yangtze Valley, but less to Southern China (Wang et al., 1981). As summer solar radiation decreased in the late Holocene the thermal contrast between the Asian landmass and the South China Sea decreased resulting in a weaker Asian monsoon that brought more precipitation to Southern China and less to Northern China (Tao and Chen, 1987; Shi and Zhu, 1996) as the monsoon front probably stayed south of Nanlin Mountain. We believe that in the past there were significant spatial variations in precipitation between Northern China, the Yangtze River Valley, and Southern China, resulting from variability in monsoon strength in response to changes in solar radiation. In fact, the present distribution of precipitation over eastern China shows that when the summer monsoon is stronger, precipitation is usually higher over Northern and Southern China but lower in the Yangtze River Valley (Domrös and Peng, 1988). The significant reduction in summer monsoon strength documented by the sharp increase in $\delta^{18}O$ values around 3.5 ka B.P. probably signifies the end of the "Holocene Climatic Optimum" in Southwestern China.

Conclusions

The steady increase in $\delta^{18}O$ values in the carbonate of a Shangdong Cave stalagmite records the gradual weakening of the Asian summer monsoon from the mid- to late-Holocene. This weakening parallels the decline in summer solar radiation over the Asian continent. In the mid-Holocene, lower $\delta^{18}O$ and higher $\delta^{13}C$ values, and lighter calcite with less luminescence, indicate a stronger Asian monsoon that brought intense rainfall and more precipitation to the Shangdong area. By contrast, higher $\delta^{18}O$ values in the calcite deposited during the late Holocene indicate that rainfall was less intense and climate was drier due to the weaker Asian

monsoon. The abrupt increase in stalagmite $\delta^{18}O$ values (~1.2‰) and the equally abrupt decline in $\delta^{13}C$ values (~0.7‰) at 3.6 ka BP probably signal the end of the "Holocene Climatic Optimum" in Southwestern China. After this transition, the climate in Northern China was drier while areas in Southern China became somewhat wetter. This study suggests that variations in precipitation during the Holocene, caused by changes in monsoon strength, were not consistent across all of China; rather there were significant spatial variations in precipitation that were not always in the same direction.

References

Al-Aasm, I. S., Taylor, B. E. and South, B., 1990. Stable isotope analysis of multiple carbonate samples using selective acid extraction. *Chemical Geology* 80, 119–125.

An, C.-B., Feng, Z.-D. and Barton, L., 2006. Dry or humid? Mid-Holocene humidity changes in arid and semi-arid China. *Quaternary Science Reviews* 25, 351-361.

An, Z. S., Wu, X. H., Wang, P. X., Wang, S. M., Dong, G. R., Sun, X. J., Zhang, D. E., Lu, Y. C., Zheng, S. H. and Zhao, S. L., 1991. Changes in the monsoon and associated environmental changes in China since the last interglacial. In: Liu, T.S. (Ed.), Loess, Environment and Global Change. Science Press, Beijing, pp. 1–29.

An, Z., 2000. The history and variability of the East Asian monsoon climate. *Quaternary Science Reviews* 19, 171-187.

Baker, A., Ito, E., Smart, P. L. and McEwan, R. F., 1997. Elevated and variable values of ^{13}C in speleothems in a British cave system. *Chemical Geology* 136(3), 263-270.

Baker, A., Mockler, N. J. and Barnes, W. L., 1999. Fluorescence intensity variations of speleothem forming groundwaters: Implications for palaeoclimate reconstruction. *Water Resources Research* 35, 407-413.

Brook, G. A., Ellwood, B. B., Railsback, L. B. and Cowart, J. B. 2006. A 164 ka record of environmental change in the American Southwest from a Carlsbad Cavern speleothem. *Palaeogeography, Palaeoclimatology, Palaeoecology* 237, 483-507.

Cai, Y., Zhang, M., Peng, Z. C., Lin, Y. S., An, Z. S., Zhang, Z. F. and Cao, Y. N., 2001. The $\delta^{18}O$ variation of a stalagmite from Qixing Cave, Guizhou province and indicated climate change during the Holocene. *Chinese Science Bulletin*. 46, 1904-1908.

Domrös, M., and Peng, G. B., 1988. Climate of China. Berlin: Springer-Verlag. 360pp.

Dykoski, C. A., Edwards, R. L., Cheng, H., Yuan, D., Cai, Y., Zhang, M., Lin, Y., Qing, J., An, Z. and Revenaugh, J., 2005. A high-resolution, absolute-dated Holocene and deglacial Asian monsoon record from Dongge Cave, China. *Earth and Planetary Science Letters* 233, 71-86.

Fleitmann, D., Bruns, S. J., Mudelsee, M., Neff, U., Kramers, J., Mangini, A. and Matter, A., 2003. Holocene forcing of the Indian monsoon recorded in a stalagmite from southern Oman. *Science* 300, 1737-1739.

Friedman, I. and O'Neil, J.R., 1977. Compilation of stable isotope fractionation factors of geochemical interest: U.S. Geological Survey, Professional Paper 440-KK, p. 1–12.

Gascoyne, M., 1992. Paleoclimate determination from cave calcite deposits. *Quaternary Science Reviews* 11, 609–632.

Genty, D. and Quinif, Y., 1996. Annually laminated sequences in the internal structure of some Belgian stalagmites; importance for paleoclimatology. *Journal of Sedimentary Research* 66(1): 275-288.

Harmon, R. S., Schwarcz, H. P., and Ford, D. C., 1978. Stable isotope geochemistry of speleothems and cave waters from the Flint Ridge-Mammoth Cave system, Kentucky: Implications for terrestrial change during the period 230,000 to 100,000 years B.P. *Journal of Geology* 86, 373-384.

Hendy, C. H., 1971. The isotopic geochemistry of speleothems, 1. The calculation of the effects of different modes of formation on the isotopic composition of speleothems and their applicability as paleoclimatic indicators. *Geochimica et Cosmochimica Acta* 35, 801-824.

Huang, C. C., Zhou, J., Pang, J. L., Han, Y. and Hou, C., 2000. A regional aridity phase and its possible cultural impact during the Holocene Megathermal in the Guanzhong Basin, China. *The Holocene* 10,135-142.

Johnson, K. R. and Ingram, B. L., 2004. Spatial and temporal variability in the stable isotope systematics of modern precipitation in China: implications for paleoclimate reconstructions. *Earth and Planetary Science Letters* 220 (3-4), 365–377.

Lauritzen, S.-E., Ford D. C. and Schwarz, H. P., 1986. Humic substances in speleothems matrix-paleoclimate significance. Proceedings of the 9th International Congress of Speleology. 2, 77-79, Barcelona, August, 1986.

Lauritzen, S.-E., and Lundberg, J., 1999. Speleothems and climate: a special issue of The Holocene. *The Holocene* 9(6), 643-647.

Lawrence, J. R. and Gedzelman, S. D., 1996. Low stable isotope ratios of tropical cyclone rains. *Geophysical Research Letters* 23, 527-530.

Li, X. Q., Zhou, W. J., An, Z. S. and John, D., 2003. The vegetation and monsoon variations at the desert-loess transition belt at Midiwan in northern China for the last 13 ka. *The Holocene* 13, 779-784.

Mattey, D., Lowry, D., Duffet, J., Fisher, R., Hodge, E. and Frisia, S., 2008. A 53 year seasonally resolved oxygen and carbon isotope record from a modern Gibraltar speleothem: Reconstructed drip water and relationship to local precipitation. *Earth and Planetary Science Letters* 269, 80-95.

McCrea, J. M., 1950. On the isotopic chemistry of carbonates and a paleotemperature scale. *Journal of Chemical Physics* 18, 849-857.

McDermott, F., 2004. Palaeo-climate reconstruction from stable isotope variations in speleothems: a review. *Quaternary Science Reviews* 23, 901-918.

Ohsawa, S., and Yusa, Y., 2000. Isotopic characteristics of typonic rainwater: typhoons no. 13 (1993) and no. 6 (1996). *Limnology* 1, 143-149.

Quade, J., 2004. Isotopic records from ground-water and cave speleothem calcite in North America, In: A. Gillespie, S. C. Porter, and B. F. Atwater, eds., Developments in Quaternary Science, v. 1, p. 205-219.

Ramsey C. B., 1995. Radiocarbon Calibration and Analysis of Stratigraphy: The OxCal Program. *Radiocarbon* 37(2): 425-430.

Ramsey C. B., 2001. Development of the Radiocarbon Program OxCal. *Radiocarbon* 43 (2A): 355-363.

Ramseyer, K., Miano, T., D'Orazio, V., Wildberger, A., Wagner, T. and Geister, J. 1997. Nature and origin of organic matter in carbonates from speleothems, marine cements and coral skeletons. *Organic Geochemistry* 26, 361–378.

Schwarcz, H. P., Harmon, R. S., Thompson, P. and Ford, D. C., 1976. Stable isotope studies of fluid inclusions in speleothems and their paleoclimatic significance. *Geochimica et Cosmochimica Acta* 40, 657-665.

Shi, Y. F. and Zhu, Q. G., 1996. An abrupt change in the intensity of the East Asian summer monsoon index and its relationship with temperature and precipitation over east China. International *Journal of Climatology* 16, 757-764.

Shopov, Y. Y., Ford, D. C. and Schwarcz, H. P., 1994. Luminescent microbanding in speleothems: high-resolution chronology and paleoclimate. *Geology* 22, 407-410.

Stuiver, M., Reimer, P. J. and Bard, E., 1998. INTCAL98 radiocarbon age calibration, 24,000–0 cal BP. *Radiocarbon* 40, 1043-1081.

Tan, M., Baker, A., Genty, D., Smith, C., Esper, J. and Cai, B., 2006. Applications of stalagmite laminae to paleoclimate reconstructions: Comparison with dendrochronology/climatology. *Quaternary Science Reviews* 25, 2103-2117.

Tao, S. Y. and Chen, L. X., 1987. A review of recent research on the East Asian summer monsoon in China. In Monsoon Meteorology, ed. C.P. Chang and T.N. Krishnamurti, 60-92. New York: Oxford University Press.

Wang, P. X., Clemens, S., Beaufort, L., Braconnot, P., Ganssen, G., Jian, Z. M., Kershaw, P. and Sarnthein, M., 2005a. Evolution and variability of the Asian monsoon system: state of the art and outstanding issues. *Quaternary Sciences Reviews* 24, 595-629.

Wang, S. M., 1992. Lake records of the Holocene climatic changes in China. In: Shi, Y. F. (Ed.), The Holocene Climatic Optimum and Associated Environment in China. Science Press, Beijing, pp.146–152 (in Chinese).

Wang, S. W., Zhao, Z. C. and Chen, Z. H., 1981. Reconstruction of the summer regime for the last 500 years in China. *Geojournal* 5, 117-122.

Wang, S., Gong, D. and Zhu, J., 2001. Twentieth-century climatic warming in China in the in the context of the Holocene. *The Holocene* 11, 313-321.

Wang, Y. J., Cheng, H., Edwards, R. L., He, Y. Q., Kong, X.G., An, Z. S., Wu, J. Y., Kelly, M. J., Dykoski, C. A. and Li, X. D., 2005b. The Holocene Asian Monsoon: links to solar changes and North Atlantic climate. *Science* 308, 854-857.

Wu, W. and Liu, T., 2004. Possible role of the "Holocene Event 3" on the collapse of Neolithic Cultures around the Central Plain of China. *Quaternary International* 117, 153-166.

Xiao, H. L., Brook, G. A., Railsback, L. B., Alexander, C., Edwards, R. L., Cheng, H., Wang, X. F., Liebig, C. M. and Dennis, W., (manuscript in prep.). Asian monsoon activity during the Holocene: stalagmite evidence from Yangzhipo Cave, Guizhou Province, Southern China.

Yonge, C. J., Ford, D. C., Gray, J. P. and Schwarcz, H. P., 1985. Stable isotope studies of cave seepage water. *Chemical Geology (Isotope Geoscience Section)* 58, 97-105.

Yuan, D. X., Cheng, H., Edwards, R. L., Dykoski, C. A., Kelly, M. J., Zhang, M .L., Qin, J. M., Lin, Y. S., Wang, Y. J., Wu, J. Y., Dorale, J. A., An, Z. S. and Cai, Y. J., 2004. Timing, Duration, and Transitions of the last interglacial Asian monsoon. *Science* 304, 575-578.

Zhang, M. L., Yuan, D. X., Lin, Y. S., Qin, J. M., Li, B., Cheng, H. and Edwards, R. L., 2004a. A 6000-year high-resolution climatic record from a stalagmite in Xiangshui Cave, Guilin, China. *The Holocene* 14, 697-702.

Zhang, Q., Zhu, C., Liu, C. L., and Jiang, T., 2005. Environmental change and its impacts on human settlement in the Yangtze Delta, P.R. China. *Catena* 60, 267-277.

Zhang, X. P., Liu, J. M, Tian, L. D., He, Y. Q. and Yao, T. D., 2004b. Variations of $\delta^{18}O$ in precipitation along vapor transport path. *Advances in Atmospheric Sciences* 21(4), 562-572.

Zhou, W. J., Yu, X. F., Timothy Jull, A. J., Burr, G., Xiao, J. Y., Lu, X. F. and Xian, F., 2004. High-resolution evidence from southern China of an early Holocene optimum and a mid-Holocene dry event during the past 18,000 years. *Quaternary Research* 62, 39-48.

CHAPTER 4

STALAGMITE EVIDENCE FROM PANIGARH CAVE OF A WETTER LITTLE ICE AGE IN THE HIMALAYAN FOOTHILLS OF INDIA *

*Fuyuan Liang, George A. Brook, Bahadur Kotlia, L. Bruce Railsback, to be submitted to *Quaternary International*

Abstract

Variations in petrography, stable isotopes, gray color, and luminescence along the central growth axis of a 14.5 cm stalagmite from Panigarh Cave that was active when collected, provide a high resolution record of paleoenvironmental change for the Himalayan foothills of Northern India for the past 750 years. Deposition of calcite from AD 1480 to 1900 suggests a wetter and cooler Little Ice Age (LIA), while precipitation of aragonite during the periods from AD 1250 to 1480 and after AD 1900 indicates drier and warmer conditions at these times. Stalagmite $\delta^{18}O$ values from AD 1250 to 1780 show that the strength of the Indian summer monsoon varied only slightly in this period. However, large-amplitude variations in stalagmite $\delta^{18}O$ point to a variable monsoon climate after AD 1780, with two distinct periods of weak monsoon activity centered on AD 1800 and 1920. These periods are defined by significantly higher $\delta^{18}O$ values. Variations in stalagmite color and luminescence correlate well with estimates of changes in northern hemisphere temperature over the past 1000 years, with lighter colors and stronger luminescence corresponding with higher temperatures, and darker colors and reduced luminescence with lower temperatures.

Key words: Little Ice Age, Stalagmite, Isotopes, Petrography, Northern India, Asian Monsoon

Introduction

The instrumental record of global average temperature indicates that the last decade of the twentieth century was the warmest period of the last 150 years (Brohan et al., 2006). Reconstructions of Northern Hemisphere temperature have allowed the magnitude of this warming to be evaluated over the past millennium (Mann, 1999; Jones, et al., 1998; Crowley and Lowery, 2000). An important episode of cooling during the last 1000 years was the Little Ice Age (LIA), which is believed to have impacted both the northern and southern hemispheres, but probably not in a globally synchronous way (Grove, 1988). There is also considerable uncertainty about the climatic characteristics and the timing of this episode in different areas (Bradley, 1992; Bradley and Jones, 1993).

As it was during other cold intervals of the Holocene, the Indian summer monsoon may have been weaker during the LIA (Gupta et al., 2003; Anderson et al., 2002) and intuitively one might think a weaker monsoon would bring less precipitation to the Asian mainland. However, the data are ambiguous with much recent evidence suggesting wetter conditions during at least certain episodes of the LIA in Nepal (Denniston et al., 2002), Northern India (Rühland et al., 2006), and Southern China (Chu et al., 2002; Chen et al., 2005). However, no high-magnitude flood deposits have been identified in the six large rivers crossing central and western India suggesting that there was no really intense precipitation at this time and in fact that conditions were probably drier from the 14^{th} to 19^{th} centuries (Vishwas et al., 2006). Given such ambiguous data on conditions during the LIA, it is clear that more information is needed to clarify the

situation. In this paper we present evidence from a stalagmite (PGH-1) from Panigarh Cave in Northern India, located in the southern foothills of the Himalayas. The stalagmite was active when collected and preserves evidence of variations in the Indian monsoon during the past 750 years, including the period of the LIA. Multi-proxy data from the stalagmite, including variations in stable isotopes, gray-scale color, luminescence, and petrography, indicate a wetter and cooler LIA in this area.

Panigarh Cave

An active, 14.5cm long stalagmite (PGH-1) was collected from Panigarh Cave (29°33′10″N; 80° 07′31″E; 1520 m amsl), which is located 300 km northeast of New Delhi and 20 km west of the western boundary of Nepal (Fig. 4.1). Panigarh Cave is only 4 m long and has a small entrance. The PGH-1 stalagmite was collected from an extremely small chamber within this cave with an entrance measuring only 20x20 cm. The cave is developed in Precambrian Thalkedar Limestone extending about 250 m above the cave. The limestone over the cave is mantled by a brownish black soil about 80 cm thick. The vegetation in the area is largely C_3 being composed predominantly of *Pinus roxburghii* with small shrubs, grasses and herbs. The climate is subtropical monsoon with a wetter and warmer summer and a drier and cooler winter. Annual precipitation is 1260 mm with about 80% of the precipitation falling during the monsoon season from May to September.

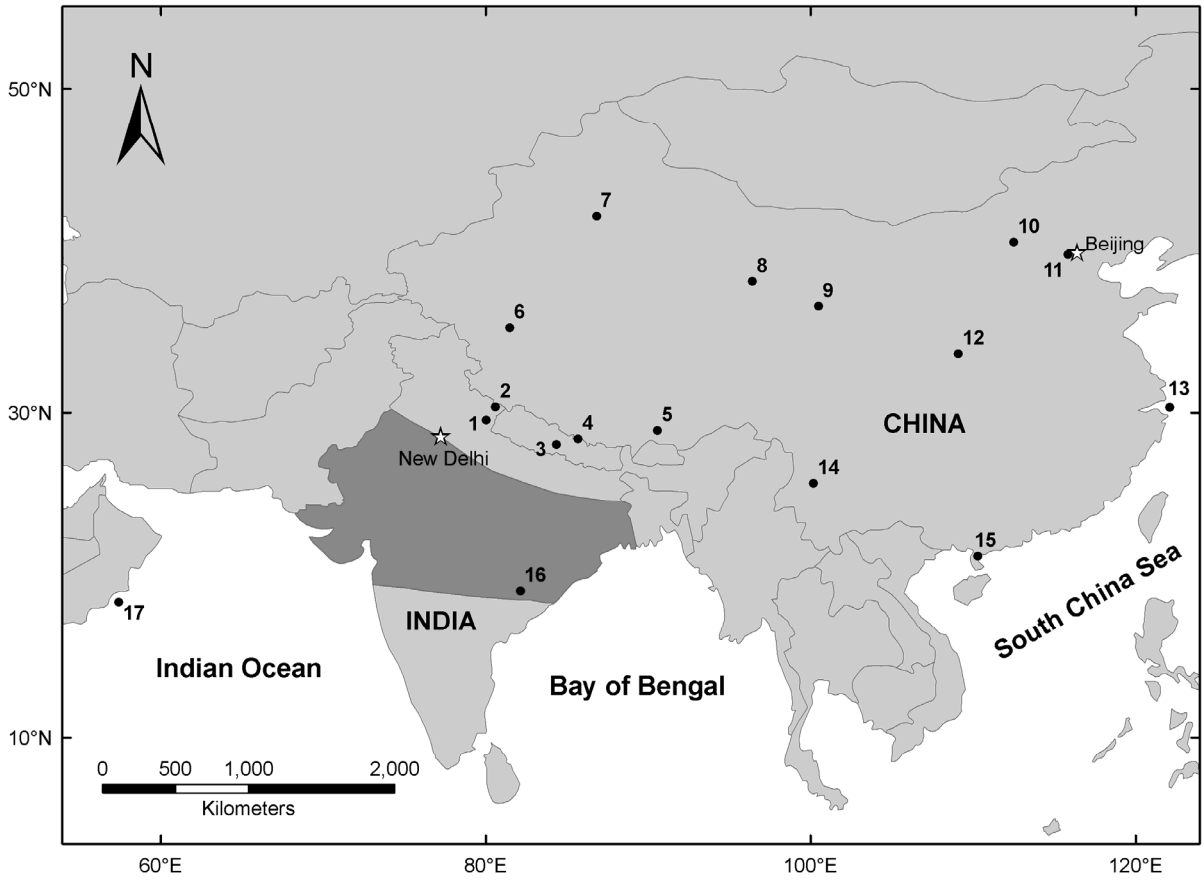

Figure 4.1. Map showing the location of Panigarh Cave and other sites discussed in the text. Dark gray shaded region shows the core monsoon zone of India. 1) Panigarh Cave (this study); 2) Pinder Valley (Rühland et al., 2006); 3) Siddha Baba Cave (Denniston et al., 2000); 4) Dasuopu ice cap (Thompson et al., 2001); 5) Chencuo (Yang et al., 2004); 6) Guliya ice cap (Yao et al., 1996); 7) Lake Bosten (Chen et al., 2006); 8) Dunde ice cap (Liu et al., 1998); 9) Lake Qinghai (Zhang et al., 2004); 10) Lake Daihai (Jin et al., 2001); 11) Sihua Cave (Ku and Li, 1998); 12) Buddha Cave (Paulsen et al., 2003); 13) Changjiang prodelta (Yi et al., 2006); 14) Lake Erhai (Chen et al., 2005); 15) Lake Huguanyan (Chu et al., 2002); 16) Dandak Cave (Sinha et al., 2007; Yadava and Ramesh, 2005); 17) Marine core RC2735 (Anderson et al., 2002).

Methods

The PGH-1 stalagmite was cut along the central growth axis and after polishing, one of the exposed surfaces was scanned on a standard flatbed scanner at 300 dpi spatial resolution and 8 bit (256 increments) gray level resolution. It was then illuminated by long-wave ultraviolet light (320 to 420 nm) from two Macken Instruments Model 22-UV lamps in a darkroom. Luminescence from the stalagmite was recorded by a Nikon D-70, 6-megapixel digital camera fitted with a Kodak Wratten Gelatin Filter #2E to prevent transmission of the UV excitation energy band. Variations in gray-scale color and luminescence were measured along a 10-pixel-wide traverse down the central growth axis of the stalagmite using image analysis software. Gray-level (0=black; 255=white) and luminescence (0=black; 255=white) values have a spatial resolution of 0.07 mm (i.e., ~0.6 year per dot).

Three large (51mm x 76 mm) thin sections were prepared from the other half of the stalagmite for petrographic study. In addition, five samples of ~100 mg were drilled at 0.6, 2.5, 7.0, 11.0, and 14.0 from the top of the stalagmite for ICP-MS U-series dating following procedures outlined in Cheng et al., (2000), Edwards et al., (1987), and Shen et al., (2002). Ages were calculated using half-lives listed in Cheng et al., (2000) and are reported with 2σ analytical errors. Finally, 30 samples of ~150 ±50 μg were drilled using a carbide dental burr at 0.5cm intervals along the central growth axis for $\delta^{13}C$ and $\delta^{18}O$ analysis. Another five samples were taken along a growth layer at 8.5 cm to test whether deposition of the stalagmite carbonate was in isotopic equilibrium with precipitating waters following criteria outlined by Hendy (1971).

Carbonate samples were processed at the Savannah River Ecology Laboratory, University of Georgia following procedures outlined in Jimenez-Lopez and Romanek (2004). Carbonate powders were loaded into 10 ml vacutainers^{TM} and flushed with helium gas. Concentrated phosphoric acid was injected into the vacutainers^{TM} to dissolve carbonate and samples were left to react overnight. Stable isotope measurements were performed on a Finnigan DeltaplusXL isotope ratio mass spectrometer operated in continuous flow mode (CF-IRMS) using a Gasbench II peripheral device. Replicates were run for every tenth sample and standards were run for every five samples. Analytical precision (1σ) was ± 0.14‰ for $\delta^{13}C$ and ± 0.23‰ for $\delta^{18}O$, respectively, based on the repeated measurement of the NBS-19 standard. All isotope measurements are reported in ‰ units versus the V-PDB standard using conventional delta (δ) notation (Craig, 1957).

Chronology

The 5 ICP-MS U-series ages for the PGH-1 stalagmite are all in stratigraphic order and range from 9 ±34 yr BP at 0.6cm to 725 ±29 yr BP at 14 cm from the top of the stalagmite (Table 4.1; Fig. 4.2). A chronology for the stalagmite was constructed through linear interpolation between ages at 0, 2.5, 7.0, 11.0, and 14.0 cm from the top of the stalagmite. The age of the top layer of the stalagmite was assumed to be AD 2005 as the stalagmite was active when collected. The age of 9 ±34 years for carbonate at 0.6 cm strongly suggests that the stalagmite was active in 2005 as we observed. This age was not used in developing a chronology for the stalagmite due to

Table 4.1. ICP-MS uranium-series age data for the PGH-1 stalagmite

Sample ID	Depth (cm)	^{238}U ppb	^{232}Th ppt	$d^{234}U$ measured[a]	$[^{230}Th/^{238}U]$ activity[c]	$[^{230}Th/^{232}Th]$ ppm[d]	Age uncorrected	Age corrected [c,e]	$d^{234}U_{initial}$ corrected
HMS-1	0.5	3214.5±150.8	13421.7±630.7	1528.2±3.8	0.00131±0.00009	5.2±0.4	57±4	9±34	1528.2±3.8
HMS-2	2.5	3510.0±5.3	4027.4±12.4	1614.3±3.3	0.00241±0.00007	34.7±1.0	101±3	88±7	1614.7±3.3
HMS-3	7	284.3±13.3	2893.1±134.8	1521.8±16.6	0.01072±0.00088	17.4±1.4	465±38	348±91	1523.3±16.6
HMS-4	11	2513.1±3.6	2815.6±10.3	1598.1±3.4	0.01407±0.00017	206.9±2.6	591±7	579±10	1600.7±3.4
HMS-5	14	3319.3±185.8	11232.6±630.6	1685.2±4.6	0.01868±0.00030	91.1±1.5	762±12	725±29	1688.7±4.7

Analytical errors are 2 of the mean. Decay constants are 9.1577 x 10^{-6} yr^{-1} for ^{230}Th, 2.8263 x 10^{-6} yr^{-1} for ^{234}U, and 1.55125 x 10^{-10} yr^{-1} for ^{238}U (Cheng et al., 2000). [a] The degree of detrital ^{230}Th contamination is indicated by the $[^{230}Th/^{232}Th]$ atomic ratio instead of the activity ratio. [b]Age corrections were calculated using an average crustal $^{230}Th/^{232}Th$ atomic ratio of 4.4 x 10^{-6} ± 2.2 x 10^{-6}. Those are the values for a material at secular equilibrium, with the crustal $^{232}Th/^{238}U$ value of 3.8. The errors are arbitrarily assumed to be 50%.

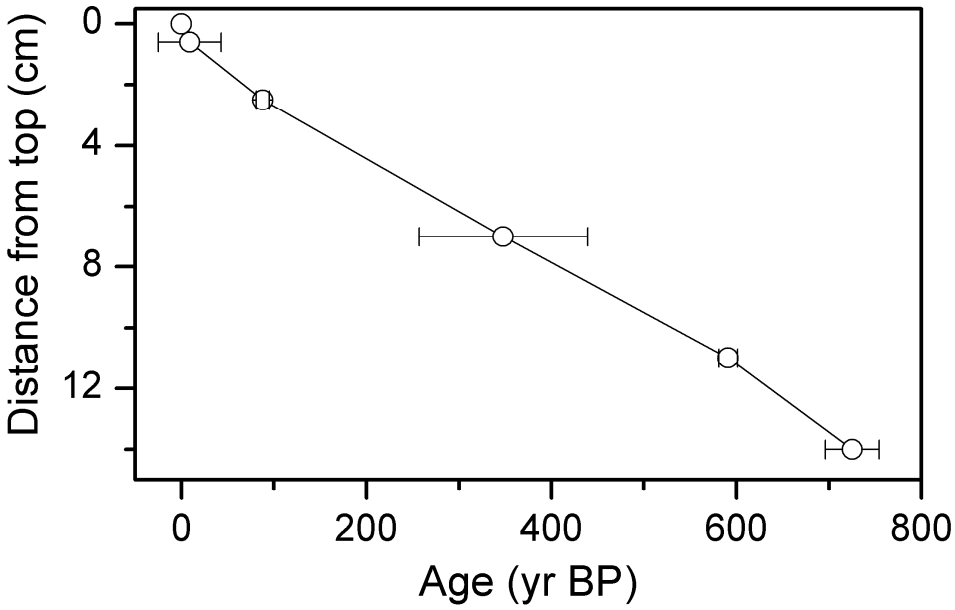

Figure 4.2. ICPMS U-series age data for the PGH-1 stalagmite in relation to distance from the top of the deposit. The age at the top of the stalagmite (depth = 0 cm) is assumed to be AD 2005 as the stalagmite was active when collected.

the relatively large uncertainty associated with it. Based on the interpolation process, 25 years was added to the oldest age obtained to account for the undated basal 0.5 cm of the stalagmite. The chronology developed indicates that stalagmite PGH-1 grew continuously over the last 750 years. During this period the growth rate varied from 0.22 mm/yr from 14.5 to 11.0 cm, 0.17 mm/yr from 11.0 to 2.5 cm, and 0.29 mm/yr from 2.5 cm to the top of the stalagmite. These variations suggest relatively slower vertical growth from AD 1400 to 1910, the approximate period of the Little Ice Age.

Petrography

The upper 3.3 cm and the basal 4.8 cm of the PGH-1 stalagmite consist entirely of aragonite, while the middle section from 9.7-3.3 cm is dominated by calcite containing several bands of aragonite (Fig. 4.3A). There is no evidence of recrystallization or of hiatuses in deposition. The basal 4.8 cm consists entirely of elongate bundles of aragonite needles. The interval from 14.5 to 13.0 cm is dominated by frothy or spongy aragonite with pores separating aragonite needle bundles. At about 13 cm from the top of the stalagmite, porous aragonite gives way upwards to dense aragonite with few voids. Banded aragonite (probably annual layers) characterizes the interval from 13-9.7 cm with typical crystals of aragonite up to 1.5 mm long and 0.8 mm wide.

The middle section of the stalagmite from 9.7-3.3 cm from the top of the stalagmite is dominated by porous calcite consisting of near-vertical columnar crystals up to 0.75 mm wide and as much as 2.2 mm long. Calcite crystals are separated by pores and porosity reaches as high as 40% in the intervals 8.4-7.4 cm and 3.3-3 cm, while calcite at 9.7-8.4 cm and 7.4-3.3 cm is much denser with porosity less than 10%. In addition to calcite, there are at least 16 aragonite layers in this interval that vary in width from 0.2 to 2 mm. These aragonite layers are thinner and

usually discontinuous near the central growth axis and become thicker and more continuous outward. In the interval 5.75-6 cm from top of the stalagmite, there are four distinct layers that contain gray, very fine non-carbonate detrital material; these become thicker and more distinct away from the central growth axis.

In the middle section of the PGH-1 stalagmite, carbonate near the central growth axis has a different mineralogy and density compared to carbonate on the stalagmite flanks in the same layer. As mentioned previously, porous calcite is typical near the central growth axis. However, from 9.5-5.8 cm, dense calcite with porosity less than 10% was deposited on the stalagmite flanks suggesting that increased evaporation favors deposition of dense calcite. In the interval from 5.8-3.5 cm there is a change from porous calcite along the stalagmite axis to dense aragonite indicating that increased evaporation favors aragonite (Mills, 1965). Thus a change from porous calcite to dense calcite or dense aragonite is probably evidence of a slow change from wetter to much drier conditions with increased evaporation.

The upper 3.3 cm of the stalagmite is mainly aragonite, with crystals up to 0.45 mm wide and 0.50 mm long. Dense aragonite dominates this part of stalagmite, except the intervals from 3.0-3.25 cm and from 1.5-1.6 cm, which consist mainly of porous aragonite needles. Two cavities at 0.9-1.1 cm and 0.20-0.25 cm from the top of the stalagmite document extremely dry conditions as evidenced by discontinuous deposition. There are four continuous detrital layers in the interval 2.85-3.05 cm and in the top 0.2 cm of the stalagmite that may record significant climate events. Detrital grains are up to 0.15 mm (find sand) in diameter showing that they were transported into the cave by water.

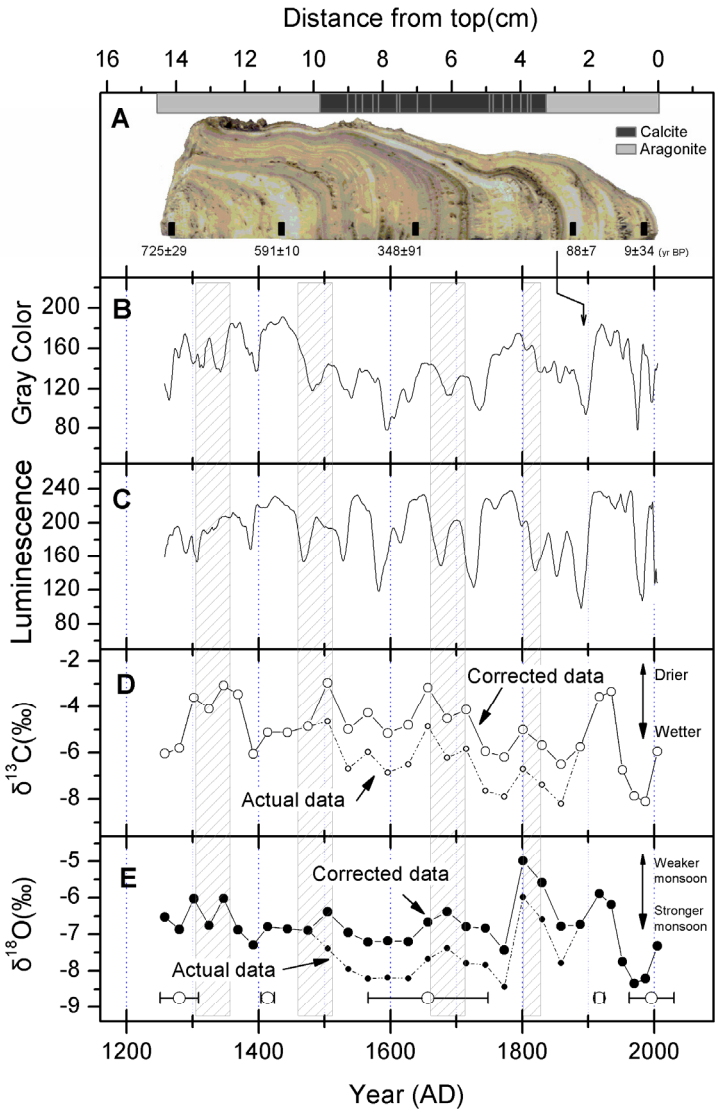

Figure 4.3. Characteristics of the PGH-1 stalagmite. (A) scanned image of internal structure and petrographic variations. (B), (C), (D), and (E) show variations in gray-scale color, luminescence intensity, $\delta^{13}C$ and $\delta^{18}O$ along the central growth axis of the stalagmite. The four shaded vertical bars show from left to right the Wolf, Spörer, Maunder, and Dalton periods of sunspot minima, respectively.

Calcite is frequently associated with wetter conditions and low evaporation and aragonite with drier conditions and higher evaporation (Siegel and Dort, 1966; Murray, 1954; Thrailkill, 1971; Reams, 1972; Cabrol and Coudray, 1982; Railsback et al., 1994). Precipitation of calcite near the growth axis of a stalagmite and aragonite on the flanks also suggests that aragonite forms when the water film thins and evaporation increases. Deposition of porous aragonite is commonly attributed to extensive evaporation and rapid growth (Hill and Forti, 1997). The presence of large cavities probably indicates much drier conditions due to a significant reduction in the volume of carbonate being precipitated. In summary, we believe that aragonite in the PGH-1 stalagmite was deposited under drier and warmer conditions while calcite was precipitated under wetter and cooler conditions.

Color and Luminescence

Luminescence along the central growth axis of the PGH-1 stalagmite ranges from 110 to 230 with higher values indicating stronger luminescence (Fig. 4.3C). There is no long-term trend in luminescence although frothy aragonite at 14.5-13.0 cm has lower luminescence than less porous calcite or compact aragonite in the upper 13 cm of PGH-1. Where detrital material with low luminescence is present, overall luminescence drops (van Beynen et al., 2001). Luminescence is also lower when pores and cavities are present in the carbonate.

Stronger luminescence can result from an increase in organic acids within the carbonate or in fluid inclusions (Lauritzen, 1986; Shopov et al., 1994; Ramseyer et al., 1997), either in the form of humic or fulvic acids (van Beynen et al., 2001). These organic acids are produced in the soil by plants and are then transported into the cave by percolating waters and may eventually become sealed in fluid inclusions in stalagmite carbonate. Increased plant activity at the surface

(usually under warmer and wetter conditions) produces more organic acids that can be transported into the cave. Under a warmer climate, humic acids are broken down by bacteria in the soil to form fulvic acids (Lauritzen, 1986; Shopov et al., 1994). Thus, increased luminescence, particularly associated by lighter colors, indicating the presence of fulvic acids that are colorless, suggests a warmer/wetter climate, while lower luminescence coupled with darker colors indicates a cooler/drier climate. Drier conditions limit plant growth and hence the production of organic acids. That is why spongy aragonite deposited at 14.5-13.0 cm has relatively low luminescence and the upper 1 cm of the stalagmite, containing cavities, has extremely low luminescence. Therefore, we assume that increased luminescence of the PGH-1 stalagmite carbonate is a proxy for warmer/wetter conditions while lower luminescence indicates cooler/drier conditions.

Reflective color of the PGH-1 stalagmite varies considerably. Generally, aragonite in the basal 4.8 cm and upper 3.3 cm has higher values (brighter in color) and calcite in the central section of the deposit at 9.7-3.3 cm is slightly darker in color (Fig. 4.3B). Superimposed on this broad pattern are high-frequency variations, with more-porous calcite/aragonite being darker, and more compact calcite/aragonite appearing lighter in color. Layers with detrital material are much darker while clean aragonite and calcite are much whiter. In addition, high-frequency fluctuations in luminescence and color along the central growth axis of PGH-1 stalagmite broadly parallel one another.

Stable Isotopes

Along the central growth axis $\delta^{18}O$ and $\delta^{13}C$ values range from −8.4‰ to −5.9‰ (PDB) and −8.2‰ to −3.1‰ (PDB) respectively (Fig. 4.3D, E). $\delta^{18}O$ and $\delta^{13}C$ values decrease steadily

upward through the stalagmite, but there are significant fluctuations in $\delta^{18}O$ in the upper 5 cm and in $\delta^{13}C$ in the top 3.5 cm. The transition to large-amplitude fluctuations in $\delta^{13}C$ coincides with a shift from calcite to aragonite, both possibly being associated with a significant climate shift. Aragonite is enriched in ^{13}C by 1.7‰ (Romanek et al., 1992) and ^{18}O (Grossman and Ku, 1986) by 1.0 ‰ compared to calcite when deposited from water with same $\delta^{18}O$ and $\delta^{13}C$ values. As the PGH-1 stalagmite consists of both calcite and aragonite, $\delta^{18}O$ and $\delta^{13}C$ values for aragonite were corrected to equivalent calcite values. After corrections were made the trend towards lower $\delta^{18}O$ values towards the top of the stalagmite is less pronounced, but still evident (Fig. 4.3D, E).

Stable isotope values along a single growth layer at 8.5 cm from the top of the stalagmite vary significantly, with a range from -7.6‰ to -8.9‰ (PDB) in $\delta^{18}O$ and from -4.7‰ to -7.3‰ (PDB) in $\delta^{13}C$ (Fig. 4.4A). Samples were drilled at 0.5 cm intervals up to 3 cm from the axis of growth. Significant variations in $\delta^{18}O$ over 3 cm along the growth layer suggest that deposition was not in isotopic equilibrium with precipitating waters, a conclusion supported by the strong relationship (R^2=0.99) between $\delta^{18}O$ and $\delta^{13}C$ along the growth layer (Fig. 4.4B). This implies that kinetic effects must have influenced the final isotopic composition of the stalagmite (Hendy, 1971). In general, when stalagmite carbonate is deposited under the influence of evaporation and rapid degassing of CO_2, $\delta^{18}O$ and $\delta^{13}C$ values tend to be enriched in heavy isotopes compared to those deposited under isotopic equilibrium conditions, and more so under increasingly evaporative conditions (Hendy, 1971).

The $\delta^{18}O$ of stalagmite carbonate is also influenced by temperature and the $\delta^{18}O$ of the precipitating water. Under warmer conditions, $\delta^{18}O$ values decrease by -0.23‰ per $^{\circ}C$ (Friedman and O′Neil, 1977). However, it is difficult to explain the large variations in O and C isotopes in

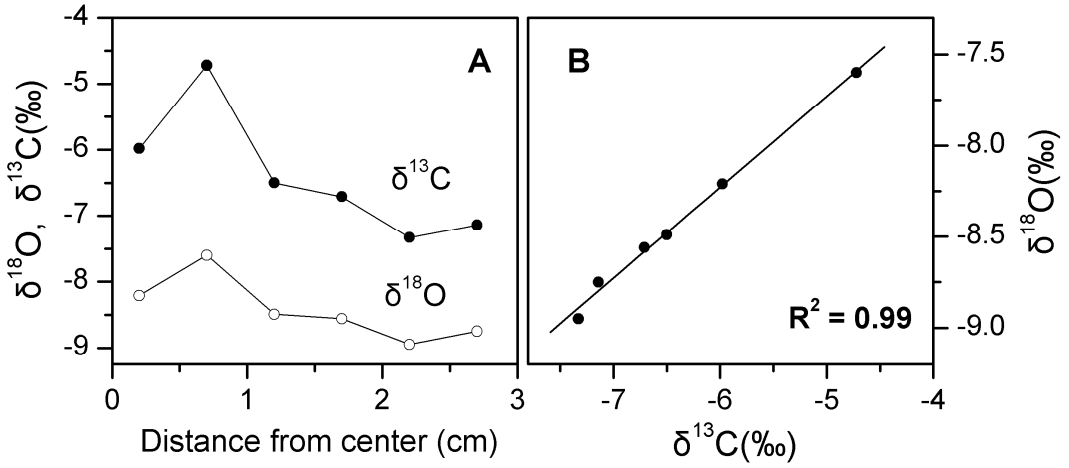

Figure 4.4. Variations in $\delta^{18}O$ and $\delta^{13}C$ values along a growth layer 8.5cm from top of the stalagmite. (A) variations in $\delta^{13}C$ and $\delta^{18}O$ with distance from the center of the stalagmite; (B) positive correlation between $\delta^{13}C$ and $\delta^{18}O$ along the layer.

the Panigarh stalagmite during the last several hundred years by variations in temperature as temperature of the Northern Hemisphere varied by less than 1°C over this time interval (Mann et al., 1999). The $\delta^{18}O$ of cave dripwaters approximates the monthly average value of meteoric rainfall (Harmon, 1979; Yonge et al., 1985), but the value can be affected by evaporation before reaching the cave and higher temperatures make this more likely. However, there is no significant relationship between mean monthly temperature and monthly weighted mean $\delta^{18}O$ of precipitation at New Delhi located ~300 km southwest of Panigarh Cave (Fig. 4.5A). By contrast, $\delta^{18}O$ is higher in months with lower relative humidity when there may be more evaporation and this signal may be transferred to the stalagmite carbonate (Fig. 4.5B).

The $\delta^{18}O$ of rainfall is also influenced by rainfall amount and this is known as the "amount effect". Forty-four years of $\delta^{18}O$ values for rainfall at New Delhi indicate that precipitation during the monsoon season generally has lower $\delta^{18}O$ (Fig. 4.5C). Long-term variations in monsoonal rainfall (June through September) in the West Utter Peridish area of Northern India during the last 130 years (AD 1870~2000) (Parthasarathy et al., 1995) parallel fluctuations in $\delta^{18}O$ of aragonite deposited during this period, with lower $\delta^{18}O$ values equating with higher monsoon rainfall and presumably lower evaporation due to higher humidities (Fig. 4.6). This is strong evidence that lower $\delta^{18}O$ values for PGH-1 are a proxy for increased monsoonal rainfall, while higher values indicate less rainfall.

In fact, the rainfall amount effect acts in the same direction on the $\delta^{18}O$ of stalagmite carbonate as kinetic fractionation, both leading to lower $\delta^{18}O$ values. This is because higher rainfall is associated with lower $\delta^{18}O$ while at the same time higher rainfall leads to higher humidities and reduced evaporation that minimize kinetic fractionation, thus maintaining the low values. During periods of lower rainfall with higher $\delta^{18}O$, humidities are lower and $\delta^{18}O$ values

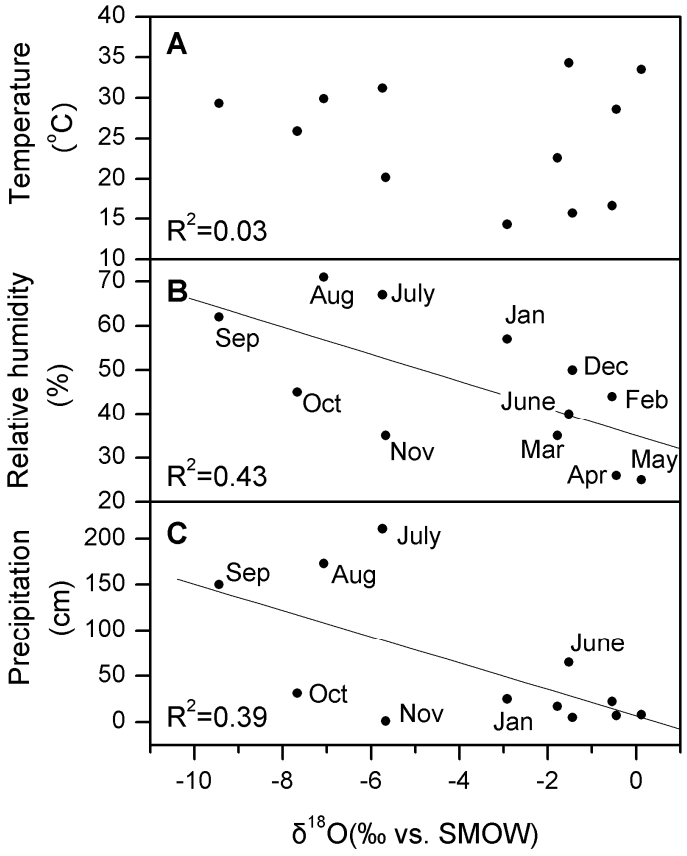

Figure 4.5. Relationship between mean monthly $\delta^{18}O$ of precipitation and temperature (A), relative humidity (B), and precipitation (C) at New Delhi, 300 km southwest of Panigarh Cave.

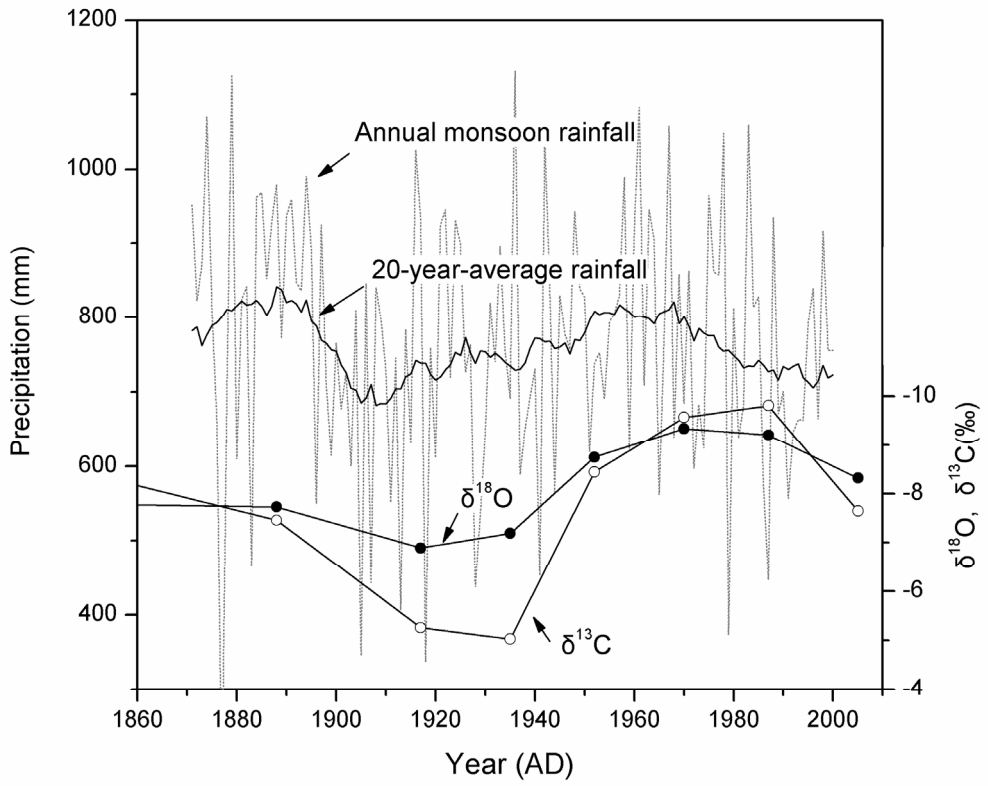

Figure 4.6. Relationship between annual monsoon rainfall in west Utter Peridish during the last 130 years and stalagmite carbonate $\delta^{18}O$ and $\delta^{13}C$ values. Lower isotopic values are clearly associated with increased monsoon precipitation and higher values with reduced precipitation.

are higher as a result of increased evaporation of the rainfall and of water on the stalagmite. Therefore we believe that lower $\delta^{18}O$ values indicate wetter conditions and/or cooler temperatures and higher values suggest a drier and/or warmer climate.

Stalagmite carbonate $\delta^{13}C$ is influenced by the $\delta^{13}C$ of CO_2 in the soil above the cave, the amount of CO_2 available in the soil, hydrological conditions at the time of limestone dissolution, and the degree of kinetic fractionation of carbon isotopes in the precipitating water (Brook et al., 2006; Webster et al., 2007 and references therein). The $\delta^{13}C$ of soil CO_2 is mainly dependent on the vegetation cover above the cave, with lower values where the plant cover is predominantly of the C_3 type and higher values when C_4 plants predominate. At present the vegetation near Panigarh Cave consists mainly of C_3 plants and it is unlikely that the vegetation has changed substantially during the last millennium. However, drier conditions in the past would have enhanced evaporation, restricted plant growth, and reduce the volume of CO_2 in the soil above the cave. Stalagmite carbonate deposited under such conditions would have higher $\delta^{13}C$ values, as more carbon would come from the limestone ($\delta^{13}C$ = 0‰) rather than soil CO_2 ($\delta^{13}C$ of C_3 plants = -27‰) due to the low levels of soil CO_2 and the likelihood that dissolution would be more closed-system than open-system due to limited exchange between carbon dissolved in water from the limestone and carbon in the soil CO_2. By contrast, stalagmite carbonate with lower $\delta^{13}C$ values would be deposited under wetter conditions, as a result of reduced evaporation and a higher volume of CO_2 in the soil. Increased plant activity and higher production of soil CO_2 would lead to an increase in open-system dissolution of the limestone, which would allow more exchange of carbon derived from dissolution of the bedrock with carbon in the soil CO_2. Thus, higher $\delta^{13}C$ values in the PGH-1 stalagmite should indicate drier/warmer conditions, while lower values should point to wetter/cooler conditions in the Panigarh Cave area. This

interpretation is supported by the relationship between long-term variations in monsoon rainfall and $\delta^{13}C$ values of speleothem aragonite during the past 130 years (Fig.4.6), with higher $\delta^{13}C$ corresponding to reduced rainfall in the period centered on AD 1920, while lower $\delta^{13}C$ values correlate with increased monsoonal rainfall in two separate periods centered on AD 1890 and 1970.

The PGH-1 Paleoclimatic Record

Multi-proxy data from the PGH-1 stalagmite provide evidence of environmental changes in Northern India over the past 750 years. Deposition of aragonite from AD 1250 to 1480 and after AD 1900 suggests drier conditions and/or more evaporation due to higher temperatures. Calcite deposition in the period AD 1480 to 1900 indicates a more humid climate and/or reduced evaporation during a cooler LIA. Continuous or discontinuous layers of aragonite in the calcite zone may record brief periods of drier conditions and possibly even droughts.

Climate changes near Panigarh Cave during the last 750 years were mainly due to variations in the strength of the Indian summer monsoon, as recorded by variations in stable isotopes along the central growth axis of the stalagmite. More or less constant $\delta^{18}O$ values for the stalagmite carbonate suggest that the summer monsoon was generally stable before AD 1770. The $\delta^{18}O$ values drop to -5.0‰ at AD 1800, indicating a significantly reduced summer monsoon at this time. A gradual decrease in $\delta^{18}O$ values from AD 1800 to 1970 appears to record an interval when the strength of the Indian summer monsoon increased. However, this period was punctuated by a short interval of weaker monsoon activity around AD 1920. The period after AD 1970 is characterized by a gradual weakening of the Indian summer monsoon, as indicated by a steady increase in stalagmite $\delta^{18}O$ values. In fact, the lowest $\delta^{18}O$ values in the record are

centered on AD 1970 suggesting that this interval witnessed the strongest India summer monsoons of the past 750 years.

Higher $\delta^{13}C$ values when $\delta^{18}O$ values increase suggests that a weaker Indian monsoon brought less precipitation to the Panigarh Cave area. In fact variations in $\delta^{18}O$ and $\delta^{13}C$ along the axis of the PGH-1 stalagmite show five distinct periods of weaker monsoon activity and drier climate during the past 750 years. These are centered on AD 1300, 1500, 1650, 1800, and 1920. Carbonate deposited at these times also has lower luminescence (Fig. 4.3). Four of these five periods correspond with the Wolf, Spörer, Maunder and Dalton periods of minimum sunspot activity indicating that the Indian monsoon weakens at times of low solar irradiance.

Comparison with other Records

The PGH-1 stalagmite provides a valuable record of climate change at the time of the LIA, which saw significant glacier advances in Europe (Lamb, 1977). The LIA was not a world-wide synchronous cold interval, but was actually a period with both warm and cold episodes which occurred at different times across the world (Bradley and Jones, 1995). Hydrological conditions during the LIA also varied geographically. For example, proxy data suggest drier conditions in the northern tropics and wetter conditions in the southern tropics due to the southward shift of the Inter-tropical Convergence Zone (Newton et al., 2006).

Deposition of calcite on the PGH-1 stalagmite during the period from AD 1480 to 1900 suggests that the climate during the LIA was probably colder and wetter in the area near the cave. Cooler episode was documented in tree rings record from AD 1600 to 1950 in western Himalayas (Yadav and Singh, 2002) and from AD 1605 to 1770 in Nepal (Cook et al., 2003).

Although there have been several palynological studies in areas near Panigarh Cave (see Phadtare, 2000; Kar et al., 2002; Chauhan et al., 2000; Rühland et al., 2006), only one study in the Pinder Valley has produced a high-resolution record for the past ~800 years allowing comparison with data from the PGH-1 stalagmite (Rühland et al., 2006). This pollen record documents a change in climate towards cold and moist conditions from ~AD 1540 to 1799, the period of calcite deposition on the PGH-1 stalagmite.

Petrographic studies of a stalagmite from Siddha Baba Cave in Central Nepal indicate that the stalagmite consists of alternating aragonite and calcite layers except in the period from AD1550 to 1640, when dense and clear calcite layers were deposited. On the basis of this, Denniston et al. (2000) argue that central Nepal was generally drier during the last 1500 years, but became wetter during the period when calcite was deposited. This change essentially parallels the evidence from PGH-1 probably indicating a major shift in climate in the foothills of the Himalayas around AD 1500. However, continuous deposition of calcite on PGH-1 until AD 1900 suggests that wetter conditions may have persisted for a longer time near Panigarh Cave than in central Nepal.

A wetter LIA is also documented by paleoclimate proxy data from ice in the Tibetan Plateau. A significant increase in decadally averaged snow accumulation in the Dasuopu Ice Cap from AD 1817 to 1880 suggests high precipitation and thus moist conditions during the later part of the LIA (Thompson et al., 2000), while generally lower snow accumulation from AD 1600 to 1817 and after AD 1880 indicates reduced precipitation. Variations in snow accumulation evident in the Guliya Ice Cap also suggest a moist climate from AD 1500 to 1880 (Yao et al., 1996). Also, high pollen concentrations and relatively low *Artemisia/Chenopodiaceae* ratios in the Dunde Ice Cap, indicate more humid conditions from AD 1400 to present (Liu et al., 1998).

Lake and subaqueous delta sediments in both north and south China also suggest a moist LIA. Reduced salinity indicated by diatoms in Lake Chencuo, southern Tibet, indicates that the last cold episode of the LIA, from AD ~1845-1885, was somewhat wetter (Yang et al., 2004). Lower concentrations of carbonate and coarser particle sizes in Lake Bosten in Xinjiang Province also suggest that the northern Tibet Plateau was humid during from AD 1500 to 1880 (Chen et al. 2006). At Qinghai Lake, the period AD 1500 to 1950 was wetter as suggested by higher organic matter and more negative $\delta^{18}O$ values of $CaCO_3$ in the lake sediment, although this long wetter period was punctuated by two drier episodes from AD 1560 to 1650 and 1780 to 1860 (Zhang et al., 2004). Jin et al. (2001) examined the Rb/Sr ratio, $CaCO_3$ concentration, and magnetic susceptibility of lake sediments in a core from Lake Daihai in Inner Mongolia. They suggest that lower $CaCO_3$ reflects a cold and moist climate during the LIA in north China. In South China, Yi et al., (2006) studied pollen variations in a sediment core (Y8) from the Yangtze prodelta. They argue that the period AD 1085 to 1815 was cool and wet, as suggested by an increase in *Pinus* and an abrupt reduction in *Quercus* and broad-leaved deciduous trees. Principle components analysis on 21 major and minor elements in a lake sediment core from Lake Erhai in Yunnan Province further to the south, suggests a warmer and drier climate from AD 1340 to 1550 and 1890-1950. By contrast, the LIA, from AD 1550 to 1890, was cooler and wetter (Chen et al., 2005). Within dating uncertainty, variations in paleoclimate indicated by the Lake Erhai record agree well with changes from aragonite/calcite to calcite/aragonite in the PGH-1 stalagmite. Local historical documents and geochemistry proxy data from Lake Huguangyan in the Leizhou Penninsula in Guangdong Province also indicate a warmer and drier Medieval Warm Period (WMP) and a wetter and cooler LIA in tropical south China (Chu et al., 2002). Their

study of historical documents also shows more frequent flood events during the LIA than during the MWP in south China, suggesting more intense rainfall.

Two stalagmite records also document a colder and wetter LIA in China. Ku and Li (1988) examined a stalagmite (S312) from Shihua Cave, located ~55 km southwest of Beijing. They found that carbonate deposited from AD 1620 to 1900 had lower $\delta^{18}O$ values suggesting a cool and wet LIA. In central China, a stalagmite (SF-1) from Buddha Cave, 80 km south of Xian in Shanxi Province, also has lower $\delta^{18}O$ values from AD 1475 to 1845 (Paulsen et al., 2003). Lower $\delta^{13}C$ values in the SF-1 stalagmite from AD 1475 to 1650 suggest a wetter climate while higher $\delta^{13}C$ values indicate that the later period of the LIA, from AD 1650 to 1845, was somewhat drier. In summary, ice core, lake sediment, and stalagmite records reveal cooler and wetter periods during the LIA in Northern India, Nepal, and China. However, it is impractical to examine whether the cooler and wetter LIA was synchronous across the Asian mainland due to the error in chronology of most currently available proxy records.

Asian Summer Monsoon Variability over the Past 750 Years

Variations in monsoon strength suggested by changes in $\delta^{18}O$ of the PGH-1 stalagmite correlate with changes of monsoon winds inferred from variations in *Globigerina bulloides* abundance in cores from the Arabian Sea, particularly after AD 1700 (Anderson et al., 2002) (Fig. 4.7). In the tropics, increased abundance of *G. bulloides* suggests stronger upwelling driven by stronger surface winds. Anderson et al. (2002) produced an index (square root of the *G. bulloides* differences from the AD 1975 average) related abundance to monsoon wind speed and so to the strength of the Asian southwest monsoon. In fact the PGH-1 $\delta^{18}O$ and *G. bulloides* records both indicate that the Indian monsoon became stronger during the past four centuries, the general

trend being punctuated by a brief period of weaker monsoon conditions around AD 1800. This brief interval is defined by more positive $\delta^{18}O$ values for stalagmite carbonate and lower *G. bulloides* indices (Fig. 4.7). The stalagmite $\delta^{18}O$ record suggests an additional interval with weaker summer monsoon conditions around AD 1920 but this is not evident in *G. bulloides* index record. A possible reason for this absence is that the $\delta^{18}O$ data have a temporal resolution of ~20 years, while the *G. bulloides* index is produced by averaging data over a 50-year interval. As a result the stalagmite data will record short-term events that are not evident in the *G. bulloides* record. However, these two records do not match well before 1700 A.D., as the stalagmite record suggests more or less constant monsoon strength while the *G. bulloides* data suggest a strong monsoon from A.D. 1200 to 1400 and a gradual decrease after that.

Century-scale variations in the Asian southwest monsoon during the past 1000 years correlate strongly with solar activity and so may be responding to it. Variations in stalagmite $\delta^{18}O$ values parallel changes in net radiative forcing inferred from variations in atmospheric ^{14}C (Crowley, 2000) (Fig.4.7). Figure 4.5 also shows that periods with higher radiative forcing centered on AD 1380, 1780, 1860 and 1970 correspond with periods of lower $\delta^{18}O$ in the carbonate of the PGH-1 stalagmite. The relationship suggests that stronger solar activity leads to a strengthening of the Indian summer monsoon.

Variations in gray level and luminescence along the central growth axis of PGH-1 parallel the northern hemisphere temperature record of Crowley and Lowery (2000). Whiter colors and stronger luminescence correspond to higher temperature, and darker colors and weaker luminescence to lower temperature (Fig. 4.8). Greater luminescence and whiter colors are associated with dense carbonate, which is more likely to be deposited at times of higher temperature and resulting increased evaporation. Also, under warmer conditions brown humic

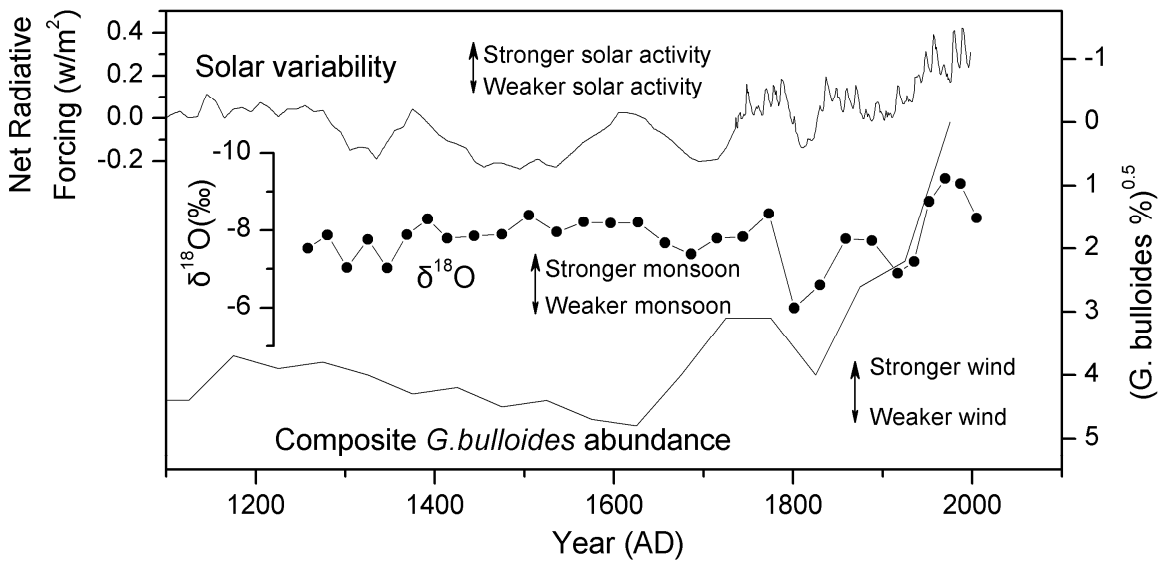

Figure 4.7. Comparison of the PGH-1 stalagmite record with *G. bulloides* data from the Arabian Sea (Anderson et al., 2002), and net radiative forcing reconstructed from variations in ^{14}C during the past 800 years (Crowley, 2000).

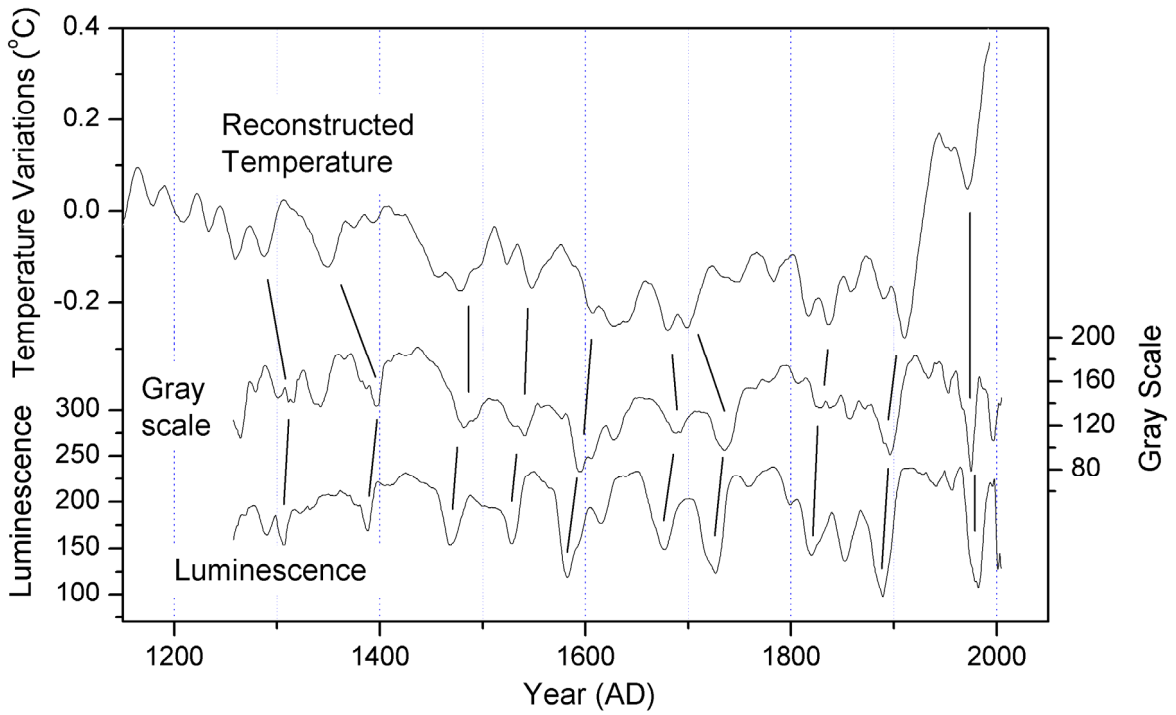

Figure 4.8. Comparison of the PGH-1 stalagmite gray color and luminescence records with northern hemisphere temperature changes during the last 1000 years (Crowley and Lowery, 2000).

acids decompose to fulvic acids (van Beynen et al., 2001), which are colorless and luminesce more. As a result, stalagmite carbonate deposited under warmer conditions would appear lighter in color and have higher luminescence.

Possible Climate Scenario in Northern India during the LIA

Evidence from marine sediments suggests a weaker Southwest Asian summer monsoon during the LIA (Anderson et al., 2002, Gupta et al., 2003). As a result, one might expect that the Indian subcontinent, particularly Northern India, would have received less rainfall as a weaker monsoon would be less likely to reach the foothills of Himalayas. However, the PGH-1 record documents a wetter, rather than a drier, climate during the LIA in Northern India. One possibility is that there was an increase in effective moisture due to reduced evaporation during a colder LIA. Another possible explanation may relate to a spatial redistribution of monsoon precipitation. At present, Indian monsoon rainfall is closely associated with active, weak, and break spells in the India core monsoon zone (Prasad and Hayshi, 2007). During break-monsoon conditions, the monsoon trough moves from the plains to the foothills of the Himalayas and the monsoon westerlies extend to the southern edge of the Tibet Plateau (Raghavan, 1973). As a result, south-facing slopes of the Himalayas, particularly the northeast Himalayas, receive more orographic precipitation brought by ascending air in the lower monsoon trough (Ramanadham et al., 1973; Gadgil and Joseph, 2003) while at the same time precipitation is below normal in the core zone of the monsoon (Gadgil and Joseph, 2003). Thus, one might expect a wetter LIA in the foothills of the Indian Himalayas if break monsoon conditions were more common, resulting in a northward movement of the monsoon trough. Under this scenario we would expect a drier LIA in the monsoon core zone. In fact, Vishwas et al., (2006) note an absence of high-magnitude

slackwater flood deposits in six large rivers in central and western India and they argue that the period from the 14th to 19th centuries was probably drier. Stable oxygen and carbon isotopes in a stalagmite from Dandak Cave, which is located near the southern boundary of the monsoon core zone, indicate less intense precipitation and probably drier conditions from ~ AD 1500 to 1850 (Yadava and Ramesh, 2005). Another stalagmite from Dandak Cave shows extremely low $\delta^{18}O$ values around AD 1400, suggesting drier conditions (Sinha et al., 2007). Deposition of this stalagmite ceased around AD 1500, probably a further indication that the climate in the surrounding area was much drier after this date.

Conclusions

The PGH-1 stalagmite was probably not deposited under isotopic equilibrium conditions. However, petrographic evidence and variations in stable isotopes along the central growth axis still provide evidence of changes in the Asian southwest monsoon over the past 750 years. The Panigarh Cave record is the first high-resolution and absolute-dated record of climate change in the southern foothills of the Indian Himalayas. Deposition of calcite with lower $\delta^{18}O$ values indicates that the LIA was a period of increased wetness in Northern India, while large-amplitude fluctuations in $\delta^{18}O$ values show that the Indian summer monsoon has varied significantly in strength during the last four centuries.

References

Anderson, D. M., Overpeck, J. T. and Gupta, A. K., 2002. Increase in the Asian southwest monsoon during the past four centuries. *Science* 297, 596-599.

Brohan, P., Kennedy, J. J., Harris, I., Tett, S. F. B. and Jones, P. D., 2006. Uncertainty estimates in regional and global observed temperature changes: a new dataset from 1850. *Journal of Geophysical Research* 111. D12106, doi:10.1029/2005JD006548.

Bradley, R. S. and Jones, P. D. 1993. 'Little Ice Age' summer temperature variations: their nature and relevance to recent global warming trends. *The Holocene* 3, 367-376.

Bradley, R. S. and Jones, P. D. 1995: Recent developments in studies of climate since A.D. 1500. In Bradley, R. S. and Jones, P. D., editors, *Climate Since AD 1500 [Revised Edition]*, London: Routledge, 666-679.

Bradley, R. S. and Jones, P. D. 1992. When was the "Little Ice Age"? Proceedings of the International Symposium on the Little Ice Age Climate. Edited by T. Mikami. 1-4.

Brook, G. A., Ellwood, B. B., Railsback, L. B. and Cowart, J. B., 2006. A 164 ka record of environmental change in the American southwest from a Carlsbad Cavern speleothem. *Palaeogeography, Palaeoclimatology, Palaeoecology* 237, 483-507.

Cabrol, P. and Coudray, J., 1982. Climatic fluctuations influence the genesis and diagenesis of carbonate speleothems in southwestern France. *National Speleological Society Bulletin* 44, 112-117.

Chauhan, M. S., Mazari, R. K. and Rajagopalan, G., 2000. Vegetation and climate in upper Spiti region, HimachalPradesh during late Holocene. *Current Science* 79, 373-377.

Chen, F., Huang, X., Zhang, J., Holmes, J. A. and Chen, J. 2006. Humid Little Ice Age in arid central Asia documented by Bosten Lake, Xinjiang, China. *Science in China Series D: Earth Sciences* 49, 1280-1290.

Chen, J., Wan, G., Zhang, D. D., Chen, Z., Xu, J., Xiao, T. and Huang, R., 2005. The 'Little Ice Age' recorded by sediment chemistry in Lake Erhai, southwest China. *The Holocene* 15, 925-931.

Cheng, H., Edwards, R. L., Hoff, J., Gallup, C. D., Richards, D. A. and Asmerom, Y., 2000. The half-lives of uranium-234 and thorium-230. *Chemical Geology* 169, 17-33.

Chu, G., Liu, J., Sun, Q., Lu, H., Gu, Z., Wang, W. and Liu, T., 2002. The 'Mediaeval Warm Period' drought recorded in Lake Huguangyan, tropical South China. *The Holocene* 12, 511-516.

Cooke, E. R., Krusic, P. J. and Jones, P. D., 2003. Dendroclimatic signals in long tree-ring chronologies from the Himalayas of Nepal. *International Journal of Climatology* 23, 707–732.

Craig, H., 1957. Isotopic standards for carbon and oxygen and correction factors for mass-spectrometric analysis of carbon dioxide. *Geochimica et Cosmochimica Acta* 12, 133-149.

Crowley, T. J. and Lowery, T. S., 2000. How Warm Was the Medieval Warm Period? *AMBIO* 29, 51-54.

Crowley, T. J., 2000. Causes of climate change over the past 1000 years. *Science* 289, 270-277.

Denniston, R. F., Gonzalez, L. A., Asmerom, Y., Sharma, R. H. and Reagan, M. K., 2000. Speleothem evidence for changes in Indian summer monsoon precipitation over the last ~2300 Years. *Quaternary Research* 53(2), 196-202.

Edwards, R. L, Chen, H. and Wasserburg, G. J., 1987. ^{238}U–^{234}U–^{230}Th–^{232}Th Systematics and the precise measurement of time over the past 500,000 years. *Earth and Planetary Science Letters* 81,175–192.

Friedman, I. and O'Neil, J. R., 1977. Compilation of stable isotope fractionation factors of geochemical interest: U.S. Geological Survey, Professional Paper 440-KK, p. 1–12.

Gadgil, S. and Joseph, P. V., 2003. On breaks of the Indian monsoon. *Journal of Earth System Science* 112, 529-558.

Grossman, E. L., and Ku, T.-L., 1986. Oxygen and carbon isotope fractionation in biogenic aragonite: temperature effects. *Chemical Geology* 59, 59-74.

Grove, J. M., 1988. The Little Ice Age. Methuen, London. 498pp.

Gupta, A. K., Anderson, D. M. and Overpeck, J. T., 2003. Abrupt changes in the Asian southwest monsoon during the Holocene and their links to the North Atlantic Ocean. *Nature* 421, 354-357.

Harmon, R. S., Schwarcz, H. P., and Ford, D. C., 1978. Stable isotope geochemistry of speleothems and cave waters from the flint ridge-mammoth cave system, Kentucky: implications for terrestrial change during the period 230,000 to 100,000 years B.P. *Journal of Geology* 86, 373-384.

Hendy, C. H., 1971. The isotopic geochemistry of speleothems, 1. the calculation of the effects of different modes of formation on the isotopic composition of speleothems and their applicability as paleoclimatic indicators. *Geochimica et Cosmochimica Acta* 35, 801-824.

Hill, C. A. and Forti, P., 1997. Cave minerals of the world (2nd Edition). National Speleological Society, Huntsville, Alabama, 463 p.

Jin, Z. D., Wang, S. M., Shen, J., Zhang, E. L., Li, F. C., Ji, J. F. and Lu, X. W., 2001. Chemical weathering since the Little Ice Age recorded in lake sediments: a high-resolution proxy of past climate. *Earth Surface Processes and Landforms* 26, 775-782.

Jimenez-Lopez, C. and Romanek, C. S., 2004. Precipitation kinetics and carbon isotope partitioning of inorganic siderite at 25°C and 1 atm. *Geochimica et Cosmochimica Acta* 68, 557-571.

Jones, P. D. and Bradley, R. S., 1992. Climatic variations over the last 500 years. In: Climate Since A.D. 1500 (Eds Raymond S. Bradley, Philip D. Jones), Routledge, London, p649-655.

Jones, P. D., Briffa, K. R., Barnett, T. P. and Tett, S. F. B., 1998. High-resolution palaeoclimatic records for the last millennium: interpretation, integration and comparison with general circulation model control-run temperatures. *The Holocene* 8, 455-471.

Kar, R., Ranhotra, P.S., Bhattacharyya, A. and Sekar, B., 2002. Vegetation vis-a-vis climate and glacial fluctuations of the Gangotri glacier since the last 2000 years. *Current Science* 82, 347-351.

Ku, T. and Li, H. 1998. Speleothems as high-resolution paleoenvironment archives: Records from northeastern China. *Journal of Earth System Science* 107, 321-330.

Lamb, H. H., 1977. Climate: present, past and future. Methuen, London, 835pp.

Lauritzen, S.-E., Ford D. C. and Schwarz, H. P., 1986. Humic substances in speleothems matrix-paleoclimate significance. *Proceedings of the 9th International Congress of Speleology* 2,77-79, Barcelona, August, 1986.

Liu, K.-b., Yao, Z. and Thompson, L. G., 1998. A pollen record of Holocene climatic changes from the Dunde ice cap, Qinghai-Tibetan Plateau. *Geology* 26, 135-138.

Mann, M. E., Bradley, R. S. and Hughes, M. K., 1999. Northern Hemisphere temperatures during the past millennium: inferences, uncertainties, and limitations, *Geophysical Research Letters* 26(6): 759-762.

Mills, P. J., 1965. Petrography of selected speleothems of carbonate caverns. Unpublished M.S. Thesis, University of Kansas. 47p.

Murray, J. W., 1954. The deposition of calcite and aragonite in caves. *Journal of Geology* 62, 481-492.

Newton, A., R. Thunell, R. and Stott, L., 2006. Climate and hydrographic variability in the Indo-Pacific Warm Pool during the last millennium, *Geophysical Research Letters* 33, L19710, doi:10.1029/2006GL027234.

Parthasarathy, B., Munot, A. A. and Kothawale, D. R., 1995. Monthly and seasonal rainfall series for all-India homogeneous regions and meteorological subdivisions: 1871-1994. Contributions from Indian Institute of Tropical Meteorolgy, Research Report RR-065, Aug. 1995, Pune 411 008 INDIA.

Paulsen, D. E., Li, H.-C. and Ku, T.-L., 2003. Climate variability in central China over the last 1270 years revealed by high-resolution stalagmite records. *Quaternary Science Reviews* 22, 691-701.

Phadtare, N. R., 2000. Sharp decrease in summer monsoon strength 4000-3500 cal yr B.P. in the central higher Himalaya of India based on pollen evidence from alpine peat. *Quaternary Research* 53, 122-129.

Prasad, V. S. and Hayashi, T., 2007. Active, weak and break spells in the Indian summer monsoon. *Meteorology and Atmospheric Physics* 95, 53-61.

Raghavan, K., 1973. Break-monsoon over India. *Monthly Weather Review* 101, 33-43.

Railsback, L. B., Brook, G. A., Chen, J., Kalin, R., and Fleisher, C. J., 1994. Environmental controls on the petrology of a late Holocene speleothem from Botswana with annual layers of aragonite and calcite. *Journal of Sedimentary Research* A64, 147-155.

Ramseyer, K., Miano, T., D'Orazio, V., Wildberger, A., Wagner, T. and Geister, J., 1997. Nature and origin of organic matter in carbonates from speleothems, marine cements and coral skeletons. *Organic Geochemistry* 26, 361–78.

Reams, M. W., 1972. Deposition of Calcite, Aragonite, and clastic sediments in a Missouri cave during four and one-half years. *National Speleological Society Bulletin* 34, 137-141.

Romanek, C. S., Grossman, E. L. and Morse, J. W., 1992. Carbon isotopic fractionation in synthetic aragonite and calcite: effects of temperature and precipitation. *Geochimica et Cosmochimica Acta* 56, 419-430.

Rühland, K., Phadtare, N. R., Pant, R. K., Sangode, S. J. and Smol, J. P., 2006. Accelerated melting of Himalayan snow and ice triggers pronounced changes in a valley peatland from northern India. *Geophysical Research Letters* 33, L15709, doi:10.1029/2006GL026704.

Shen, C.-C., Edwards, R. L., Cheng, H., Dorale, J. A., Thomas, R. B., Moran, S. B., Weinstein, S. and Edmonds, H.N., 2002. Uranium and thorium isotopic and concentration measurements by magnetic sector inductively coupled plasma mass spectrometry, *Chemical Geology* 185,165–178.

Shopov, Y. Y., Ford, D. C., and Schwarcz, H. P., 1994. Luminescent microbanding in speleothems: high-resolution chronology and paleoclimate. *Geology* 22, 407-410.

Siegel, F. R. and Dort, W. Jr., 1966. Calcite-aragonite speleothems from a hand-dug cave in northeast Kansas. *International Journal of Speleology* 2, 165-169.

Sinha, A., Cannariato, K. G., Stott, L. D., Cheng, H., Edwards, R. L., Yadava, M. G., Ramesh, R. and Singh, I. B., 2007. A 900-year (600 to 1500 AD) record of the Indian summer monsoon precipitation from the core monsoon zone of India. *Geophysical Research Letters* 34, 16707, doi:10.1029/2007GL030431.

Thompson, L. G., Yao, T., Mosley-Thompson, E., Davis, M. E., Henderson, K. A. and Lin, P. N. 2000. A High-Resolution Millennial Record of the South Asian Monsoon from Himalayan Ice Cores. *Science* 289, 1916-1919.

Thrailkill, J., 1971. Carbonate deposition in Carlsbad Caverns. *Journal of Geology* 79, 683-695.

van Beynen, P., Bourbonniere, R., Ford, D. C. and Schwarcz, H. P., 2001. Causes of colour and fluorescence in speleothems. *Chemical Geology* 175, 319-341.

Vishwas, K. S. and Baker, V. R., 2006. An extraordinary period of low-magnitude floods coinciding with the Little Ice Age: Palaeoflood evidence from central and western India. *Journal of the Geological Society of India* 68(3), 477-483.

Webster, J. W., Brook, G. A., Railsback, L. B., Cheng, H., Edwards, R. L., Alexander, C. and Reeder, P. P., 2007. Stalagmite evidence from belize indicating significant droughts at the time of preclassic abandonment, the Maya hiatus, and the classic Maya Collapse. *Palaeogeography, Palaeoclimatology, Palaeoecology* 250, 1-17.

Yadav, R. R. and Singh, J., 2002. Tree-ring-based spring temperature patterns over the past four centuries in western Himalaya. *Quaternary Research* 57, 299– 305.

Yadava, M. G. and Ramesh, R., 2005. Monsoon reconstruction from radiocarbon dated tropical Indian speleothems. *The Holocene* 15, 48-59.

Yang, X. D., Wang, S. M., Kamenik, C., Schmidt., R., Shen, J., Zhu, L. P. and Li, S. F., 2004. Diatom assemblages and quantitative reconstruction for paleosalinity from a sediment core of Chencuo Lake, southern Tibet. *Science in China Series D (Earth Sciences)* 47(6), 522-528.

Yao, T., Thompson, L. G., Qin, D., Tian, L., Jiao, K., Yang, Z. and Xie, C., 1996. Variations in temperature and precipitation in the past 2000 a on the Xizang(Tibet) Plateau-Guliya ice core record. *Science in China Series D (Earth Sciences)* 39, 425-433.

Yi, S., Saito, Y., Chen, Z. and Yang, D.Y., 2006. Palynological study on vegetation and climatic change in the subaqueous Changjiang (Yangtze River) delta, China, during the past about 1600 years. Geosciences Journal, 10(1) 17-22.

Yonge, C. J., Ford, D. C., Gray, J. P. and Schwarcz, H. P., 1985. Stable isotope studies of cave seepage water. *Chemical Geology (Isotope Geoscience Section)* 58, 97-105.

Zhang, J. W., Jin, M., Chen, F. H., Battarbee, R. W. and Henderson, A. C. G., 2003. High-resolution precipitation variations in the Northeast Tibetan Plateau over the last 800 years documented by sediment cores of Qinghai Lake. *Chinese Science Bulletin* 48, 1451-1456.

CHAPTER 5

PALEOCLIMATE VARIATIONS IN THE SOUTHEASTERN USA DURING THE LATE HOLOCENE: STALAGMITE EVIDENCE FROM DESOTO CAVERNS, ALABAMA*

*Fuyuan Liang, George A. Brook, L. Bruce Railsback, to be submitted to *Palaeogeography, Palaeoclimatology, Palaeoecology*

Abstract

Variations in stable isotopes, color, and luminescence along the growth axes of two vertical cores drilled from two large, active DeSoto Caverns stalagmites provide the first absolute-dated and high-resolution paleoenvironmental record for the Southeastern USA for the last 4400 years. More negative stable isotopic values and stronger luminescence of the stalagmite carbonate indicate wetter conditions. The record shows alternating wetter and drier regimes with wetter conditions centered at ~4300, 3400, 2500, 1400, 770, 420, and 120 years, and drier conditions at ~3900, 3000, 2700, 530, and 130 years B.P. Periods of wetter (drier) conditions generally correspond to higher (lower) Bermuda Rise ocean temperatures, suggesting that variations in the location of the Bermuda High Pressure cell, controlled by the ocean temperature regime, influences the amount of moisture reaching the Southeastern USA. The stalagmite record also indicates that the Medieval Warm Period in the Southeastern USA was wetter than today and the Little Ice Age drier. In particular, two distinct drier periods in the stalagmite records during Little Ice Age match two prominent cooling events in the North Atlantic, suggesting a linkage between ocean and atmosphere and between the North Atlantic and Southeastern USA.

Key words: stalagmite, vertical core, Medieval Warm Period, Little Ice Age, Holocene, Southeastern USA

Introduction

The late Pleistocene and Holocene of the Southeastern USA are poorly known due to a lack of continuous high-resolution records for the area. Our present understanding comes mainly from fossil pollen and fluvial evidence. Pollen records for Florida and south Georgia indicate drier conditions than present during the early Holocene (e.g. Watts, 1969, 1971, 1975, 1980; Rich, 1984), while evidence from further north points to wetter conditions (e.g. Seielstad, 1994; Brook, 1996; LaMoreaux, 1999; Goman and Leigh, 2004). Large paleomeanders along the Ogeechee River of southeast Georgia indicate that early Holocene river discharges were 1.6 to 4.0 times bankfull discharges today (Leigh, 2006) and precipitation was higher and more seasonal (Leigh and Feeney, 1995). Larger floods are also indicated by overbank sandy vertical accretion deposits along river channels in the lower Piedmont (Leigh, 2008 and references therein). By contrast, OSL- and TL-dated sand dunes along the Gulf of Mexico coast document increased aeolian activity and drier conditions at 10.5-8.5 ka and 6.8-5.7 ka B.P. (Otvos and Price, 2001; Otvos, 2004, 2005, 2006). However, Goman and Leigh (2005) argue that aeolian activity in the Southeastern USA was brief and sporadic and that the first half of the Holocene generally was wetter than present.

Pollen assemblages and paleochannels of late Holocene age are similar to modern counterparts and so cannot be used to unravel centennial or decadal climate changes during the last 5000 years. High-resolution records have been obtained for Georgia and the Carolinas from tree rings, but only for the past ~1000 years (Stahle and Cleaveland, 1994). These data indicate

no significant variations in spring rainfall during the past 1053 years, with weak evidence of drier conditions from ca. AD 1040-1275 and wetter conditions from AD 1475-1620. Obviously more evidence is needed to clarify what happened in the Southeastern USA during the Holocene.

This paper presents stalagmite data from DeSoto Caverns in Alabama documenting centennial and decadal variations in climate during the last ~4400 years. This is the first continuous, high-resolution, accurately-dated record of climate change for the Southeastern USA for this time interval. The proxy data were acquired from vertical cores drilled from two large stalagmites. Large stalagmites have the potential to provide long records of past climate change, but are rarely used because they cannot be removed from the cave for study. Our newly-developed drilling system can be used to extract vertical cores from large formations with little damage to the stalagmites or to the cave. In the future, this method should help the scientific community to obtain longer paleoclimate records from the many large stalagmites caves around the world.

DeSoto Caverns

DeSoto Caverns (33°18′24″N, 86°16′39″W, 160 m amsl) is located at the southern end of the Appalachian Mountains 8 km northeast of Childersburg and 55 km southeast of Birmingham, Alabama (Fig. 5.1A). The cave is essentially one large chamber 170 m long, 36 m high and ~4800 m^2 in area, which contains numerous stalagmites, stalactites, and flowstones,

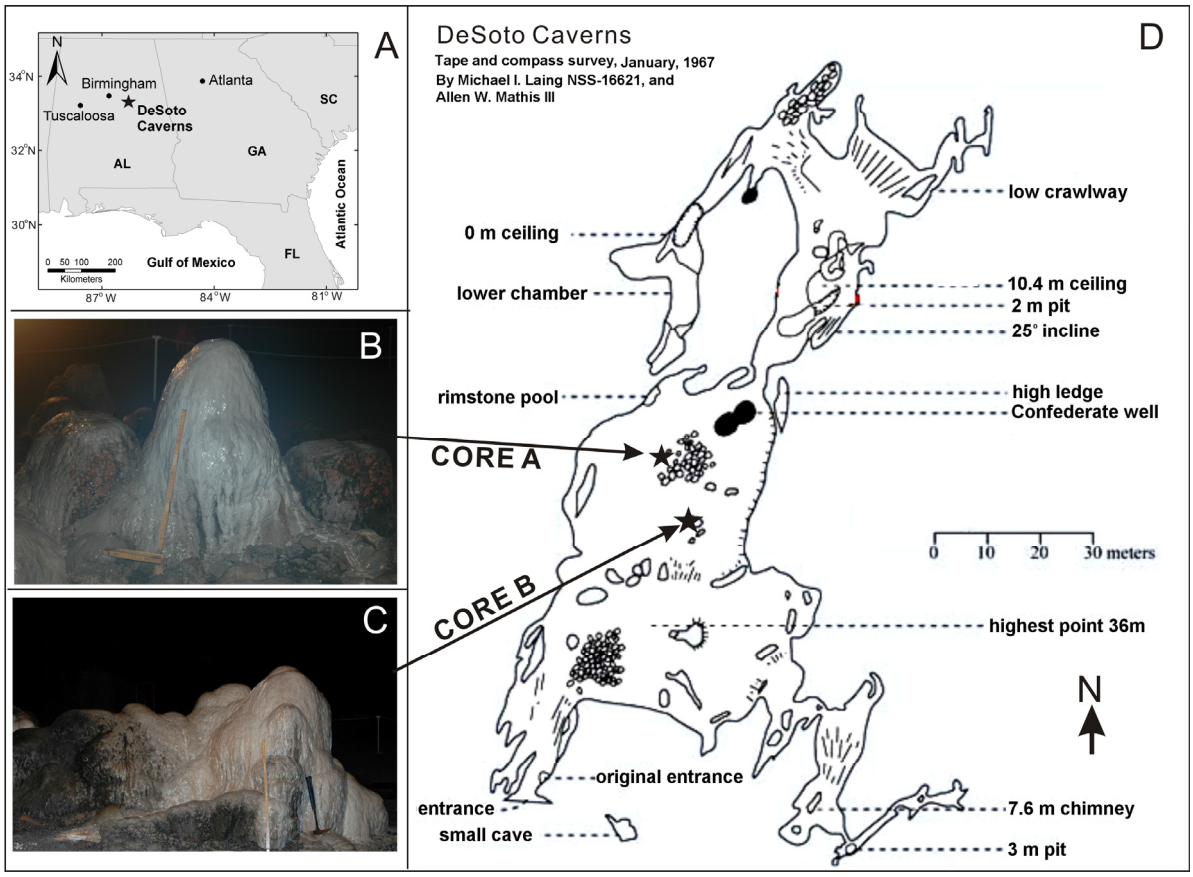

Figure 5.1. Location and map of DeSoto Caverns, Alabama (A and D) and the stalagmites examined in this study (B and C). The map of DeSoto Caverns was created by Michael I. Laing and Allen W. Mathis III. Locations of stalagmites from which cores A and B were drilled are shown by black stars.

many of them active (Fig. 5.1D). The cave has developed in undifferentiated Knox Group Ordovician-Cambrian Ordovician Dolomite. The climate of the area near the cave is humid and warm; with an annual average temperature of 17.2°C. Annual precipitation averages 1423 mm and is fairly well distributed through the year with slightly more rainfall in winter.

Methods

Stalagmites have been widely used to derive paleoclimate information and usually entire formations are removed for analysis. As a result, previous studies have mainly targeted stalagmites of relatively small size, despite the fact that large stalagmites hold the promise of long records of climate change. We have developed a new coring system that can be used to recover vertical, axial cores from large stalagmites without significantly damaging either them or the area of the cave around them. This coring system is a modified version of equipment used previously to extract 3 m-long, horizontal cores from two stalagmites in Carlsbad Caverns, New Mexico (Brook et al., 2006).

In this study two 5 cm-diameter vertical cores, 75 cm (core A) and 120 cm (core B) long, were recovered from two stalagmites (Fig. 5.1B and C) in DeSoto Caverns. The stalagmites are 15 m apart on the flat floor in the center of the main chamber of the cave. Drilling was stopped when bedrock was encountered. In the laboratory the cores were cut in half along the growth axis and, after polishing, one half was scanned and photographed for gray-scale color and luminescence analysis. The other half was cut lengthwise into two quadrants; slabs about 0.6

cm thick were cut from one quadrant for thin section preparation. Samples for U-series dating and stable isotope analysis were taken from the other quadrant.

Eighteen ~100 mg samples were drilled from the two cores and were dated by ICP-MS U-series in the Isotope Laboratory at the University of Minnesota following procedures described in Cheng et al., (2000), Edwards et al., (1987), and Shen et al., (2002). Ages were calculated using half-lives listed in Cheng et al., (2000) and are reported with analytical errors of 2σ of the mean (Tables 5.1 and 5.2). Petrographic studies indicate that core A is mostly aragonite, but contains sections or areas that have inverted to calcite. As a result, sample sites for dating and isotope analysis were chosen carefully to avoid areas of recrystallization. Samples were obtained from unaltered aragonite because of possible U, C and O mobilization during recrystallization, which would affect the ages and isotopic values obtained (Railsback et al., 2002).

Samples of ~100 μg were drilled for stable isotopes analysis at intervals of ~0.5 cm along the stalagmite growth axes using a carbide dental burr. Again, samples were taken from unaltered aragonite. Measurements were performed in the Isotope Laboratory at Nanjing Normal University, China. Samples were first prepared with an on-line and automated carbonate preparation system (Kiel III) and then analyzed by a Finnigan MAT-253 gas source mass spectrometer. Reliability was checked by running standards (NBS-19) every nine samples, with calculated standard deviation of 0.06‰ for $\delta^{18}O$ and 0.03‰ for $\delta^{13}C$ values.

Table 5.1 Uranium and thorium isotopes and ICP-MS ^{230}Th ages by for DeSoto stalagmite core A.

Sample ID	Depth (cm)	^{238}U ppb	^{232}Th ppt	d^{234}U measured[a]	[^{230}Th/^{238}U] activity[c]	[^{230}Th/^{232}Th] ppm[d]	Age uncorrected	Age corrected [c,e]	d^{234}U$_{initial}$ corrected
A-1	1	2775.1±12.7	3513.6±14.2	575.7±4.5	0.00178±0.00012	23.1±1.6	123±8	100±14	575.8±4.5
A-2	9	9602.1±71.9	582.5±8.4	585.6±5.3	0.01066±0.00014	2893.7±52.4	734±10	733±10	586.9±5.3
A-3	17.2	6800.9±515.9	916.3±70.1	526.9±2.3	0.02083±0.00020	2552.2±35.5	1498±15	1496±15	529.1±2.3
A-4	26.2	5983.6±24.7	2255.4±11.7	553.8±3.1	0.03475±0.00030	1518.6±14.1	2461±22	2454±22	557.6±3.1
A-5	33	5078.4±17.2	1060.5±8.2	546.6±2.6	0.04185±0.00036	3300.9±36.5	2984±26	2980±26	551.3±2.6
A-6	39	1781.8±134.5	1321.5±100.2	598.9±2.5	0.06946±0.00072	1545.9±19.5	4835±53	4821±54	607.1±2.5
A-7	71	2042.8±8.2	1067.3±8.2	522.9±4.2	0.25304±0.00171	7978.7±75.3	19594±155	19,585±155	552.7±4.4

Analytical errors are 2σ of the mean. Decay constants are 9.1577 x 10^{-6} yr^{-1} for ^{230}Th, 2.8263 x 10^{-6} yr^{-1} for ^{234}U, and 1.55125 x 10^{-10} yr^{-1} for ^{238}U (Cheng et al., 2000). [a] The degree of detrital ^{230}Th contamination is indicated by the [^{230}Th/^{232}Th] atomic ratio instead of the activity ratio. [b]Age corrections were calculated using an average crustal ^{230}Th/^{232}Th atomic ratio of 4.4 x 10^{-6} ± 2.2 x 10^{-6}. Those are the values for a material at secular equilibrium, with the crustal ^{232}Th/^{238}U value of 3.8. The errors are arbitrarily assumed to be 50%.

Table 5.2 Uranium and thorium isotopic composition and ICP-MS ^{230}Th ages for DeSoto stalagmite core B.

Sample ID	Depth (cm)	^{238}U ppb	^{232}Th ppt	d^{234}U measured[a]	[^{230}Th/^{238}U] activity[c]	[^{230}Th/^{232}Th] ppm[d]	Age uncorrected	Age corrected [c,e]	d^{234}U$_{initial}$ corrected
B-1	1.7	1557.7±5.5	828.5±7.8	681.9±3.6	0.00145±0.00012	45.1±3.6	94±7	85±9	682±3.6
B-2	3.2	2160.4±8.2	196.2±7.3	741.2±3.6	0.005±0.00011	908.7±39.2	314±7	312±7	741.9±3.6
B-3	7	3193.8±13.2	178.9±6.2	619.8±2.9	0.01991±0.0002	5868±209.2	1349±14	1348±14	622.1±2.9
B-4	12	121.6±0.2	72.2±0.8	630.3±2.7	0.02346±0.00027	651.1±10.4	1578±19	1567±19	633.1±2.7
B-5	16.3	1798.6±131.2	2717.3±198.5	628.7±2.5	0.03069±0.00043	335.3±4.9	2073±31	2046±37	632.4±2.6
B-6	23	3241.6±9.0	309.0±6.4	616.9±2.9	0.03667±0.00023	6337.4±136.7	2496±17	2494±17	621.2±2.9
B-7	31	2851.8±9.3	347.5±8.3	645.4±3.9	0.04414±0.00028	5966.9±146.2	2958±21	2955±21	650.8±3.9
B-8	39.6	3093.5±231.0	1211.0±91.1	656.0±2.3	0.05052±0.00064	2130.3±33.0	3375±44	3368±45	662.3±2.3
B-9	47.5	741.9±1.4	1471.2±7.6	672.9±3.3	0.05629±0.00049	467.6±4.6	3721±34	3686±38	680.0±3.3
B-10	59.8	945.8±1.5	995.8±6.0	693.3±2.3	0.06127±0.00053	958.6±10.0	4006±36	3988±37	701.1±2.3
B-11	76	1105.6±2.0	1030.6±5.8	713.6±2.6	0.06905±0.00038	1220.3±9.3	4469±26	4453±27	722.7±2.6
B-12	79	1161.5±2.6	592.1±6.5	751.0±2.9	0.08324±0.00052	2690.0±33.7	5289±35	5280±35	762.3±2.9
B-13	93	1504.6±3.0	333.7±8.1	787.6±3.2	0.11998±0.00069	8911.2±220.9	7533±47	7529±47	804.6±3.3
B-14	117	2315.3±5.7	3098.3±13.1	587.7±2.7	0.16979±0.00087	2090.1±12.9	12240±70	12,215±71	608.4±2.8

Analytical errors are 2σ of the mean. Decay constants are 9.1577 x 10^{-6} yr^{-1} for ^{230}Th, 2.8263 x 10^{-6} yr^{-1} for ^{234}U, and 1.55125 x 10^{-10} yr^{-1} for ^{238}U (Cheng et al., 2000). [a] The degree of detrital ^{230}Th contamination is indicated by the [^{230}Th/^{232}Th] atomic ratio instead of the activity ratio. [b]Age corrections were calculated using an average crustal ^{230}Th/^{232}Th atomic ratio of 4.4 x 10^{-6} ± 2.2 x 10^{-6}. Those are the values for a material at secular equilibrium, with the crustal ^{232}Th/^{238}U value of 3.8. The errors are arbitrarily assumed to be 50%

In addition, samples for $\delta^{18}O$ and $\delta^{13}C$ analysis were also drilled from two layers in core A and three layers in core B to determine if the stalagmite carbonate was deposited in isotopic equilibrium with the precipitating water following the criteria of Hendy (1971). Although most of the primary aragonite in core A has inverted to calcite, some growth layers have clearly-defined areas of primary aragonite and secondary calcite. These occurrences provided an opportunity to determine whether stable isotope values are significantly modified during the recrystallization process. So, three unaltered aragonite and four secondary calcite samples were drilled along one growth layer 5.5 cm from the top of core A.

The polished half of each core was scanned on a standard flatbed scanner at 300 dpi spatial resolution and 8-bit gray level resolution. Variations in gray-scale color along the growth axis of each stalagmite were measured along a 0.8 mm wide traverse (10 pixels) on the scanned image. The polished half of the core was then illuminated by long-wave ultraviolet light emitted from two Macken Instruments Model 22 UV lamps in a darkroom. Induced luminescence was recorded using a Nikon D-70, 6-megapixel digital camera fitted with a Kodak Wratten Gelatin Filter #2E to prevent transmission of the UV excitation energy band. Variations in luminescence were measured along a 0.8 mm wide (10 pixels) transverse along the growth axis of the resulting digital images.

Chronology

The 18 samples dated were all in stratigraphic order, with a typical 2 σ error of about 1%. Most have low concentrations of detrital thorium, indicated by high [$^{230}Th/^{232}Th$] atomic ratios, showing that they can be dated accurately and so provide reliable chronologies for the two cores. The low [$^{230}Th/^{232}Th$] atomic ratio of sample (A-1), 1 cm from the top of core A is due to the low

concentration of ^{230}Th because the sample is very young and very little ^{230}Th has accumulated. The ages obtained indicate that the oldest section of core A was deposited before 19,589 years ago, but this period was followed by a hiatus with growth resuming at 4821 years ago. The base of core B is more than 12,215 years old and the age data suggest that growth was interrupted prior to 7529 years ago (Table 5.2).

The basal sections of both cores, 40-75 cm in core A and 77-120 cm in core B, consist mainly of altered or unaltered aragonite with complex layering. Further work will be necessary to clarify the record in these parts of the cores. This paper will focus on the upper 40 cm of core A and the upper 75 cm of core B that show continuous growth and have excellent chronologies for the last 5000 and 4400 years, respectively.

The ages indicate significant variations in the growth of both stalagmites over time (Fig. 5.2). Stalagmite A grew more slowly before 3000 years ago, at an average rate of 5.6 cm/ka; the rate doubled to 11 cm/ka in the last 3000 years. Stalagmite B grew gradually slowly over time, from 30 cm/ka from 3400-4400 years ago, 16.1 cm/ka from 1400-3300 years ago, to only 5.2 cm/ka during the last 1400 years. Clear differences in the growth of the two stalagmites suggest that growth rate is at least in part related to the unique hydrological condition of the dripping points and not entirely to past changes in regional climate.

Petrography

Core A is secondary calcite interspersed with zones of unaltered aragonite, which is present as bundles of elongated needles (Fig. 5.3A). Secondary calcite crystals are generally equant in

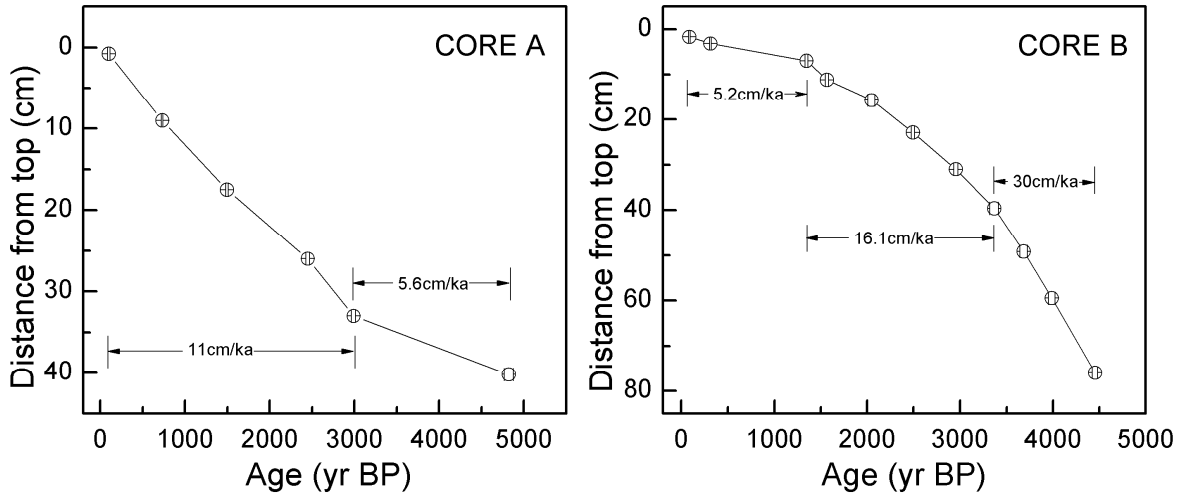

Figure 5.2. ICPMS U-series age data for core A and B in relation to distance from top of the stalagmites. Numbers in the diagrams show the average growth rate of these two cores over time.

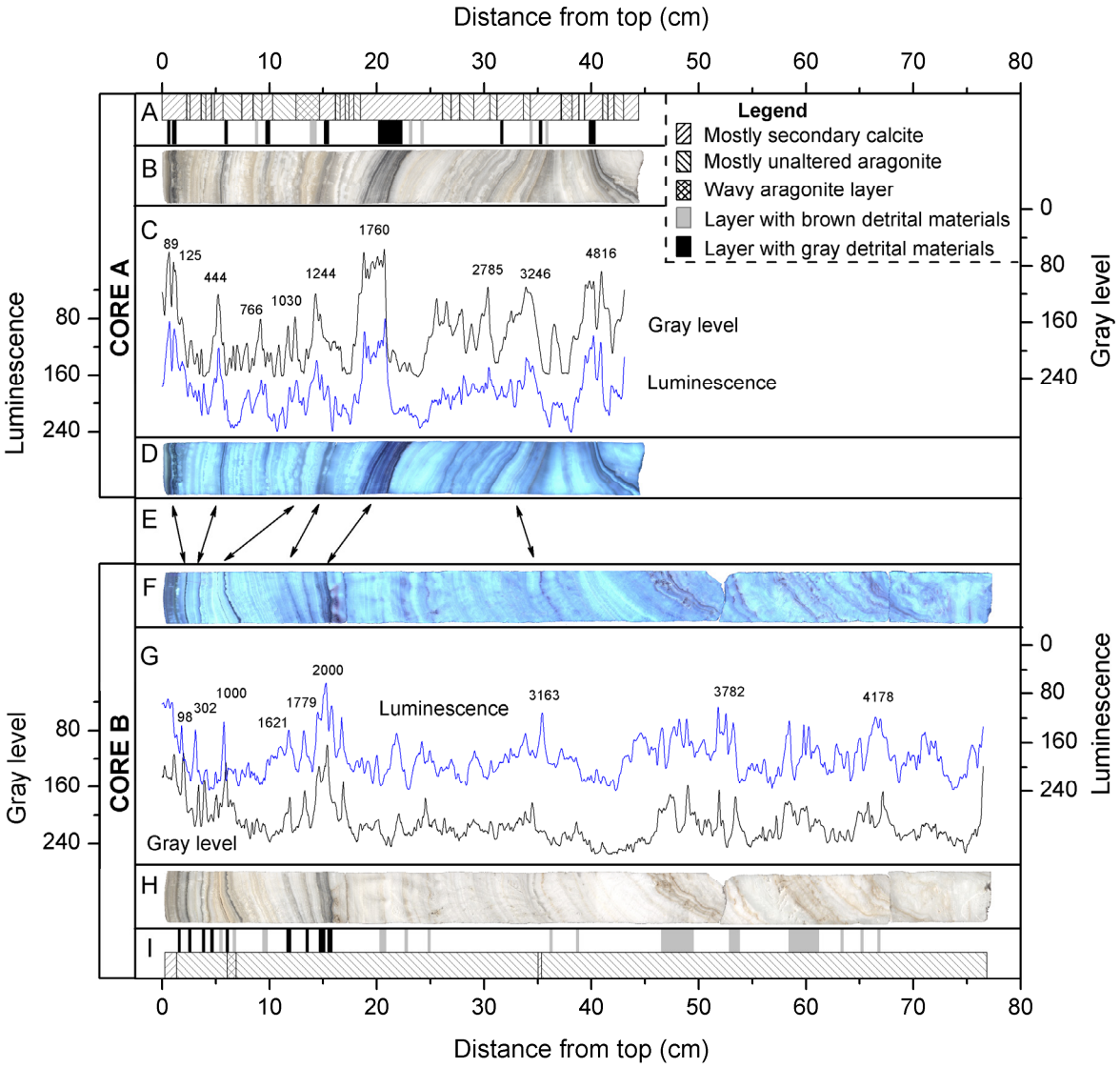

Figure 5.3. Petrography (A, I), gray scale color images (B, H), luminescence images (D, F), and variations in gray color and luminescence along the growth axes of cores A and B (C, G). Arrows in E show dark gray layers in cores A and B that may have been deposited at the same time.

form and usually engulf unaltered aragonite within it. Although most of the primary aragonite has been replaced, layering is still evident and can be traced across the thin sections and the core itself. In core A there is a prominent wavy layer of aragonite 13-14.2 cm from the top (Fig. 5.3A). Core B is mainly unaltered elongate aragonite in bundles of radiating needles, except for secondary calcite in the upper 1.5 cm and in a layer from 33.4-33.7 cm (Fig. 5.3I). As with core A, the secondary calcite in core B is generally equant with some unaltered aragonite within it.

Although the unaltered aragonite and secondary calcite generally contain few detrital particles, 15 layers, 0.2 to >2 cm thick, in the upper 44 cm of core A are rich in dark gray or brown, fine to very fine, non-carbonate detrital material (Fig. 5.3A). Similar to core A, most of the aragonite in core B is clear and dense, although there are 8 layers containing dark gray, non-carbonate detrital material in the upper 16 cm (Fig. 5.3I). Detrital materials are apparent at 5.7- 6 cm and 8-10 cm from top of the core and from 48-75 cm the core appears light brown to brown in reflective color. In total, there are 14 layers with brown detrital materials in core B (Fig. 5.3I), including a wavy aragonite layer 6.4 cm from the top of the core (Fig. 5.3I).

XRD analysis indicates that the dark gray, non-soluble detrital materials are mainly quartz and phlogopites (a mica mineral), which may account for the reflectance properties of these layers. Fine-grained phlogopites are more likely to be present in weakly weathered soils (Brady and Weil, 1999). The brown detrital materials in the cores are mainly quartz and probably chlorite. Particles in these detrital materials are too small to resolve with a light microscope and are thus classified as clay. As the particle size is up to 0.05 mm, these detrital materials were more likely to be transported into the cave from the overlying soil, possibly by increased rainfall after a dry interval (e.g. El-Farhan et al., 2000).

Given dating uncertainties, the aragonite layers containing detrital materials in the two cores correlate well, particularly for the dark layers in the upper 20 cm of core A and the upper 15 cm of core B (Fig. 5.3E). For example, one prominent aragonite layer with dark gray detrital material at 18-20 cm from the top of core A appears to correlate with a similar layer at 14.8-15.8 cm in core B; both were deposited around 1800-2000 years BP. Four other dark layers in the upper 16 cm of core A have counterparts in core B (Fig. 5.3E). Aragonite layers with brown detrital materials in both cores may also have been deposited at the same time. This certainly appears to be the case for the layer at 8.5 cm in core A, which appears to correspond with the aragonite layer at 5.8 cm in core B that was deposited 700 years B.P. Wavy aragonite layers in both cores were deposited around 1100 years B. P. The deposition of detrital materials in both cores at similar times suggests that climate changes above the cave affected both stalagmites in a similar way. Differences in stalagmite hydrology may explain why most aragonite in core A has inverted to calcite while most in core B is still unaltered. When conditions favoring aragonite deposition persist, this limits inversion of aragonite to the more stable calcite form (Frisia et al., 2002). As a result, it appears that in the past the drip rate to stalagmite A was more rapid and had a lower Mg content than was the case with stalagmite B; this resulted in more rapid and more complete inversion to calcite in stalagmite A.

Color and Luminescence

Luminescence and gray scale color vary significantly along the growth axis of core A, but there is no significant long-term trend in either variable (Fig. 5.3B, C, and D). Layers containing detrital materials have lower luminescence and are darker in color, while clear aragonite layers have stronger luminescence and are lighter. Petrographic analysis of aragonite layers 18.5-21 cm

from the top of the core reveal fine, non-carbonate detrital material and so not surprisingly these layers are dark gray in reflection color and have low luminescence, in fact recording the lowest values of gray scale color and luminescence in the entire record. Darker colors and low luminescence at 0.6, 1.3, 5.3, 9.2, 12.4 20, 30, 34, 36, and 39 cm are also associated with detrital materials.

Luminescence and gray color of clear carbonate in core A appear to be related to mineral type. Unaltered aragonite is generally lighter in color than secondary calcite, while secondary calcite has stronger luminescence than unaltered aragonite. Thus the paleoclimatic significance of variations in luminescence and color in core A have probably been affected to some degree by recrystallization.

Luminescence and gray color of core B also are correlated and there is no long-term trend (Fig. 5.3F, G, and H). Clear aragonite layers are lighter in color and emit stronger luminescence, while layers with detrital materials at 0.7, 1.8, 3.1, 5.8, 11.9, 13.4, 15.3, 21.8, 24.2, 29, 35, 38, 45, 52, 58, and 66 cm depth are darker and have lower luminescence. Peaks in luminescence and gray level are closely associated with aragonite layers consisting of shorter radiating needles, such as occur at 4.5, 13.4, and 42.2 cm from top of the stalagmite.

Variations in luminescence have been explained in terms of the content of organic acids sealed in the speleothem (Lauritzen, 1986; Shopov et al., 1994; Ramseyer et al., 1997). These acids are produced in the overlying soil and transported into the cave by percolating water, so that luminescence is partly associated with vegetation productivity above the cave (Shopov et al., 1994, Webster et al., 2007), which is affected by temperature and water availability. During the later Holocene, plant growth in the DeSoto cave area was probably not significantly affected by temperature variations, and so the content of soil organic acids is likely to have been determined

by moisture availability. Therefore, stronger luminescence is taken to indicate enhanced plant growth under wetter conditions although, as described above, petrography and detrital content complicate this simple relationship.

Stable Isotopes

Equilibrium Tests

Samples along four of the five growth layers used to test for isotopic equilibrium deposition had very similar $\delta^{18}O$ values with standard deviations less than 0.06, which is within the magnitude of instrumental error (Figs 5.4C and 5.5A, C, E). The high standard deviation (0.11) of samples drilled from the layer 3.2cm from the top of core A is due to the unusually low $\delta^{18}O$ value of the sample 0.6 cm from the edge of the core (Fig. 5.4A). Excluding this value reduces the standard deviation to 0.04, which is within instrumental error. Although the $\delta^{18}O$ values along individual growth layers are positively correlated with $\delta^{13}C$ (Figs 5.4B and D, 5.5 B, D, and F), variation of $\delta^{18}O$ values along the growth layers in both cores are basically constant suggesting that deposition was in isotopic equilibrium with precipitating waters. In the past, the cave had only one entrance 1.2 m high and 2.4 m wide on the side of the hill (located above the current entrance which was built in the 1990s). At this time, ventilation between the cave and the outside would have been limited. A Confederate well at one end of the main chamber, probably helped to maintain high humidity in the cave thus reducing evaporation. As a result, it is reasonable to expect that stalagmites in the cave were deposited under isotopic equilibrium conditions. If this was the case, and our results suggest it was, then the stable isotopic composition of speleothem

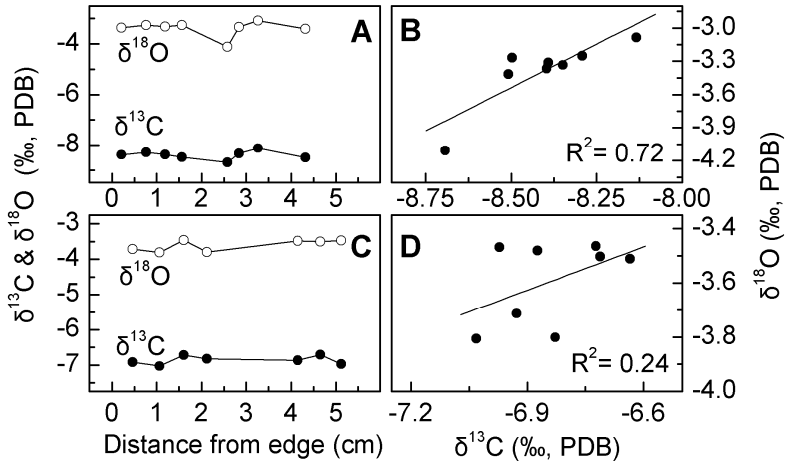

Figure 5.4. Variations in $\delta^{18}O$ and $\delta^{13}C$ values with distance from the edge of core B along three growth layers. The growth layers are 11.2 (A), 41.7 (C), and 62.7 cm (E) from top of the stalagmite; there is a positive relationship between $\delta^{18}O$ and $\delta^{13}C$ (B, C, and D).

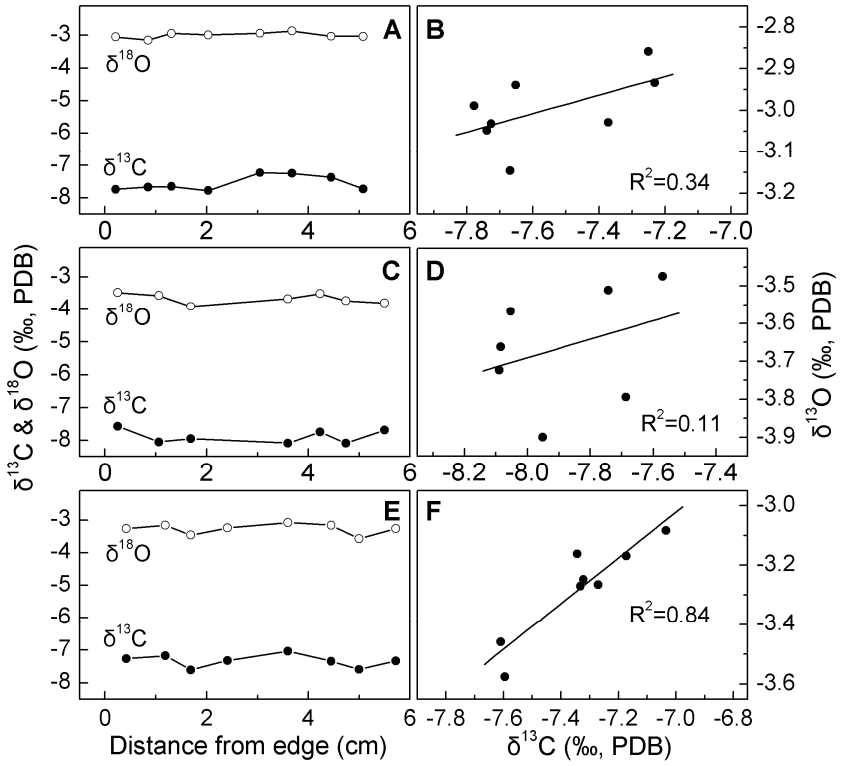

Figure 5.5. Variations in $\delta^{18}O$ and $\delta^{13}C$ values along a growth layer 5.5 cm from the top of stalagmite core A. This layer consists of both unaltered aragonite (symbols not circled by ellipse) and secondary calcite (symbols circled by ellipse). Secondary calcite has lower $\delta^{18}O$ values but higher $\delta^{13}C$ values compared to unaltered aragonite.

carbonate is related to changes in temperature and in the isotopic composition of the water entering the cave.

Possible Kinetic Fractionation of Dripwaters

Rapid degassing may have influenced the stable isotope composition of dripwaters dropping ~30 m from the ceiling to the floor of the cave. When the climate was dry and there was less CO_2 in the soil, less water would have entered the cave and there would have been limited outgassing of CO_2 due to lower partial pressures of CO_2 in the dripwaters and in the cave air itself. However, the cave air would have been much drier than today and so evaporation may have led to enrichment of both ^{18}O and ^{13}C in the dripwaters before they reached stalagmites on the floor of the cave. By contrast, higher PCO_2 of the cave air and increased humidity due to an increase in dripwater volume suppresses CO_2 degassing and limits evaporation leading to somewhat lower values of ^{18}O and ^{13}C in the dripwaters.

Isotopic Values and Recrystallization

Four samples were drilled from secondary calcite and three from unaltered aragonite within a single growth layer 5.5 cm from the top of core A (Fig. 5.6). The $\delta^{18}O$ values for the four samples from secondary calcite average 0.7‰ lower than the samples from primary aragonite, and $\delta^{13}C$ values are 0.2‰ higher. These differences are too high to be explained by instrument error and so we believe that either sampling problems or recrystallization to be responsible. This finding suggests that great caution is needed when using isotope data from recrystallized carbonate as a climate proxy.

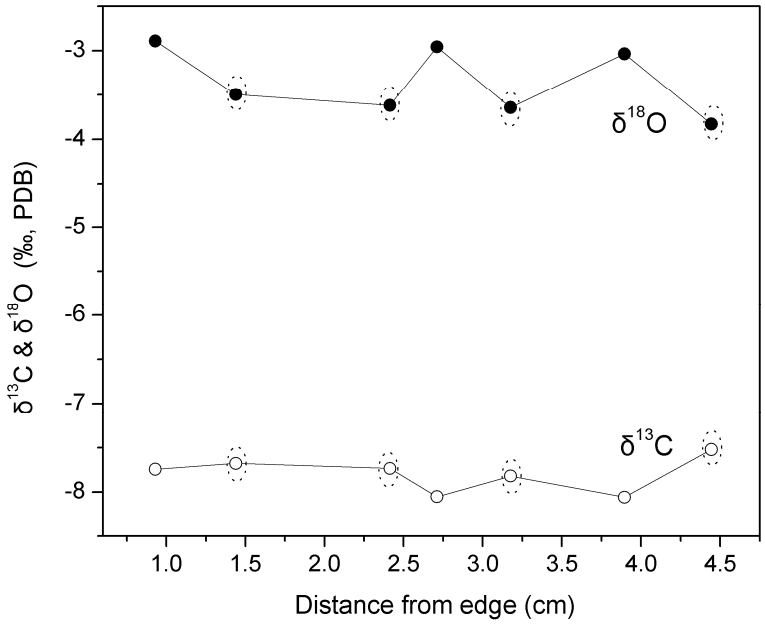

Figure 5.6. Variations in $\delta^{18}O$ and $\delta^{13}C$ values along a growth layer 5.5 cm from the top of stalagmite core A. This layer consists of both unaltered aragonite (symbols not circled by eclipse) and secondary calcite (symbols circled by eclipse). Secondary calcite has lower $\delta^{18}O$ values but higher $\delta^{13}C$ values compared to the unaltered aragonite.

Isotopic Variations along the Growth Axes

Values of $\delta^{18}O$ along the growth axes of the two cores ranged from -2.3 to -4.9 ‰ and -2.5 to -4.1 ‰ respectively relative to PDB (Fig. 5.7). Values of $\delta^{13}C$ ranged from -4.6 to -11.8 ‰ and -5.8 to -10.8‰ (PDB) respectively. Due to different growth rates and sampling strategy, core A provides a higher temporal resolution for the last 2000 years than earlier. By contrast, data from core B are of higher temporal resolution before 2000 years ago than after. Although at different temporal resolutions, the $\delta^{18}O$, $\delta^{13}C$, luminescence records from cores A and B match well suggesting that the observed variations are due to regional climate changes and not to stalagmite-specific hydrological conditions. The four variables in both cores show relatively higher values before 2000 years ago than after, although the long-term variation is less striking in $\delta^{18}O$ values for core B (Fig. 5.7). The long-term trends in the records are punctuated by millennial-scale fluctuations, with lower values at 3800, 3000, 2000, and 500 years B.P., and higher values at 4200, 3500, 2500, 1400, 700, and 200 years B.P.

Environmental Interpretation of the Oxygen and Carbon Isotope Data

As discussed above, both cores were deposited in isotopic equilibrium conditions with precipitating water and, as a result, $\delta^{18}O$ values would have been affected by changes in temperature and the $\delta^{18}O$ values of precipitating water. Although stalagmite carbonate is enriched in O^{18} when deposited in lower temperature, the temperature effect would have been negligible due to the limited carbonate/water fractionation of oxygen isotopes with temperature (-0.23‰ per $^{\circ}C$, Friedman & O'Neil, 1977) and because of restricted temperature fluctuations during the Late Holocene. The observed large-amplitude variations in the two cores (2.7‰ for core A

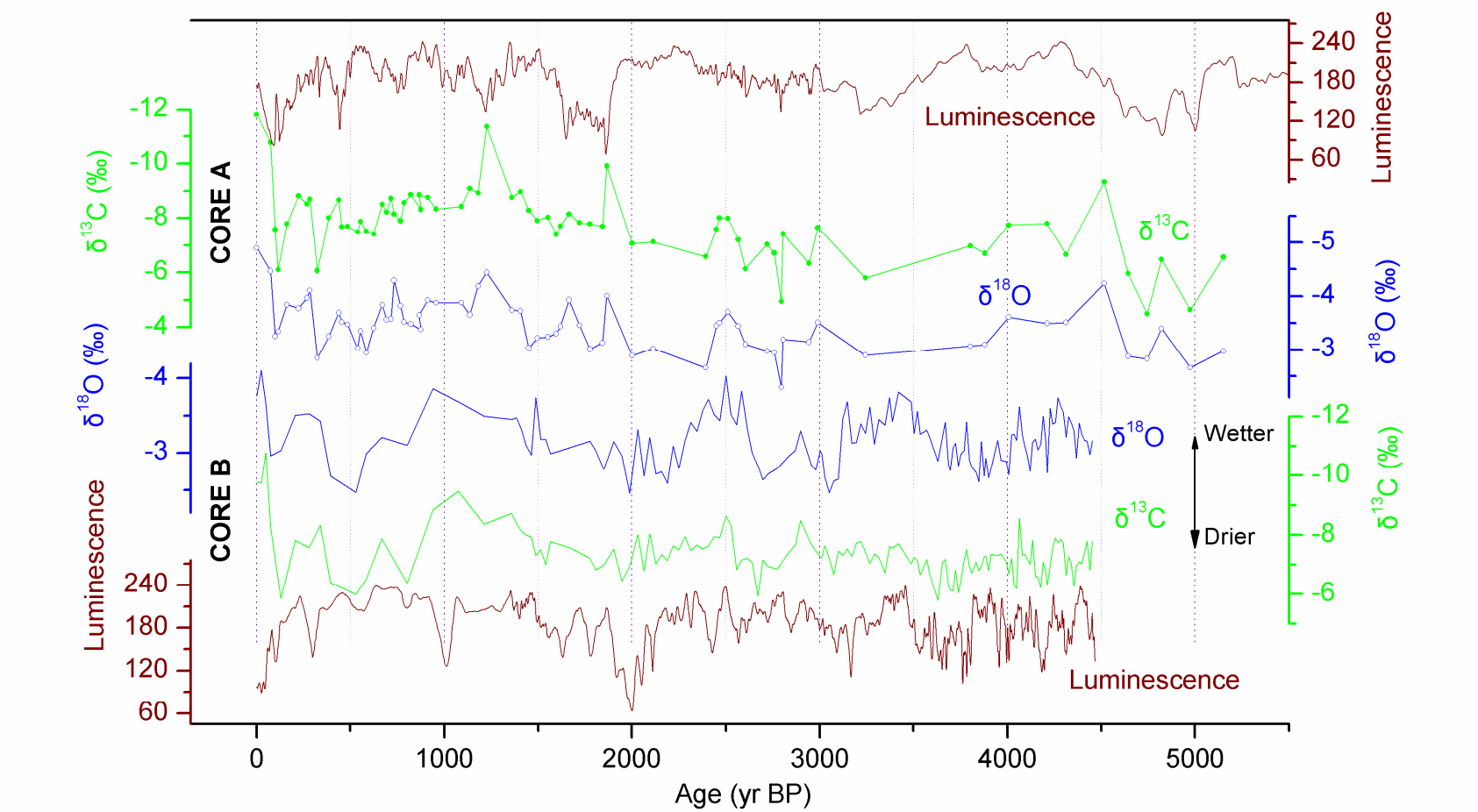

Figure 5.7. Variations in stable isotopes and luminescence along the growth axes of stalagmite cores A and B. Similar patterns of change in $\delta^{18}O$ strongly suggest that broad regional climate changes were responsible for the variations. Stronger luminescence in core B is generally associated with lower $\delta^{18}O$ and $\delta^{13}C$ values.

and 1.6 ‰ for core B) are therefore interpreted to be caused by variations in the $\delta^{18}O$ value of precipitating water from which the speleothem carbonate was deposited.

In most cases, $\delta^{18}O$ value of precipitating water is believed to be the same as that of dripwaters. However, this is not true in the DeSoto Caverns, as the discussion above indicates that rapid degassing might result in more positive values in dripwaters after it fell from the ceiling and before it reached the top of the stalagmite. Subsequently this enrichment in O^{18} was transferred to the stalagmite carbonate. It is obvious that, when deposition of stalagmite carbonate is affected by rapid degassing, usually under drier conditions, speleothem carbonate would have elevated $\delta^{18}O$ values. By contrast, under wetter conditions, evaporation and rapid degassing may not be as important and the stalagmite carbonate will have generally lower values of $\delta^{18}O$.

Although there are no published rainfall isotope data for Alabama, preliminary results of a study at the University of Alabama in Tuscaloosa, about 150 km west of DeSoto Caverns, show more negative monthly rainfall $\delta^{18}O$ values in winter when there is slightly more rainfall and temperature is lower (Joe Lambert, personal communication, 2008). So, lower $\delta^{18}O$ values in the core carbonate might indicate wetter conditions and/or more winter precipitation and higher values drier conditions and/or more summer rains. This relationship affects $\delta^{18}O$ values in speleothem carbonate in the same direction as the kinetic fractionation due to rapid degassing. As a result, higher $\delta^{18}O$ values in DeSoto Caverns speleothem carbonate are to be expected at times of reduced rainfall and increased outgassing in a drier cave environment. By contrast, lower $\delta^{18}O$ values are to be expected during periods of increased rainfall when degassing of dripwaters in the cave is limited by higher cave air CO_2 levels due to increased dripwater volume and therefore

an increase in CO_2 degassed. In summary, we believe that higher $\delta^{18}O$ values in DeSoto stalagmite carbonate indicate drier conditions, and lower values wetter conditions.

Environmental Interpretation of the Carbon Isotope Data

Factors controlling $\delta^{13}C$ values of speleothem carbonate include vegetation type above the cave (C_3 or C_4), abundance of soil CO_2, as well as extent of degassing (Brook et al., 2006, Webster et al., 2007, references therein). The $\delta^{13}C$ values of the DeSoto stalagmites are not likely to be influenced by vegetation type since the study area has been dominated by temperate broad-leaved forest, with C_3 vegetation, during the past several thousand years (Delcourt, 1980). Abundance of soil CO_2, with $\delta^{13}C$ = -22 ‰ under a C_3 biomass, is closely related to vegetation growth conditions, which are influenced by climate. Under drier conditions with reduced plant growth above the cave, a lower level of CO_2 is to be expected in the soil and in any percolating water. Under this situation, relatively more carbon in the drip water would come from the overlying carbonate bedrock ($\delta^{13}C = 0$) and $\delta^{13}C$ values of deposited carbonate would be enriched in ^{13}C. By contrast, $\delta^{13}C$ values of speleothem carbonate would be lower when there was enhanced plant growth under wetter conditions and a greater abundance of soil CO_2. Dissolution of limestone is also more likely to occur under more open-system conditions and more of the carbon deposited on the speleothem would originate from soil CO_2 with its lower $\delta^{13}C$ values. Speleothems deposited under this situation would have lower $\delta^{13}C$ values. As mentioned previously, rapid degassing of dripwaters are more likely under drier conditions so that speleothem carbonate deposited with kinetic fractionation tends to be enriched in ^{13}C. Therefore, higher values of $\delta^{13}C$ in the DeSoto stalagmites are taken to indicate drier conditions

(probably with enhanced rapid degassing), while lower $\delta^{13}C$ values would suggest wetter conditions.

In summary, we believe that elevated $\delta^{13}C$ and $\delta^{18}O$ values indicate drier conditions while lower values record wetter conditions. The general correspondence between variations in $\delta^{13}C$ and $\delta^{18}O$ strongly suggest that variations in these two proxy indexes simultaneously document moisture variability during the past 4400 years.

The DeSoto Paleoclimatic Record

Variations in petrography, stable isotopes, luminescence, and reflectance color are considered to be climate proxies that record changes in climate outside the cave. Higher stable isotope values, lower luminescence, and darker colors indicate drier conditions. The dominance of aragonite in both cores suggests relatively dry conditions at DeSoto Cavern during the last 4400 years. A weak trend towards depletion in both O^{18} and C^{13} from older to younger deposit suggests a gradual shift over time to wetter conditions. Relatively higher values of $\delta^{18}O$ and $\delta^{13}C$ in both cores indicates drier conditions before 2000 years ago, while lower values after 2000 years suggest relatively wetter conditions.

The shift from drier to wetter condition is punctuated by sub-millennial climate fluctuations. As Fig. 5.7 shows, the proxy data appear to document wetter periods at 4300, 3400, 2500, 1400, 770, 420, and 70 year B.P., as suggested by lower $\delta^{18}O$ and $\delta^{13}C$ values, stronger luminescence, and lighter speleothem carbonate colors. Drier periods centered at 3800, 3000, 2700, 2000, 500, and 100 years ago are recorded by relative higher $\delta^{18}O$ and $\delta^{13}C$ values, lower luminescence and darker deposits.

The period 4400-2600 years ago is characterized by elevated $\delta^{13}C$ values with an average of 7.2‰ in core B, documenting general drier conditions during the cooler Neoglaciation period after the Holocene Optimum ended at around 4500 years B.P. in the Southeastern USA (LaMoreaux, manuscript in review). In core B, wetter episodes are suggested by lower $\delta^{18}O$ values centered at 4300 and 3400 years B.P. These were probably relatively short warmer spells during the Neoglaciation. These short-term fluctuation in climate are not well documented in core A as the temporal resolution of this core is too coarse. However, data for core A extend the record back to 4800 years B.P. Lower values for both $\delta^{18}O$ and $\delta^{13}C$ at 4500 years BP suggest wetter conditions while higher stable isotope values, lower luminescence, and darker color of formation deposited at 4800-4600 years BP suggest a period of drier conditions.

Significantly lower $\delta^{18}O$ and $\delta^{13}C$ values, stronger luminescence and lighter colors in both cores appear to record a 300-year wetter period centered at 2500 years BP during the Roman Warm Period (RWP), a period when Europe was warmer than today (Lamb, 1985). The following period, the Dark Age, 2200-1800 years BP was apparently drier at DeSoto Caverns as suggested by elevated stable isotope values in both cores. As mentioned above, by this time the climate at DeSoto Caverns had shifted from drier in the early ~2400s to wetter during the last 2000 years. The presence of abundant detrital materials at 20 cm in core A and 15 cm in core B also marks this climate shift and suggests that the materials were washed into the cave when the climate became wetter after a prolonged period of dry conditions.

After 1800 years ago, the stalagmites show a gradual trend toward lower values of $\delta^{13}C$ and $\delta^{18}O$ suggesting that the climate became wetter. This trend culminates at 1000 years BP and appears to end 800 years ago. As a result, lower $\delta^{18}O$ and $\delta^{13}C$ values and increased luminescence in the period 1100-770 years B.P. suggest wetter conditions during the Medieval

Warm Period (MWP). Marked peaks in $\delta^{18}O$ centered at 330 and 100 years B.P. in core A, and at 530 and 130 years B.P. in core B, may document significantly drier periods during the LIA. These peaks are separated by a trough in stable isotope values centered at 350 years ago.

Comparison with other Records

Proxy fluvial (Goman and Leigh, 2005; Leigh and Feeney, 1995; Leigh, 2006; 2008), sand dune (Otvos and Price, 2001; Otvos, 2004, 2005, 2006), and fossil pollen (Watts, 1969, 1971, 1975; Rich, 1984; Seielstad, 1994; Brook, 1996; LaMoreaus, 1999) data document millennial-scale climate variations in the Southeastern USA during the Holocene. These suggest that the Southeastern USA was generally drier in the late Holocene after the Holocene Optimum. By this time, the Laurentide ice sheet had completely melted (Dyke and Prest, 1987) and seasonality lessened (Berger and Loutre, 1991) due to reduced temperature differences between summer and winter in the Northern Hemisphere. As a result, processes influencing the climate of the Southeastern USA varied significantly compared to the Holocene Optimum. Enhanced ENSO activity beginning at 5 ka (Moy et al., 2002) probably played a more important role in late Holocene climate variation (LaMoreaux et al., manuscript in review). High-frequency alternating El Niño and La Niño events in the late-Holocene brought a more changeable climate to the Southeastern USA. This record is consistent with data presented here, which shows alternating wet and dry periods. Wetter periods documented by the DeSoto Caverns stalagmites centered at 260, 940, 2500, 3400 and 4300 years B.P. generally correspond with periods with an increase in the number of warmer ENSO events indicated by lake sediment data from southern Ecuador (Moy et al., 2002) (Fig. 5.8). As El Niño brings more winter and spring precipitation

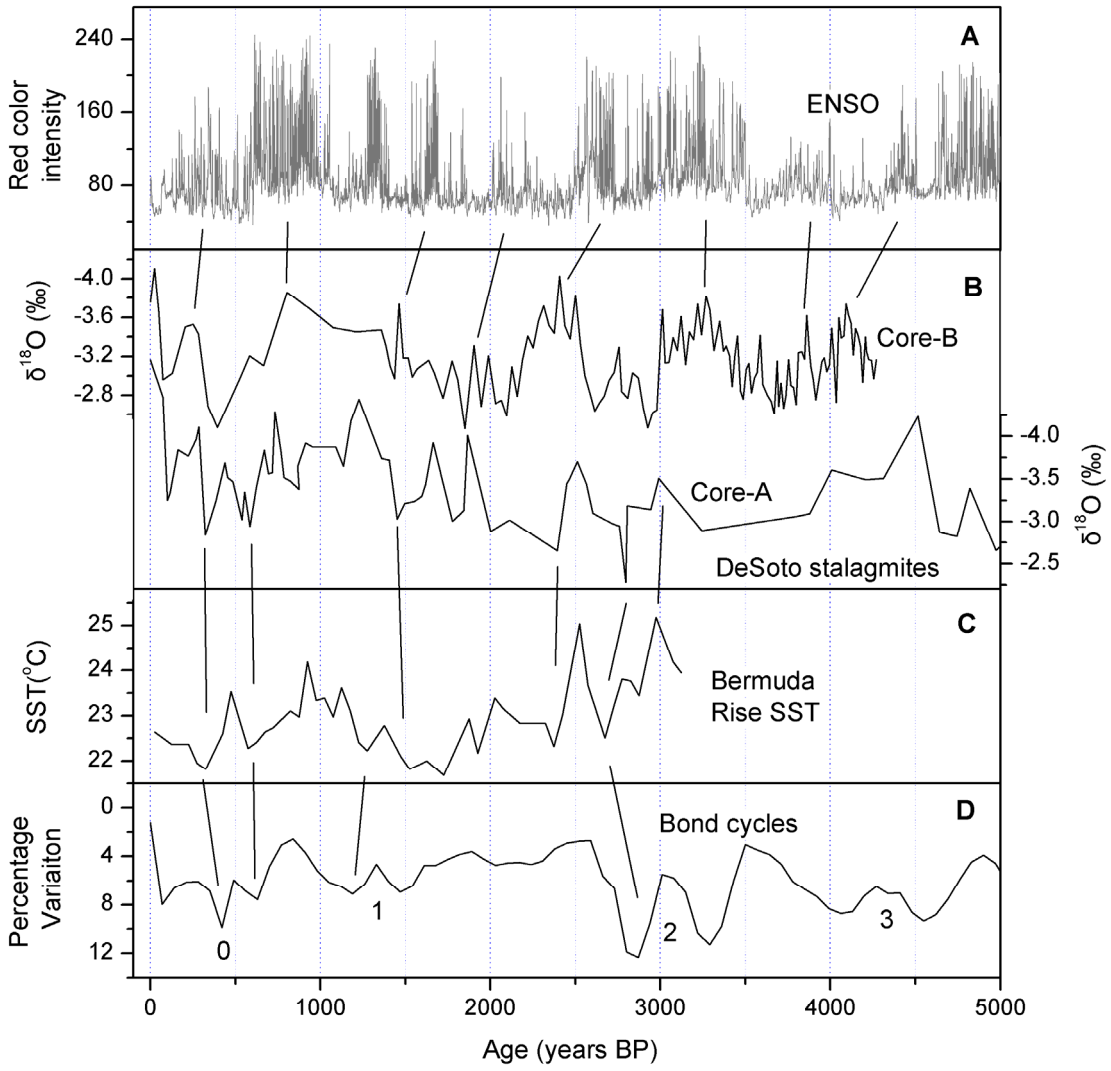

Figure 5.8. Comparison of the DeSoto $\delta^{18}O$ record (B) with reconstructed ENSO activity (A) from Laguna Pallcacocha of Ecuador (Moy et al., 2002), Bermuda Rise temperature (C) over the past 3500 years (Keigwin, 1996) and Bond Cycles of ice cover in the North Atlantic (D) over the last 5000 years (Bond et al., 2001).

with lower $\delta^{18}O$ to the southeastern USA today, it is likely that it also did so in the past. In fact, $\delta^{18}O$ values of carbonate in the two stalagmites examined here decreased slightly over the past 4400 years suggesting a slight increase in warm ENSO phases, and perhaps an increase in moisture availability in the Southeastern USA.

By comparing fossil and modern pollen abundances, Prentice et al. (1991) modeled Holocene climate at 3000-year intervals and found that precipitation 3000 years ago was slightly less than present. However, previous modeling by Kutzbach (1987) using the Community Climate Model (CCM) shows that the Southeastern USA received 20% more precipitation at 3000 years ago than present. The more recent results of Prentice et al. (1991) are supported by the DeSoto stalagmite data.

Drier conditions suggested by higher $\delta^{18}O$ values of stalagmite carbonate generally correlate with lower temperature in the Sargasso Sea (Keigwin et al., 1996), as well as in the high-latitude North Atlantic (Bond et al., 2001) (Fig. 5.8). This indicates that changes in moisture availability at DeSoto Caverns are probably linked to variations in sea surface temperature in the North Atlantic. Precipitation in the Southeastern USA mainly results from circulation around the western side of the Bermuda High situated over the Atlantic Ocean. During the past 100 years the Gulf of Mexico has been the dominant source of moisture and precipitation over both the Southeastern and Southwestern USA. According to Forman et al. (1995) the amount of precipitation is controlled mainly by the location of Bermuda High and this was probably also important during the late-Holocene. When the Bermuda High is located farther to the north and east, moisture from the Gulf of Mexico moves into the Southeastern USA and the east coast of North America. By contrast, the Central USA is wetter and the Southeastern USA drier when the Bermuda High is located more to the south and west, in which case moisture is mainly

transported to the Central United States instead of the Southeastern USA. This suggests that wetter periods at DeSoto Caverns may have been caused by a northeasterly movement of the Bermuda High and drier conditions by a southwesterly movement. It is likely that variations in ENSO activity linked with the position of the Bermuda High controlled the climate of the Southeastern USA during the late-Holocene.

The high temporal resolution of the DeSoto stalagmite record allows identification of conditions during "Holocene Event 3", the Roman Warm Period, the Dark Age, the Medieval Warm Period and the Little Ice Age, which are not apparent in published, lower-resolution pollen and fluvial records (Leigh, 2008). Elevated O^{18} and C^{13} values around 4000 years ago suggest a drier climate over the Southeastern USA during "Holocene Event 3" (Bond et al., 1997). Evidence for the possible global extent of this event is recorded by a reduction of ice cover on Kilimanjaro (Thompson et al., 2002), an increase in dolomite in sediment core M5-422 from the Gulf of Oman (Cullen et al., 2000), the collapse of the Akkadian Empire in Mesopotamia (deMenocal, 2000), a weakened Asian summer monsoon (Wang et al., 2005), collapse of Neolithic Cultures around the Central Plains of China (Wu and Liu, 2004), and an increase in dust in ice cores from the Andes of Northern Peru (Thompson et al., 2000). During this event, sea surface temperature in the North Atlantic dropped by 1º to 2ºC (Bond, 1997).

During the Roman Warm Period, the climate of Europe appears to have been warmer at ~2000 yr BP (Lamb, 1985). This warmer event is also documented by elevated O^{18} values at 2500-2000 years BP in the CC3 stalagmite from southwest Ireland (McDermott et al., 2001). Reconstructed temperatures from corals in the northern South China Sea also suggest a warmer period during this event (Yu et al., 2005). Although different in timing, the Roman Warm Period

may be represented in the DeSoto records by lower O^{18} and C^{13} values during the period from ~2600 to 2300 years B.P.

The Roman Warm Period was followed by a cooling of climate with glacial advances during the Dark Age, the period from 1500 to 1000 years BP (Lamb 1985). Data in both the CC3 (McDermott, 2001) and DeSoto stalagmites (this study) suggest that the Dark Age started shortly after 2000 years BP. During this event, the temperature in northern South China Sea was ~1º to 3.8ºC lower than during the 1990s (Yu et al., 2005).

The warmest part of the Medieval Warm Period in Europe was from AD 950-1100 (Lamb, 1985). However, it is not clear from the available data whether this was a synchronous global climate event (Bradley, 2000; Bradley et al., 2003). The Little Ice Age was a cool period lasting from AD 1550-1850, although there is significant regional variation in the timing (Bradley and Jones, 1995). Although the terms Medieval Warm Period and Little Ice Age were first used to describe climate events emphasizing temperature variations, they are also associated with hydrological anomalies (Stine, 1994). As mentioned above, the DeSoto stalagmites document a wetter Medieval Warm Period and a drier Little Ice Age in the Southeastern USA. Annual tree ring data from the Carolinas and Georgia have revealed a prolonged spring rainfall deficit during the mid-18^{th} century (Stahle et al., 1988) that corresponds with a dry spell during the Little Ice Age in the DeSoto record. However, there are no proxy records for the Southeastern USA on moisture availability during the Medieval Warm Period. Evidence from the Great Plains and Southwestern USA suggests prolonged drier conditions at this time and a wetter Little Ice Age (e.g, Stine, 1994, Fritz et al., 1994; Laird et al., 1996; Cook et al., 2004; Sridhar et al., 2006; Meyer et al., 1995; Castiglia and Fawcett, 2006), indicating significant regional climate variations across North America at this time.

The two drier periods in the DeSoto stalagmite records during the Little Ice Age, centered at ~AD 1530 and ~1800, correspond well with two distinct cooling events in sediment cores from the Bermuda Rise (Keigwin, 1996) and eastern subtropical North Atlantic (deMenocal et al., 2000). The correspondence suggests that climate change during the Medieval Warm Period and Little Ice Age at DeSoto Caverns, and possibly during earlier periods, was associated with variations in conditions in the low-latitude North Atlantic.

Conclusions

Vertical cores drilled from two active stalagmites in DeSoto Caverns in Alabama have provided the first absolute-dated, high-resolution record of climate change for the Southeastern USA during the last 4400 years. Good correspondence between the stable isotope and luminescence data from the two stalagmites strongly suggests that these variables are recording regional climate change and not stalagmite-specific hydrological events. Both records document alternating wetter and drier climates over the past 4400 years and clearly indicate a wetter Roman Warm Period and Medieval Warm Period, and a drier Dark Age and Little Ice Age in the Southeastern USA. The stalagmite records correspond well with Bermuda Rise sea surface temperature variations suggesting that moisture availability in the Southeastern USA during the Holocene was associated with the thermal contrast between the North American landmass and the North Atlantic Ocean.

References

Berger, A. and Loutre, M. F., 1991. Insolation values for the climate of the last 10 million years. *Quaternary Science Reviews* 10, 297–317.

Bond, G., Showers, W., Cheseby, M., Lotti, R., Almasi, P., deMenocal, P., Priore, P., Cullen, H., Hajdas, I. and Bonani, G., 1997. A Pervasive Millennial-Scale Cycle in North Atlantic Holocene and Glacial Climates. *Science* 278, 1257-1266.

Bradley, R., 2000. 1000 Years of Climate Change. *Science* 288, 1353-1355.

Bradley, R. S. and Jones, P. D., 1995: Recent developments in studies of climate since A.D. 1500. In Bradley, R. S. and Jones, P. D., editors, Climate Since AD 1500 [Revised Edition], London: Routledge, 666-679.

Bradley, R. S., Hughes, M. K. and Diaz, H. F., 2003. Climate change: Climate in Medieval Time. *Science* 302, 404-405.

Brady, N.C. and Weil, R.R., 1999. The nature and properties of soils. 12th ed. Prentice Hall, Upper Saddle River, NJ. 881p.

Brook, F. Z., 1996. A late-quaternary pollen record from the Middle Ogeechee River Valley, Southeastern Coastal Plain, Georgia. Master Thesis, University of Georgia, Athens, Georgia.

Brook, G. A., Ellwood, B. B., Railsback, L. B. and Cowart, J. B., 2006. A 164 ka record of environmental change in the American southwest from a Carlsbad Cavern speleothem. *Palaeogeography, Palaeoclimatology, Palaeoecology* 237, 483-507.

Castiglia, P. J. and Fawcett, P. J., 2006. Large Holocene lakes and climate change in the Chihuahuan Desert. *Geology* 34, 113-116.

Cheng, H., Edwards, R.L., Hoff, J., Gallup, C.D., Richards, D.A. and Asmerom, Y., 2000. The Half-lives of uranium-234 and thorium-230. *Chemical Geology* 169, 17-33.

Cook, E. R., Woodhouse, C. A., Eakin, C. M., Meko, D. M. and Stahle, D. W., 2004. Long-term aridity changes in the western United States. *Science* 306, 1015-1018.

Cullen, H. M., deMenocal, P. B., Hemming, S., Hemming, G., Brown, F. H., Guilderson, T. and Sirocko, F. 2000. Climate change and the collapse of the Akkadian empire: Evidence from the deep sea. *Geology* 28, 379-382.

Delcourt, P. A., 1980. Goshen Springs: Late Quaternary Vegetation Record for Southern Alabama. *Ecology* 61, 371-386.

deMenocal, P. B., 2001. Cultural Responses to Climate Change During the Late Holocene. *Science* 292, 667-673.

deMenocal, P., Ortiz, J., Guilderson, T. and Sarnthein, M., 2000. Coherent high- and low-latitude climate variability during the Holocene warm period. *Science* 288, 2198-2202.

Dyke, A.S. and Prest, V.K., 1987. Late-Wisconsinan and Holocene history of the Laurentide Ice Sheet. *Geographie Physique et Quaternaire* 41, 237– 263.

Edwards, R. L, Chen, H. and Wasserburg, G. J., 1987. ^{238}U–^{234}U–^{230}Th–^{232}Th Systematics and the precise measurement of time over the past 500,000 years, *Earth and Planetary Science Letters* 81,175–192.

El-Farhan, Y. H., Denovio, N. M., Herman, J. S. and Hornberger, G. M., 2000. Mobilization and transport of soil particles during infiltration experiments in an agricultural field, Shenandoah Valley, Virginia. *Environmental Science and Technology* 34, 3555-3559.

Forman, S. L., Oglesby, R., Markgraf, V. and Stafford, T., 1995. Paleoclimatic significance of late quaternary eolian deposition on the piedmont and high plains, central United States. *Global and Planetary Change* 11, 35-55.

Friedman, I. and O'Neil, J. R., 1977. Compilation of stable isotope fractionation factors of geochemical interest: U.S. Geological Survey, Professional Paper 440-KK, p. 1–12.

Frisia, S., Borsato, A., Fairchild, I. J., McDermott, F. and Selmo, E. M., 2002. Aragonite-Calcite Relationships in Speleothems (Grotte De Clamouse, France): Environment, Fabrics, and Carbonate Geochemistry. *Journal of Sedimentary Research* 72, 687-699.

Fritz, S. C., Engstrom, D. R. and Haskell, B. J., 1994. 'Little Ice Age' aridity in the North American Great Plains: a high-resolution reconstruction of salinity fluctuations from Devils Lake, North Dakota, USA. *The Holocene* 4, 69-73.

Goman M. Leigh D. S., 2005. Comment on "Holocene aridity and storm phases, Gulf and Atlantic Coasts, USA" by Ervin G. Otvos, 2005, *Quaternary Research* 63, 368-373 Quaternary Research 66,182-184.

Goman, M. and Leigh, D. S., 2004. Wet early to middle Holocene conditions on the upper Coastal Plain of North Carolina, USA. *Quaternary Research* 61, 256-264.

Hendy, C. H., 1971. The isotopic geochemistry of speleothems, 1. the calculation of the effects of different modes of formation on the isotopic composition of speleothems and their applicability as paleoclimatic indicators. *Geochimica et Cosmochimica Acta* 35, 801-824.

Keigwin, L. D., 1996. The Little Ice Age and Medieval Warm Period in the Sargasso Sea. *Science* 274, 1504-1508.

Kutzbach, J. E., 1987. Model simulations of the climatic patterns during the deglaciation of North America. In: Ruddiman, W.F., H.E. Wright, Jr., (Eds.). North America and Adjacent Oceans During the Last Deglaciation. Geological Society of America, Boulder, CO, pp. 425-446.

Laird, K. R., Fritz, S. C., Maasch, K. A. and Cumming, B. F., 1996. Greater drought intensity and frequency before AD 1200 in the Northern Great Plains, USA. *Nature* 384, 552-554.

Lamb, H. H., Climatic history and the future. Princeton University Press, 1985.

LaMoreaux, H. K., Brook, G. A. and Knox, J. A., 2008. Late Pleistocene and Holocene environments of the southeastern USA from the stratigraphy and pollen content of a peat deposit on the Georgia Coastal Plaint. Submitted to *Palaeogeography, Palaeoclimatology, Palaeoecology*.

LaMoreaux, H.K., 1999. Human-environmental relationships in the coastal plain of Georgia based on high-resolution paleoenvironmental records from three peat deposits. Ph.D. Dissertation, University of Georgia, Athens, GA.

Lauritzen, S.-E., Ford D. C. and Schwarz, H. P., 1986. Humic substances in speleothems matrix-paleoclimate significance. *Proceedings of the 9th International Congress of Speleology* 2, 77-79, Barcelona, August, 1986.

Leigh, D. S., 2006. Terminal Pleistocene braided to meandering transition in rivers of the southeastern USA. *Catena* 66, 155-160.

Leigh, D. S. and Feeney, T. P., 1995. Paleochannels indicating wet climate and lack of response to lower sea level, Southeast Georgia. *Geology* 23, 687-690.

Leigh, D.S., 2008. Late Quaternary climates and river channels of the Atlantic Coastal Plain, Southeastern USA. Geomorphology, doi: 10.1016/j.geomorph.2008.05.024

McDermott, F., Mattey, D. P. and Hawkesworth, C., 2001. Centennial-Scale Holocene Climate Variability Revealed by a High-Resolution Speleothem delta ^{18}O Record from SW Ireland. *Science* 294, 1328-1331.

Meyer, G.A., Wells, S.G. and Jull, A.J.T., 1995, Fire and alluvial chronology in Yellowstone National Park: Climatic and intrinsic controls on Holocene geomorphic processes. Geological Society of America Bulletin 107, 1211–1230.

Moy, C. M., Seltzer, G. O., Rodbell, D. T. and Anderson, D. M., 2002. Variability of El Nino/Southern Oscillation activity at millennial timescales during the Holocene epoch. *Nature* 420, 162-165.

Otvos, E. G., 2004. Prospects for interregional correlations using Wisconsin and Holocene aridity episodes, northern Gulf of Mexico Coastal Plain. *Quaternary Research* 61, 105-118.

Otvos, E. G., 2005. Holocene aridity and storm phases, Gulf and Atlantic Coasts, USA, *Quaternary Research* 63, 368–373.

Otvos, E. G., 2006. Reply to letter to the editor from Goman and Leigh re: Quaternary Research 63, 368-373. *Quaternary Research* 66, 185-186.

Otvos, E. G. and Price, D. M., 2001. Late Quaternary inland dunes of southern Louisiana and arid climate phases in the Gulf Coast Region. *Quaternary Research* 55,150-158.

Prentice, I.C., Bartlein, P.J., Webb, T., 1991. Vegetation and climate change in eastern North America since the Last Glacial Maximum. *Ecology* 72(6), 2038-2056.

Railsback, L. B., 2000. An atlas of speleothem microfabrics: http://www.gly.uga.edu/speleoatlas/SAindex1.html.

Railsback, L. B., Dabous, A. A., Osmond, J. K. and Fleisher, C. J., 2002. Petrographic and geochemical screening of speleothems for u-series dating: an example from recrystallized speleothems from Wadi Sannur Cavern, Egypt. *Journal of Cave and Karst Studies* 64, 108-116.

Ramseyer, K., Miano, T., D'Orazio, V., Wildberger, A., Wagner, T. and Geister, J., 1997. Nature and origin of organic matter in carbonates from speleothems, marine cements and coral skeletons. *Organic Geochemistry* 26, 361–78.

Rich, F. J., 1984. An ancient flora of the eastern okefenokee swamp as determined by palynology. In: The Okefenokee Swamp: Its Natural History, Geology, and Geochemistry. Cohen, A.J., Casagrande, D.J., Andrejko, M.J., Best, G.R., (eds) Wetland Surveys, Los Alamos, NM.

Seielstad, C.A., 1994. Holocene environmental history at Chatterton Springs on the southern Coastal Plain of Georgia. Unpublished Master Thesis. Department of Geography, University of Georgia. Athens. 153pp.

Shen, C.-C., Edwards, R. L., Cheng, H., Dorale, J. A., Thomas, R. B., Moran, S. B., Weinstein, S. and Edmonds, H. N., 2002. Uranium and thorium isotopic and concentration measurements by magnetic sector inductively coupled plasma mass spectrometry. *Chemical Geology* 185,165–178.

Shopov, Y. Y., Ford, D. C. and Schwarcz, H. P., 1994. Luminescent microbanding in speleothems: high-resolution chronology and paleoclimate. *Geology* 22, 407-410.

Sridhar, V., Loope, D. B., Swinehart, J. B., Mason, J. A., Oglesby, R. J. and Rowe, C. M., 2006. Large wind shift on the Great Plains during the Medieval Warm Period. *Science* 313, 345-347.

Stahle, D. W. and Cleaveland, M. K., 1994. Tree-ring reconstructed rainfall over the Southeastern U.S.A. during the Medieval Warm Period and Little Ice Age. *Climatic Change* 26, 199-212.

Stahle, D. W., Cleaveland, M. K. and Hehr, J. G., 1988. North Carolina climate changes reconstructed from tree rings: A.D. 372 to 1985. *Science* 240, 1517-1519.

Stine, S. 1994. Extreme and persistent drought in California and Patagonia during mediaeval time. *Nature* 369, 546-549.

Thompson, L. G., Mosley-Thompson, E. and Henderson, K. A., 2000. Ice-core palaeoclimate records in tropical South America since the Last Glacial Maximum. *Journal of Quaternary Science* 15, 377-394.

Thompson, L. G., Mosley-Thompson, E., Davis, M. E., Henderson, K. A., Brecher, H. H., Zagorodnov, V. S., Mashiotta, T. A., Lin, P.-N., Mikhalenko, V. N., Hardy, D. R. and Beer, J., 2002. Kilimanjaro Ice Core Records: Evidence of Holocene Climate Change in Tropical Africa. *Science* 298, 589-593.

Wang, Y., Cheng, H., Edwards, R. L., He, Y., Kong, X., An, Z., Wu, J., Kelly, M. J., Dykoski, C. A. and Li, X., 2005. The Holocene Asian Monsoon: Links to Solar Changes and North Atlantic Climate. *Science* 308, 854-857.

Watts, W. A., 1969. A pollen diagram from Mud Lake, Marion County, North-central Florida. *Geological Society of America Bulletin* 80, 631-642.

Watts, W. A., 1971. Postglacial and interglacial vegetation history of southern Georgia and central Florida. *Ecolog*y 52,676-690.

Watts, W. A., 1975. A Late-Quaternary record of vegetation from Lake Annie, South-Central Florida. *Geology* 3, 344-346.

Watts, W. A., 1980. Late-Quaternary vegetation history at White Pond on the Inner Coastal-Plain of South-Carolina. *Quaternary Research* 13, 187-199.

Webster, J. W., Brook, G. A., Railsback, L. B., Cheng, H., Edwards, R. L., Alexander, C. and Reeder, P. P., 2007. Stalagmite evidence from belize indicating significant droughts at the time of Preclassic Abandonment, the Maya Hiatus, and the Classic Maya Collapse. *Palaeogeography, Palaeoclimatology, Palaeoecology* 250, 1-17.

Wu, W. and Liu, T., 2004. Possible role of the "Holocene Event 3" on the collapse of Neolithic Cultures around the Central Plain of China. *Quaternary International* 117, 153-166.

Yu, K.-F., Zhao, J.-X., Wei, G.-J., Cheng, X.-R., Chen, T.-G., Felis, T., Wang, P.-X. and Liu, T.-S. 2005. $\delta^{18}O$, Sr/Ca and Mg/Ca records of Porites lutea corals from Leizhou Peninsula, northern South China Sea, and their applicability as paleoclimatic indicators. *Palaeogeography, Palaeoclimatology, Palaeoecology* 218, 57-73.

CHAPTER 6

PALEOENVIRONMENTAL CHANGE IN THE SOUTHEASTERN USA DURING THE LATE PLEISTOCENE AND HOLOCENE: EVIDENCE FROM A SPELEOTHEM IN DESOTO CAVERNS, ALABAMA*

*Fuyuan Liang, George A. Brook, L. Bruce Railsback, to be submitted to *Quaternary Research*.

Abstract

Evidence from mineralogy, stable isotopes, gray color, and luminescence along the growth direction of a slab cut from a collapsed column obtained near the entrance of DeSoto Caverns, Alabama, provides an absolute-dated record of paleoenvironmental change over the Southeastern USA during the periods from ~37 to 30 ka and from ~13 to 3ka B.P. Dominance of calcite with more negative $\delta^{13}C$ values, darker color, and weaker luminescence in the inner section of the slab (from 12 to 7 cm) indicates a generally wetter climate during the periods from ~37 to 30 ka and from ~13 to 6 ka. Conversely, climate over the Southeastern USA was generally drier during period from 6 to 3 ka B.P., as suggested by deposition of aragonite with more positive $\delta^{13}C$ values, lighter color, and stronger luminescence in the outer part of the slab (from 7 cm to the edge). Paleoenvironmental variations inferred from our DeSoto slab agree well with records of fossil pollen, fluvial sediment, and river channel patterns from the Southeastern USA, suggesting a wetter early Holocene and drier later Holocene. Our study also illustrates that record derived from the horizontal direction of a speleothem deposited in cave also has potential to provide useful information about past climate change, although the $\delta^{18}O$ variable is not as reliable as that derived from the vertical direction along the central growth axis of stalagmite. In addition, our study also suggests that dirty speleothem formation is valuable in recording paleoenvironmental conditions in spite of the relative large uncertainty of chronology due to the possible thorium contamination in the samples.

Key words: Speleothem, stable isotopes, Luminescence, Holocene, Southeastern USA

Introduction

Cave speleothems are a valuable archive of paleoclimatic information because they can provide long records of environmental change and at the same time can be dated precisely by U-series techniques. So far, stalagmites have been the main focus of paleoclimatic research as they may be deposited in isotopic equilibrium with precipitating waters and so can potentially provide proxy temperature data, but some studies have examined other speleothem deposits including stalactites and flowstones (e.g. Baker et al., 1995; Yadava and Ramesh, 2005). Most previous studies have targeted clean formations as these contain little detrital ^{230}Th and so can be dated more reliably. However, detrital materials can in some cases be evidence of important paleoclimate events. For example, detrital non-carbonate materials in two Holocene stalagmites from Southern China record intense rainfall events, which washed the materials into the cave (Liang et al., Chapter 3 of this dissertation, Xiao et al., manuscript in prep.). Also, clay-size materials in a Belize stalagmite recorded a drier climate favoring airborne transportation and preservation because a reduction in drip water rate failed to wash them from the top of the stalagmite (Webster et al., 2007).

Most published stalagmite records are based on variations in isotopes along the central growth axis of the formation, although variations along a horizontal radial axis can also provide valuable information (Brook et al., 2006). Here we present a record from a collapsed column that formed near the expanded natural entrance of DeSoto Caverns, Alabama. The column was broken when the artificial entrance was expanded by blasting to make it large enough for

vehicular access. A portion of the broken column was recovered with the permission of Al Mathis, the owner of the cave. In the laboratory two horizontal slabs about 5 cm thick were cut from the column for analysis. The slabs show distinct radial layering with bands of relatively clear carbonate interspersed with reddish-brown layers containing abundant detrital clay.

Paleoenvironmental conditions in the Southeastern USA during the Holocene are hotly debated (Goman and Leigh, 2004, 2005; Otovos et al., 2005, 2006), with records from pollen and fluvial sediments suggesting wetter conditions during the early Holocene while evidence from sand dunes indicates drier conditions. In this paper a record of environmental conditions from DeSoto Caverns is presented that adds information to this debate. The record is the first absolute-dated Holocene record derived from speleothems in the Southeastern USA.

DeSoto Caverns

DeSoto Caverns is a tourist cave (33°18′24″N, 86°16′39″W, 160 m above mean sea level) situated in the Ridge and Valley province of southern foothills of the Appalachian Mountains. The cave is 8 km east of Childersburg and 70 km southeast of Birmingham, Alabama (Fig. 6.1). Speleothems are common in DeSoto Caverns, which has formed in undifferentiated Knox Group Ordovician-Cambrian dolomite. The modern climate near the cave is humid and warm, with 1410 mm of annual precipitation. Rainfall is well distributed through the year with slightly more during the winter months. Summers are hot and winters mild; mean annual temperature is 17.2°C.

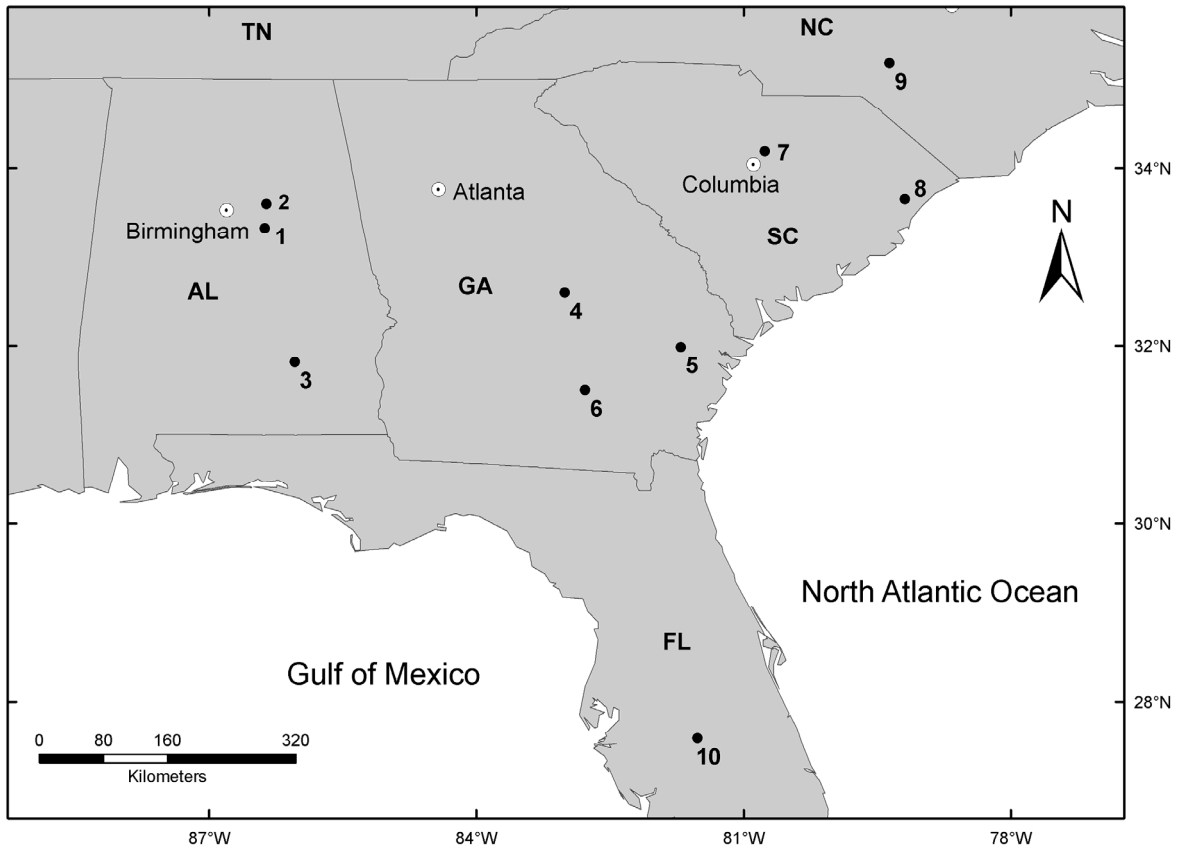

Figure 6.1. Map showing the location of DeSoto Caverns and other key paleoenvironmental sites in the Southeastern USA.: 1) DeSoto Caverns (this study); 2) Cahaba Pond, AL (Delcourt et al., 1983); 3) Goshen Spring, AL (Delcourt, 1980); 4) Sandy Run Creek (LaMoreaux, 1999); 5) Cooperville, GA (Brook, 1996); 6) Chatterton Springs, GA (Seielstad, 1994); 7) White Pond, SC (Watts, 1980); 8) Clear Pond, SC (Watts et al., 1996); 9) PAW, NC (Goman and Leigh, 2004); 10) Lake Tulane, FL (Huang et al., 2006).

Methodology

Two 5 cm thick slabs were cut from the broken column and one face was polished and then scanned at 300 dpi resolution and 8 bits gray level using a flat-bed scanner (Fig. 6.2). The polished surface was then illuminated by ultraviolet light in a darkroom and resulting luminescence was recorded by a 6-megapixel Nikon D70 digital camera. The camera was fitted with a Kodak Wratten Geltain Filter #2E to prevent transmission of the UV excitation energy band. Variations in gray level and luminescence were measured using Erdas Imagine along a series of linear transects on the digital images that were oriented perpendicular to the growth direction (Fig. 6.3B). Based on our dating results, the scanned data provide proxy information at decadal resolution (15 years per pixel for gray color and 30 years for luminescence).

Seventeen samples were drilled from relatively clean carbonate for ICP-MS U-series dating in the Stable Isotope Laboratory at the University of Minnesota following procedures described in Cheng et al., (2000), Edwards et al., (1987), and Shen et al., (2002). The ages of detritus-rich layers were bracketed by dating older and younger clear carbonate layers. Ages were calculated using half-lives determined by Cheng et al., (2000) and are reported with analytical errors of 2σ of the mean (Table 6.1).

Four 51mm x 76 mm thin sections were prepared from chips cut from the slab. Speleothem carbonate microfabrics, including mineralogy, and the shape and size of crystal layering were studied by examining thin sections with a Leica DMLP petrographic microscope. A ~0.5 cm thick slice was cut from the slab and mounted to the stage of a New Wave micromilling system

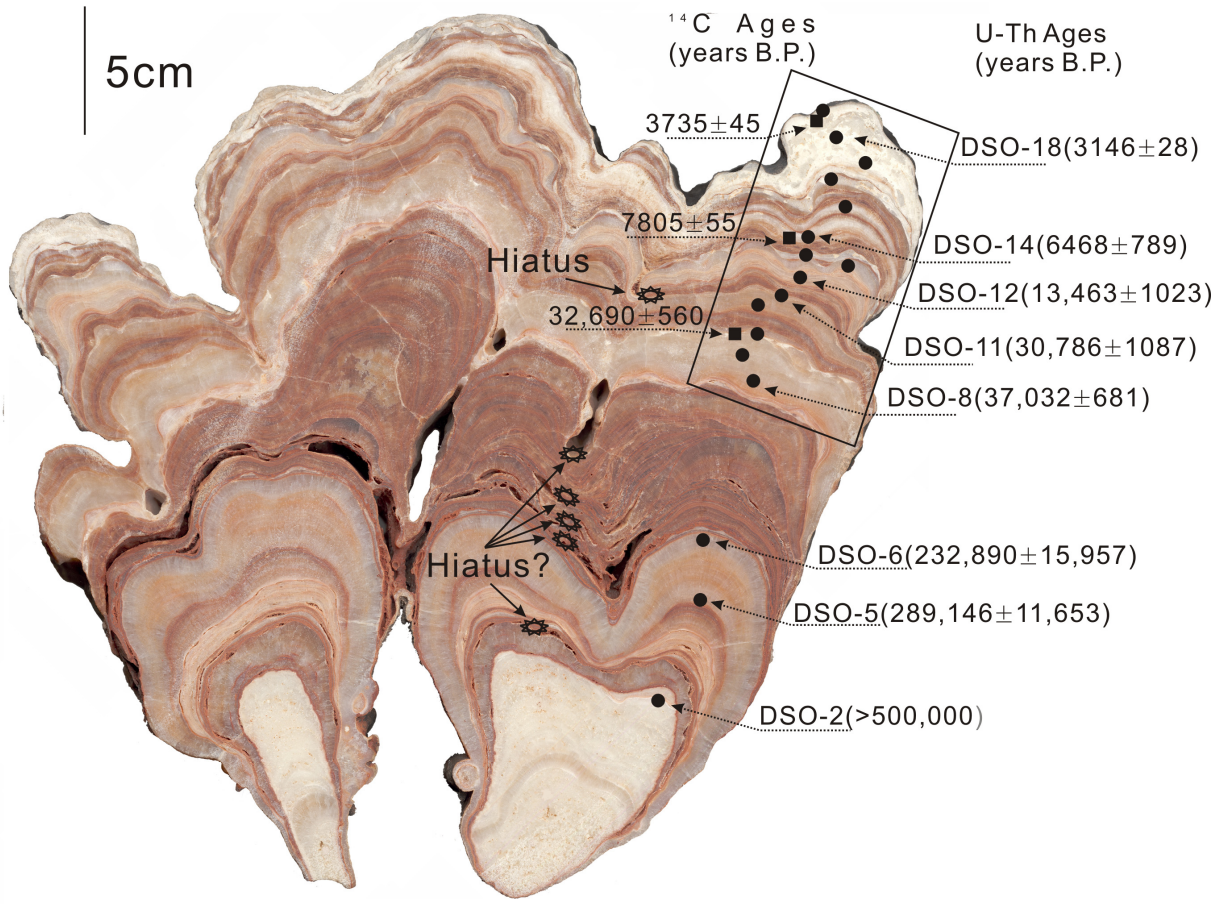

Figure 6.2. Scanned image of the DeSoto Caverns column showing radiocarbon (black solid square) and major U-series ages (black solid circle). The rectangle shows the area of Figure 6.3B.

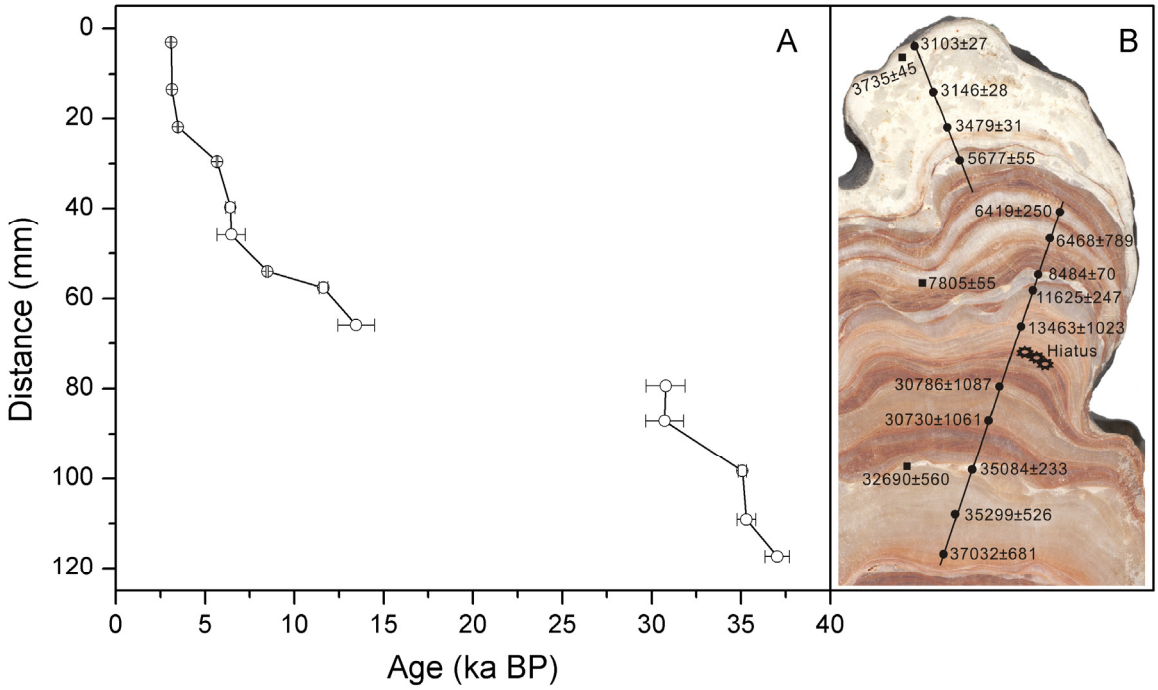

Figure 6.3. Characteristics of the outer 12 cm of the DeSoto Caverns column. (A) Relationship between depth and age, (B) scanned image showing radiocarbon (solid square) and U-series ages (solid circle), and transects used to determine variations in color, luminescence and O and C isotopes (see Fig. 6.4).

using double sided tape. Samples were milled from the slice along a transect at an interval of 3mm in the outer section (from the edge to 7 cm) and at 0.6mm in the inner section (from 7 to 12 cm). In total, 109 samples were obtained for stable isotope analysis at the Savannah River Ecology Laboratory of the University of Georgia following procedures outlined in Jimenez-Lopez and Romanek (2004). Approximately 150 ±50 μg of carbonate powder was loaded into 10 ml vacutainers^{TM} and flushed with helium gas. Concentrated phosphoric acid was injected into the vacutainers^{TM} to dissolve carbonate and samples were left to react overnight. Stable isotope measurements were then performed on a Finnigan DeltaplusXL isotope ratio mass spectrometer operated in continuous flow mode (CF-IRMS) using the Gasbench II peripheral device. Replicates were run for every tenth sample and standards were run for every five samples. The analytical precision was ±0.2‰ (1σ) based on the repeated measurement of standard NBS-19. All isotope measurements are reported in ‰ units versus the V-PDB standard using conventional delta (δ) notation (Craig, 1957).

Chronology

The ages obtained are in stratigraphic order within dating uncertainty (Table 6.1). Errors range from 0.6% to 12% with lower values for white, clean carbonate. For example, samples from 9.8, 5.4, 22, 14, and 0.2 cm depth provided ages with errors less than 1%. In contrast, large errors are associated with samples drilled from light-brown bands (e.g. DSO-12 and DSO-14) that appear to contain significant detrital ^{232}Th, as suggested by generally low

Table 6.1. Uranium and thorium isotopes and ^{230}Th ICP-MS ages for the DeSoto column.

Sample ID	Depth (mm)	^{238}U ppb	^{232}Th ppt	d^{234}U measured[a]	[^{230}Th/^{238}U] activity[c]	[^{230}Th/^{232}Th] ppm[d]	Age uncorrected	Age corrected [c,e]	d^{234}U$_{initial}$ corrected
DSO-19	3	1733±3.8	1164.34±7.8	406.26±2.5	0.03972±0.00033	973.8±10.1	3117±27	3103±27	409.8±2.5
DSO-18	13.4	1574.22±3.6	889.39±8	395.86±2.4	0.03992±0.00033	1164±14	3157±27	3146±28	399.4±2.4
DSO-17	21.9	1099.86±2.5	457.56±6.5	407.11±2.5	0.04439±0.00037	1757.9±28.8	3488±30	3479±31	411.1±2.6
DSO-16	29.6	1356.89±2.6	3259.87±11.8	436.82±2.3	0.07374±0.00062	505.6±4.5	5725±50	5677±55	443.9±2.4
DSO-15	39.7	136.35±0.3	2572.81±10.3	436.98±4.2	0.0872±0.00201	76.1±1.8	6800±163	6419±250	445±4.3
DSO-14	45.9	128.74±9.4	6178.32±451.2	422.28±5.2	0.09432±0.00407	32.4±1.4	7449±378	6468±789	430.1±5.4
DSO-13	54	99.39±0.2	365.23±1.1	415.35±2.2	0.10732±0.00069	481.1±3.3	8559±59	8484±70	425.4±2.3
DSO-12A	57.6	110.61±0.3	472.38±7.4	373.06±4.6	0.1406±0.00273	542.3±13.5	11,715±243	11,625±247	385.5±4.8
DSO-12	65.8	196.15±0.4	17662.57±66.4	393.85±3.5	0.18414±0.00443	33.7±0.8	15,337±396	13,463±1023	409.1±3.8
DSO-11	79.4	89.16±0.2	8039.67±20.8	378.85±4.5	0.36156±0.00514	66.1±0.9	32,657±549	30,786±1087	413.3±5.1
DSO-10	87.1	57.76±0.2	4562.52±16.2	401.04±6.3	0.36373±0.0066	76±1.4	32,340±695	30,730±1061	472.7±2.1
DSO-9	98.3	1893.29±93.1	10968.36±539.5	428.06±1.9	0.399315±0.00206	1137.8±1.4	35,198±218	35,084±233	437.4±7.0
DSO-8A	109.1	97.56±0.3	1570.43±8.7	391.93±5.1	0.39361±0.00453	402.8±5	35,626±502	35,299±526	433.1±5.6
DSO-8	117.3	90.51±0.2	3514.83±13.2	416.87±4.6	0.421±0.00515	179±2.2	37,807±563	37,032±681	462.9±5.2
DSO-6	173.9	23.99±0.1	3373.72±12.9	218.87±12.9	1.13072±0.0197	132.5±2.3	235801±16313	232,890±15957	422.7±32.3
DSO-5	198.1	42.97±0.1	3091.34±8.4	237.95±6	1.22002±0.00897	279.4±2.1	290,514±11773	289,146±11653	538.8±23.1
DSO-2	236.2	1442.6±70.1	1106±54	42.1±1.6	1.060596±0.00380	2831±97	>500,000	>500,000	

Analytical errors are 2 of the mean. Decay constants are 9.1577 x 10^{-6} yr^{-1} for ^{230}Th, 2.8263 x 10^{-6} yr^{-1} for ^{234}U, and 1.55125 x 10^{-10} yr^{-1} for ^{238}U (Cheng et al., 2000). [a] The degree of detrital ^{230}Th contamination is indicated by the [^{230}Th/^{232}Th] atomic ratio instead of the activity ratio. [b]Age corrections were calculated using an average crustal ^{230}Th/^{232}Th atomic ratio of 4.4 x 10^{-6} ± 2.2 x 10^{-6}. Those are the values for a material at secular equilibrium, with the crustal ^{232}Th/^{238}U value of 3.8. The errors are arbitrarily assumed to be 50%.

$^{230}Th/^{232}Th$ ratios (Table 6.1). One sample from the clear carbonate core of the formation 23.6 cm from the outer surface gave an age of >500 ka, showing that deposition of the column began more than half a million years ago. Two samples at 17.4 and 19.8 cm depth dated to 289 ±12 and 233 ±16 ka respectively indicating periodic deposition of the column for a considerably period after it began forming. Partings after the >500 ka and 289 ±12 ka samples suggest major hiatuses in deposition and input of detrital material that covered the column at these times. Relatively clean calcite was deposited from 289 ±12 ka to 233 ±16 ka, a colder period of OIS 8 and the early part of OIS 7. Carbonate deposited after 233 ±16 ka and before 37 ±0.7 ka consists mainly of light-brown layers and could not be dated precisely. Development of cavities in this section suggests at least four hiatuses in deposition, although we cannot determine the duration of these no-growth periods.

Layers of the column from 12-7.9 cm depth date from 37 ±0.7 ka to 31 ±1 ka (corresponding to part of OIS 3) indicating rapid deposition in this time period. A hiatus is apparent at ~7 cm, which lasted from ~31-13.5 ka B.P. (mainly OIS 2). After this, deposition was continuous until ~3 ka ago when the column finally stopped growing (Figs 6.3A & B). Hence, the DeSoto column provides paleoenvironmental information for intervals back to >500 ka but only continuous records for the intervals 37-30 and ~13.5-3 ka ago. This paper will focus on these two periods of continuous deposition. Three calibrated radiocarbon ages shown in Figure 6.3B generally agree with the U-series chronology for the periods of interest, providing a further indication that the chronology is reliable and these ages are not affected by the presence of detrital material. Using the ages in Table 6.1, a chronology was established and assigned to the proxy variables of $\delta^{18}O$, $\delta^{13}C$, gray level, and luminescence.

Petrography

The more recent part of the column to 3 cm depth consists mainly of zones of primary aragonite interspersed with zones of secondary calcite. However, from 3-12 cm the carbonate is mainly columnar calcite with several layers of aragonite and possibly some secondary calcite. Aragonite in the outer part of the column forms bundles of needles, with typical crystals up to 3 mm in length. About half of the aragonite has converted to secondary columnar or equant calcite, usually with aragonite relicts within the crystals of secondary calcite. Almost all aragonite in this section is clean, except for two layers at 2.3 and 2.8 cm depth that contain dark brown detrital minerals. Most of the aragonite in these two layers has been replaced by calcite.

The older, inner section of the column, from 3-12 cm depth, consists mainly of columnar calcite, with typical crystals up to 0.5 mm long and 0.2 mm wide, except for a chaotic and probably secondary calcite layer from 7-7.2 cm, which probably developed at the beginning or end of the hiatus from 30-13.5 ka. Zones of columnar calcite at 3.94-3.98, 4.1-4.6, 5.72-5.79, and 9.8-11.8 cm are relative clear, while calcite in other parts of the column is light or dark brown in color, suggesting the presence of detrital clay. Particle size of these materials is up to 0.1 mm, suggesting that they were mainly transported into the cave by water, probably by increased flow as a result of periodic intense rainfalls.

At least three layers of unaltered or partly altered aragonite are evident in this section. The first layer at 4.5 cm depth is ~2 mm thick and is characterized by porous short bundles of aragonite needles. The second and the third layers occur at 5.4 and 9.8 cm depth and here the aragonite has been replaced by equant calcite, although some small patches of unaltered aragonite remain. These two aragonite layers contain little detrital material and as a result are white in color.

Deposition of aragonite cannot be ascribed solely to the lithology of the dolomitic host rock, as both calcite and aragonite can be deposited in caves in dolomite (e.g. this study) and in limestone caves (Ch. 4, this dissertation, Xiao et al., manuscript in prep.). Transformation from calcite dominance in the inner part of the column (from 12 to 3 cm) to aragonite dominance in the outer part (from 3 cm to the edge) suggests a shift from wetter to drier conditions at the cave as calcite is usually deposited under wetter/cooler conditions while aragonite is more likely to be deposited under warmer/drier conditions (Siegel and Dort, 1966; Murray, 1954; Thrailkill, 1971; Reams, 1972; Cabrol and Coudray, 1982; Railsback et al., 1994; Denniston et al., 2002). As a result, layers of aragonite in the inner part of the column suggest brief stages of drier/warmer climate during a prolonged period of relatively wet climate. White calcite layers are more likely to suggest periods with less intense precipitation, while those of light or dark brown color were probably deposited when there were intense rains, which washed soil into the cave and onto the column.

Luminescence and Gray Color

Gray color and luminescence vary significantly along the linear transects, ranging from 90 to 253 and 45 to 254 respectively (Fig. 6.4A, B). Variations in gray color generally parallel those of luminescence, layers with less or no detrital material having higher values while light or dark brown bands containing varying amounts of detrital particles have much lower values. The reddish to reddish-brown color of layers rich in detrital particles suggests addition of red clay washed in from soils overlying the cave. When detrital materials are present this quenches luminescence emitted by organic acids (van Beynen et al., 2001). As a result, darker layers with detrital materials also have lower values of luminescence.

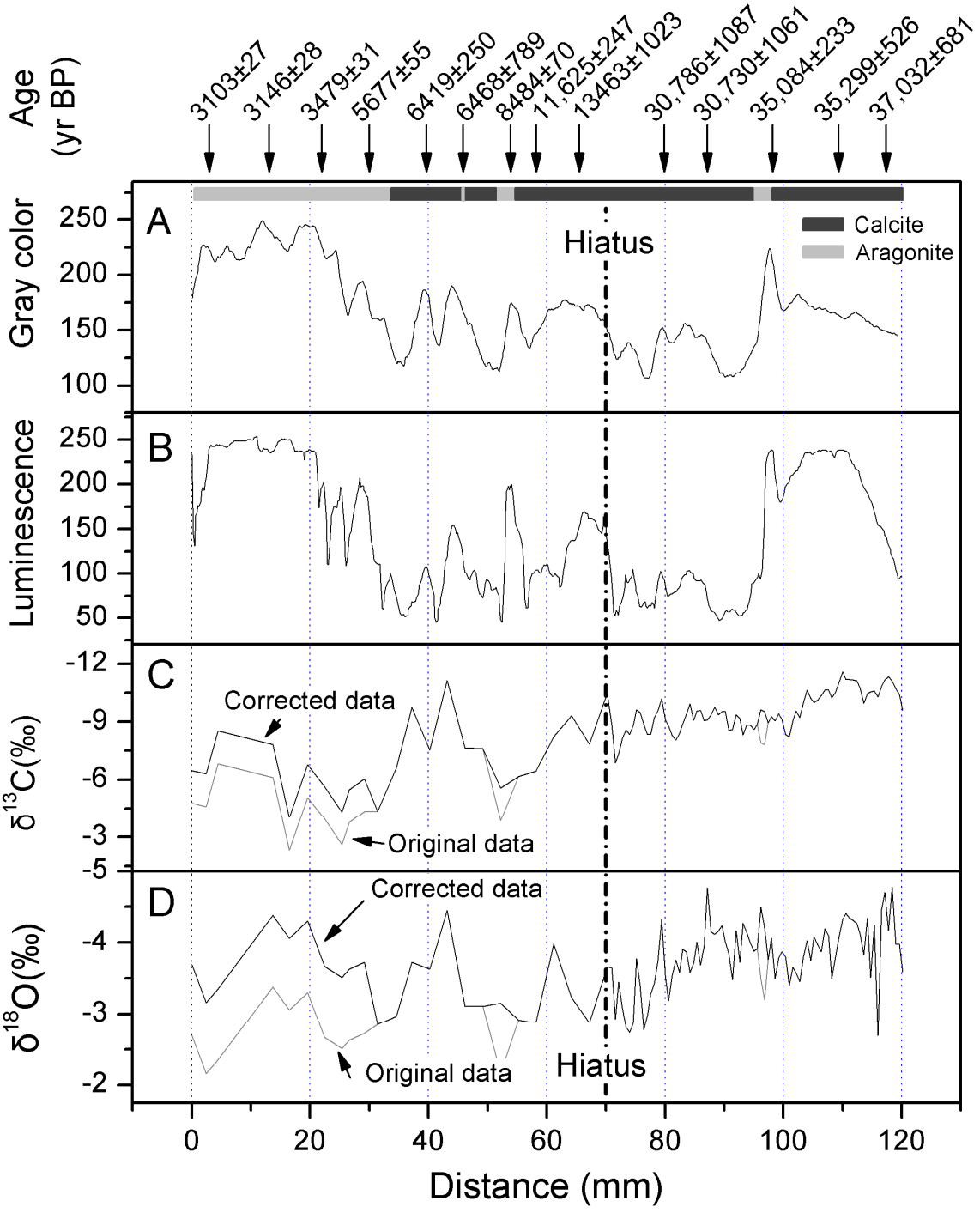

Figure 6.4. Variations in gray color (A), luminescence (B), $\delta^{13}C$ (C), and $\delta^{18}O$ (D) along transects shown on Figure 6.3B. Chronology and mineralogy of the slab are also indicated at the top of the diagram.

Variations in luminescence of clean calcite or aragonite are closely related to the content of organic matter transported into the cave and sealed into the speleothem carbonate (Lauritzen, 1986; Shopov et al., 1994; Ramseyer et al., 1997). Hence luminescence intensity is also an index of plant growth above the cave, with enhanced growth producing more organic acid in the soil. As climate is the main factor influencing plant growth, variations in luminescence should reflect variations in temperature and/or moisture availability.

Gray color and luminescence of speleothem carbonate are also affected by carbonate mineralogy. Unaltered aragonite in the column is generally whiter than secondary calcite, as in the outer section of the column and in the two layers at 5.4 and 9.8 cm depth. By contrast, secondary calcite emits a stronger luminescence than unaltered aragonite (Fig. 6.5). However, differences in gray color and luminescence between unaltered aragonite and secondary calcite are much less than variations caused by the presence of detrital materials (Fig. 6.4).

In summary, we believe that variations in gray color and luminescence through the column are proxies of climate change with lighter gray colors and stronger luminescence suggesting less detrital material, probably due to less intense precipitation and drier conditions. Conversely, darker colors and weaker luminescence suggest an increase in the transport of detrital particles into the cave as a result of more intense rains and dilution of organic acids because of the large input of water to the soil and cave.

Stable Isotopes

$\delta^{18}O$ and $\delta^{13}C$ values along the transects vary significantly, with a general trend toward enrichment in heavy isotopes from the older to younger deposits, and with large-amplitude

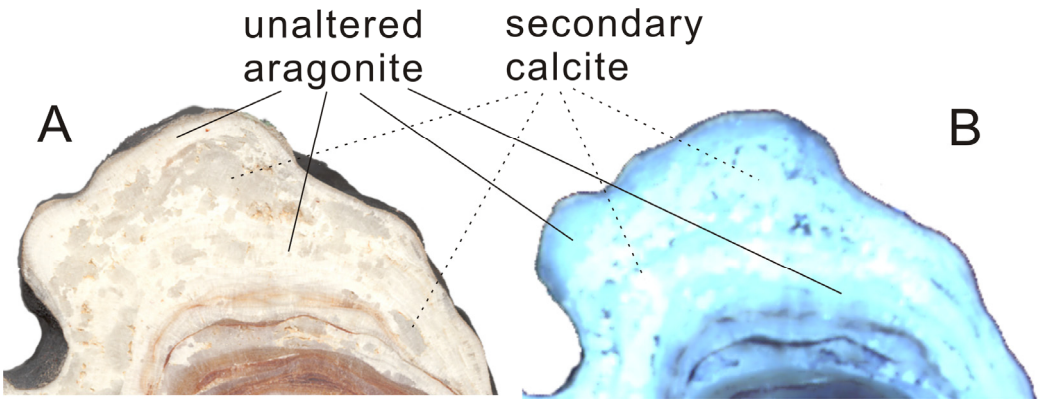

Figure 6.5. Color and luminescence affected by conversion of aragonite to calcite. Unaltered aragonite appears white in color and luminesces less than secondary calcite as shown in scan image (A) and luminescence image (B).

fluctuations in the outer part of the column from 0-7 cm, and less marked variations from 7-12 cm, particularly in the case of $\delta^{13}C$ (Figs 6.4C & D). As the DeSoto column consists of aragonite and calcite, a correction was applied for the different fractionation coefficients of these two minerals with respect to the stable isotopic composition of the depositing fluid before paleoclimatic significance of isotopic variations was assessed. When precipitated from water with the same isotopic composition, aragonite is enriched in ^{13}C by 1.7‰ (Romanek et al., 1992) and ^{18}O by 1.0‰ (Grossman and Ku, 1986) compared to calcite. In order to compare the aragonite and calcite sections of the column, stable isotope time series were converted to a calcite base (i.e. $\delta^{18}O$ and $\delta^{13}C$ values of aragonite samples were reduced by 1.0‰ and 1.7‰ respectively).

After correction, $\delta^{13}C$ values ranged from -4.0‰ to -11.6‰ with an average of -8.9‰ and still show a striking trend toward more positive values in younger deposits. By contrast, $\delta^{18}O$ values ranged from -4.8‰ to -2.7‰ and illustrate a general trend toward higher values in the interval from 12-7 cm and a trend toward lower values in younger deposits. The trends in both $\delta^{18}O$ and $\delta^{13}C$ are punctuated by high-frequency fluctuations.

Interpretation of variations in $\delta^{18}O$

Under isotopic equilibrium conditions, variations in $\delta^{18}O$ of speleothem carbonate would be affected by changes in temperature and the $\delta^{18}O$ of the moisture source (e.g. Gulf of Mexico). Speleothem carbonate deposited in warmer conditions has $\delta^{18}O$ values that are 0.22‰ lower for each 1ºC increase in water temperature (O'Neil et al., 1969). The $\delta^{18}O$ value of sea water is related to the volume of continental ice, and is estimated to have been 1.5‰ higher during the last glacial maximum (Shackleton, 1987). If long-term variations in the $\delta^{18}O$ of the DeSoto

column were mainly controlled by temperature and ice volume, we would expect late-Holocene deposits to have much lower $\delta^{18}O$ values with more positive values in older deposits. This is because the late-Holocene is much warmer and there was less continental ice. However, no such trend is apparent so we believe that other factors have played a more important role in affecting variations in $\delta^{18}O$ values of the column.

As the DeSoto column grew close to the original natural entrance to the cave, and as it accumulated by deposition from a water film moving vertically down the side of the formation, there is no doubt that deposition was influenced by kinetic fractionation. In fact, the surface area of the column increased over time (Fig. 6.2) so if there was no increase in the volume of water flowing over the surface of the column, water film thickness would have decreased over time. This might have led to increased kinetic fractionation in younger deposits increasing both $\delta^{18}O$ and $\delta^{13}C$ values. However, changes due to climate variations, particularly in rainfall, are superimposed upon any long-term trend, and indeed as Figure 6.4 shows, mid-Holocene deposits on the column have lower values of $\delta^{18}O$ than early Holocene deposits.

So, the large amplitude of $\delta^{18}O$ fluctuations may record variations in the $\delta^{18}O$ of the precipitating water, with increased rainfall and rainfall intensity leading to lower values (Chapter 5, this dissertation). Increased kinetic fractionation, particularly in the form of evaporation would have increased $\delta^{18}O$ values as would rapid outgassing. As a result, drier conditions should produce speleothem carbonate with relatively high $\delta^{18}O$ (less intense rainfall and increased evaporation), while wetter conditions should produce carbonate with lower values (heavier rainfall and reduced evaporation).

Interpretation of variations in $\delta^{13}C$

Variations in speleothem carbonate $\delta^{13}C$ values are mainly influenced by the following factors: 1) vegetation type above the cave that affects $\delta^{13}C$ of soil CO_2; 2) local hydrological conditions that affect the proportion of carbon in percolating water derived from soil CO_2 and bedrock; 3) kinetic fractionation of carbon isotopes in the precipitating cave waters due to rapid degassing or evaporation (McDermott, 2004; Quade, 2006, Brook et al., 2006).

The isotopic characteristics of soil CO_2 generally depend on the photosynthetic pathway used by vegetations above the cave, with a limit of -22.2 and -8.5‰ for the $\delta^{13}C$ of soil CO_2 beneath pure C_3 and pure C_4 biomasses, respectively (Cerling, 1984). Speleothem calcite deposited under a pure C_3 or C_4 biomass is likely to have $\delta^{13}C$ ranging from -12 to -9‰ or -2.3 to +1.5‰, respectively (Brook et al., 1999). Evidence from Lake Tulane in south-central Florida, indicates a vegetation with about 15% C_4 plants from 40-30 ka and almost no C_4 plants after 14 ka B.P. (Huang, et al., 2006). If the same change occurred near DeSoto Caverns, we should expect calcite during OIS 3 to be more enriched in $\delta^{13}C$ than that deposited during the Holocene. However, our ^{13}C record illustrates more negative values in OIS 3, probably suggesting that changes in C_3/C_4 composition may not have been a major factor in controlling $\delta^{13}C$ of the DeSoto column. In fact, fossil pollen from Goshen Springs (~200 km south of DeSoto Caverns) suggests that South-Central Alabama was covered by C_3 forest from ~ 33,000 ^{14}C years ago (Delcourt, 1980). Pollen from Cahaba Pond, ~50 km north of DeSoto Caverns, also suggests that forest dominated this area during the last 12000 years (Delcourt et al., 1983).

The proportion of carbon absorbed by percolating water from the bedrock/soil is mainly determined by the mode of dissolution, whether this is more open system or more closed system (McDermott, 2004; Quade, 2006, Brook et al., 2006). An increase in open-system solution

increases the carbon in the water derived from soil CO_2 ($\delta^{13}C$ =-22.2 under C_3 vegetation). As a result, speleothem calcite has more negative values of $\delta^{13}C$. In contrast, when solution is more closed-system more carbon in the water is derived from bedrock ($\delta^{13}C$ = 1%) and speleothem carbonate has higher $\delta^{13}C$ values. Open-system dissolution in generally enhanced when CO_2 partial pressures in the soil are higher due to wetter conditions and higher temperatures, both of which stimulate plant growth. By contrast, more carbon is derived from bedrock under closed-system conditions due to the limited contact between C in the water and C in the soil CO_2. This effect is enhanced during times with dry and cold conditions that result in reduced plant growth and thus reduced CO_2 production above the cave.

If temperature was the main factor influencing vegetation growth from 6-3 ka (warmer climate and enhanced vegetation growth) $\delta^{13}C$ should have been lower than in carbonate deposited from ~37-30 ka (much cooler climate and reduced plants growth). However, this is not what the data show (Fig. 6.4C). As a result, we believe that more negative $\delta^{13}C$ values in the column are associated with wetter conditions, while more positive values suggest drier conditions.

Speleothem carbonate deposited from waters affected by kinetic fractionation (including evaporation and rapid degassing) is enriched in $\delta^{13}C$ compared to carbonate deposited under isotopic equilibrium conditions (Hendy, 1971). In DeSoto Caverns, kinetic fractionation influences the isotopic composition of speleothem carbonate in the same direction as the hydrological conditions so that speleothem carbonate deposited under more open-system conditions due to a wetter climate is likely to have more negative $\delta^{13}C$ values as also expected due to less evaporation and slower degassing under wetter conditions. By contrast, speleothem carbonate deposited under drier conditions tends to have more positive $\delta^{13}C$ values due to

enhanced kinetic fractionation and more closed-system dissolution of the bedrock. In summary, we conclude that more positive $\delta^{13}C$ values in the DeSoto record suggest drier conditions in the past while more negative values indicate wetter conditions. Following this logic, conditions were wetter from ~37-30 ka and probably from ~13-6 ka, but drier after ~6 ka.

The DeSoto Column Paleoenvironmental Record

Deposition of calcite with lower luminescence, darker gray color, and more negative $\delta^{13}C$ values, suggests wet conditions during the periods from ~37-30 and ~13-6 ka B.P. By contrast, aragonite with higher luminescence, lighter color, and more positive $\delta^{13}C$ values, indicates drier conditions from 6-3ka B.P.

The generally wet conditions from ~37-30 ka and ~13-6 ka were punctuated by short drier periods around 34, 8.2 and 6.5 ka ago, as suggested by deposition of three aragonite layers 9.6, 5.4 and 4.2 cm from the outer surface of the column. Deposition of relatively clean calcite layers with dirty bands during this period suggest sub-millennial periods of intense rain when clay was washed into the cave. In contrast, clean calcite layers with fewer detrital grains indicate less intense rainfall and probably drier conditions. Fluctuations in $\delta^{18}O$ values also suggest significant high-frequency variations in rainfall intensity during this wet period.

The dry period from 6-3 ka also probably witnessed short spells of intense rain as suggested by more negative $\delta^{18}O$ values at 3.2 and ~3.4 ka. These intense rains appear to have been of short duration and did not transport clay into the cave, as indicated by fewer detrital grains in the column carbonate of these periods.

Comparison with other Records

Variations in paleoenvironmental conditions reconstructed from the DeSoto column agree well with late Wisconsin and Holocene records from the Southeastern USA derived from fossil pollen, fluvial geomorphology, and sand dune activity. As discussed above, the dominance of primary calcite from 12-7 cm from the surface of the column suggests generally wet conditions from ~37-30 ka. Two large paleomeanders in the Middle Ogeechee River in Southeast Georgia dated to 31,000- 28,000 ^{14}C years (circa 36 to 32 ka calendar age) (Leigh and Feeney, 1995) also suggest a wet paleoclimate during this period. However, sand dune activity at 32.8 ±3 ka (Ivester et al., 200) and 34.0 ±2.6 ka (Leigh, 2008) on the Canoochee River fluvial terraces in the Georgia Coastal Plain, appears to correspond with an aragonite layer deposited shortly after 35 ka in the DeSoto column slab suggesting a drier spell over the Southeastern USA at this time. The depositional hiatus visible in the column from ~30-13 ka generally corresponds to a cold and dry late Wisconsin episode, characterized by enhanced aeolian dune activity on the Georgia Coastal Plain (Ivester et al, 2001; Leigh et al., 2004) and dominance of braided river patterns in Georgia and the Carolinas (Leigh et al., 2004).

For the Southeastern USA there are more records of climate change at the Pleistocene-Holocene transition than during the Holocene itself. The transition from calcite dominance ~13-6 ka to aragonite formation in the DeSoto column clearly suggests a wetter climate before 6 ka, which supports the fossil pollen and river channel pattern evidence. Vegetation around Cahaba Pound from ~14 to ~12 ka (12000 to 10000 ^{14}C yr BP) was dominated by mesic broadleaved deciduous trees and was replaced by more xeric forests after ~12 ka (Delcourt et al., 1983). Water levels in Cahaba Pond increased after ~9 ka suggesting an increase in effective precipitation in central Alabama. However, the Cahaba Pond record does not show

the mid-Holocene climate shift visible in the DeSoto Caverns record, possibly because of a significant reduction in lake sedimentation rates in this period.

Pollen records from Clear Pond (Watts et al., 1996) and White Pond (Watts, 1980) suggest that the period 16 to ~6 ka was moister than today, as indicated by the abundance of beech (*Fagus*). An increase in gum pollen at Chatterton Springs (Seielstad, 1994), Cooperville (Brook, 1996), Sandy Run Creek (Lamoreaux, 1999), and Fort Bragg (Goman and Leigh, 2004) in the Southeastern USA suggests that the early and mid-Holocene were moister than the later Holocene (Fig. 6.6). Stream meanders formed at 16-11 ka have wider channels with pronounced scroll bars (Leigh and Feeney, 1995; Leigh, 2006). Modeled bankfull stage paleodischarges for these larger channels range from 1.3 to 4.2 times modern values and late Holocene channels (Leigh, 2006) (Fig. 6.6). In the period 9-6.1 ka, there are 15 large overbank flood events visible in a Fort Bragg, North Carolina peat core from an abandoned river channel (Goman and Leigh, 2004), suggesting episodic intense rainfall in the Southeastern USA. Intense rainfall events are also apparent in the DeSoto column as calcite layers with reddish detrital materials. They record an increased flow of water into the cave that washed red-colored detrital grains into the cave and onto the column (Fig. 6.6). During the wetter early Holocene a discontinuous, lens-shaped, white aragonite layer, dated to 8400 years B.P., suggests at least one significant drier episode. The timing of this interval raises the possibility that it corresponds to the 8200 year cold event (Alley, 1997). There is also OSL- and TL-dated evidence of enhanced aeolian activity in the Georgia Coastal Plain (Ivester et al., 2001) and along the Gulf Coast (Otvos and Price, 2001; Otvos, 2004). However, Goman and Leigh (2006) suggest that sand dune reactivation in the Southeastern USA during early Holocene was short-lived and sporadic and probably does not represent a regional shift to drier climatic conditions.

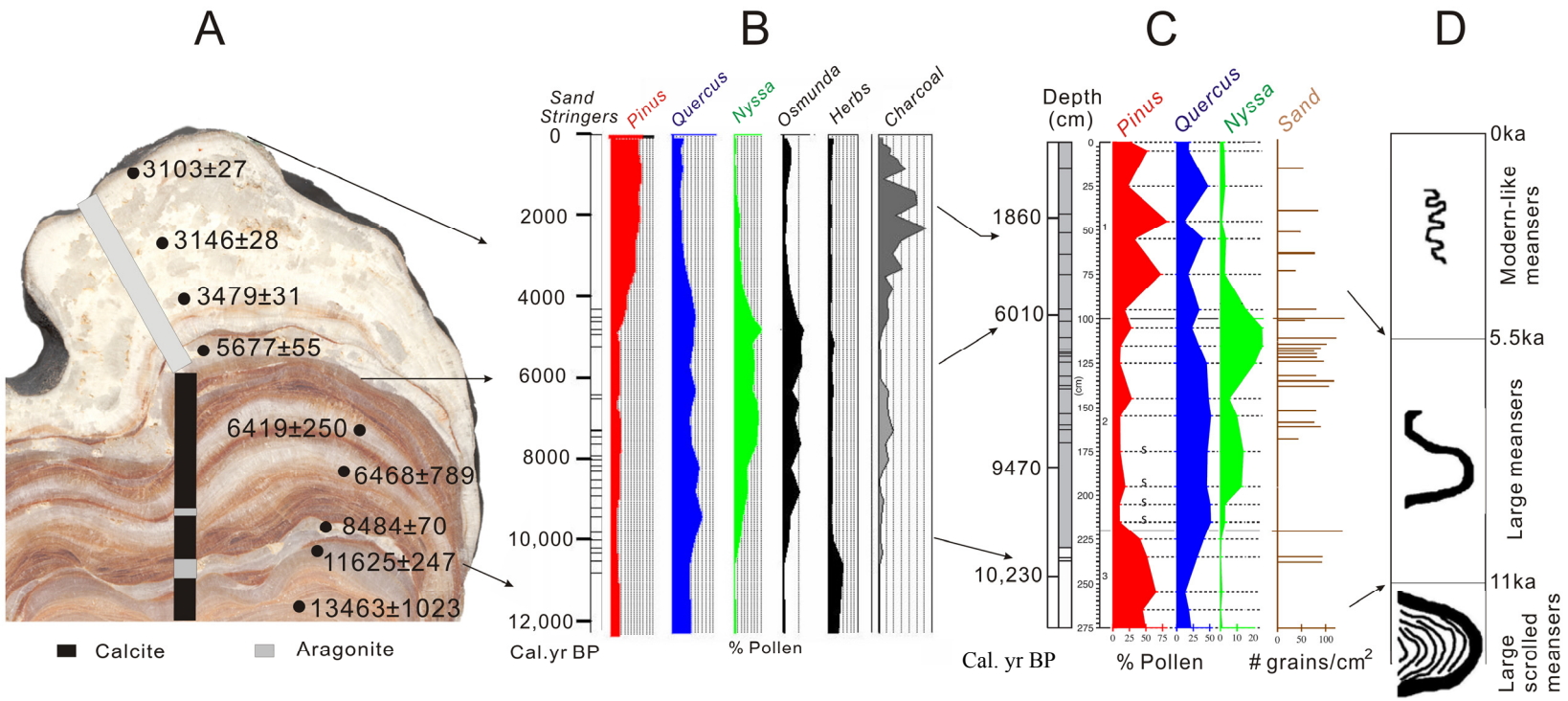

Figure 6.6. Comparison of the DeSoto column record for the last 13 ka with other paleoclimate proxy data from the Southeastern USA. (A) DeSoto column record (this study); (B) Sandy Run Creek pollen record (LaMoreaux, manuscript in review); (C) Selected sediment and pollen data from a Fort Bragg, North Carolina peat core (Goman and Leigh, 2004); (D) Stream channel pattern changes in the Atlantic coastal plain (Leigh, 2008).

Deposition of aragonite after 6 ka suggests drier and possibly warmer conditions in the DeSoto Caverns area and the limited amount of detrital material indicates less intense rainfall. This is consistent with evidence of fewer flood events in the Fort Bragg peat core after 6 ka (Goman and Leigh, 2004). Development of relatively small, modern-like paleochannels after 5.5 ka (Leigh, 2008) also suggests drier climatic conditions in the Atlantic Coastal Plain (Fig. 6.6).

Climate modeling so far has produced inconsistent results for the Holocene of the Southeastern USA. Kutzbach (1987) used the Community Climate Model (CCM) of the National Center for Atmospheric Research to model climate change. His results showed that the Southeastern USA was warmer and wetter than present at 11-3 ka mainly due to an intensified summer monsoon in response to higher northern hemisphere summer solar radiation in the early Holocene. By contrast, inferred climates based on six pollen taxa (spruce, birch, northern pines, oak, southern pines, and prairie forbs) suggest that precipitation in Alabama was slightly lower at 12-9 ka, and increased to present levels (1400 mm/yr) after 6 ka followed by a slight decrease aftert 3 ka (Prentice et al., 1991). However, using two coupled ocean-atmosphere climate models, Harrison (2003) found that the Southeastern USA was slightly drier at 6 ka than at present.

Paleoclimate simulations for North America by Bartlein et al. (1998) indicate that climate in Central Alabama was as wet as today at 11 ka but drier at 6 ka. By modeling the potential effect of mid-Holocene insolation forcing and sea surface temperature on summer precipitation, Diffenbaugh et al. (2006) concluded that three of four models suggest drier conditions in Alabama and Mississippi during the mid-Holocene. As there is a clear lack of agreement between climate modeling results and the interpretation of proxy data, it is clear that more high-resolution data for the Southeastern USA are needed. Fine-resolution climate modeling may

cast new insights and help us better understand what had happened to the climate during Holocene.

The transition from wetter to drier conditions at 6 ka, suggested by the deposition of aragonite rather than calcite on the DeSoto column, suggests a significant regional climate shift in the Southeastern USA. Before 6 ka, a more poleward subtropical jet over eastern North America due to the presence of the Laurentide Ice Sheet in the north (Dyke and Prest, 1987) and increased summer insolation in the northern hemisphere probably brought more moisture to the Southeastern USA (Leigh and Webb, 2006; LaMoreaux et al., manuscript in review). During the early Holocene, the Bermuda High shifted to a more northerly and easterly position and probably also transported more moisture from the Gulf of Mexico bringing more intense rainfall to the Southeastern USA (Goman and Leigh, 2004). As the Laurentide Ice Sheet had melted by 6 ka and summer solar radiation was on the decline, the subtropical jet may have weakened or shifted southward (LaMoreaux et al., manuscript in review) bringing less rainfall to the DeSoto Caverns area. In addition, a shift in the Bermuda High to a more westerly and southerly location would have brought more moisture to the Central USA and less to the Southeastern USA (Forman et al., 1995). By this time, the present-day climate pattern was in place and the DeSoto area experienced alternating drier and wetter periods (Chapter 5, this dissertation) due to the strong influence of increased ENSO activity (Moy et al., 2002).

Conclusions

The record derived from a column near the entrance to DeSoto Caverns in Alabama documents a wetter climate in the periods ~37-30 ka and ~13-6 ka. At these times calcite was deposited with lower luminescence, darker gray color, and more negative $\delta^{13}C$ values. By

contrast, from 6-3 ka B.P. deposition was mainly of aragonite with higher luminescence, lighter color, and more positive $\delta^{13}C$ values, all indicating drier and possibly warmer conditions in this time interval. These findings agree well with published fossil pollen, sand dune, river channel pattern, and fluvial sediment records. The DeSoto data thus add to the growing body of evidence on paleoclimate variations in the Southeastern USA during the late-Pleistocene and Holocene.

This study also illustrates that like stalagmites, columns deposited in caves have the potential to provide useful information of past climates. It has also shown that valuable paleoenvironmental information can be derived from dirty speleothem formations, although some clean layers are necessary for developing a reliable chronology for the data.

References

Alley, R., Mayewski, P., Sowers, T., Stuiver, M., Taylor, K. and Clark, P., 1997. Holocene climate instability: a prominent, widespread event 8200 yr ago. *Geology* 25, 483–486.

Baker, A., Smart, P. L. and Edwards, R. L., 1995. Paleoclimate implications of mass spectrometric dating of a British flowstone. *Geology* 23, 309-312.

Bartlein, P. J., Anderson, K. H., Anderson, P. M., Edwards, M. E., Mock, C. J., Thompson, R. S., Webb, R. S., Webb Iii, T. and Whitlock, C., 1998. Paleoclimate simulations for North America over the past 21,000 years features of the simulated climate and comparisons with paleoenvironmental data. *Quaternary Science Reviews* 17, 549-585.

Brook, F. Z., 1996. A Late-Quaternary Pollen Record from the Middle Ogeechee River Valley, Southeastern Coastal Plain, Georgia. Master Thesis, University of Georgia, Athens, Georgia.

Brook, G. A., 1999. Arid zone paleoenvironmental records from Cave Speleothems. In: Singhvi, A.K., Derbyshire, E. (Eds.), Paleoenvironmental Reconstruction in Arid Lands. Oxford & IBH, New Delhi, pp. 217–262.

Brook, G. A., Ellwood, B. B., Railsback, L. B. and Cowart, J. B., 2006. A 164 ka record of environmental change in the American southwest from a Carlsbad Cavern speleothem. *Palaeogeography, Palaeoclimatology, Palaeoecology* 237, 483-507.

Cabrol, P. and Coudray, J., 1982. Climatic fluctuations influence the genesis and diagenesis of carbonate speleothems in southwestern France. *National Speleological Society Bulletin* 44, 112-117.

Cerling, T. E., 1984. The stable isotopic composition of modern soil carbonate and its relationship to climate. *Earth and Planetary Science Letters* 71, 229-240.

Cheng, H., Edwards, R. L., Hoff, J., Gallup, C. D., Richards, D. A. and Asmerom, Y., 2000. The half-lives of uranium-234 and thorium-230. *Chemical Geology* 169, 17-33.

Craig, H., 1957. Isotopic standards for carbon and oxygen and correction factors for mass-spectrometric analysis of carbon dioxide. *Geochimica et Cosmochimica Acta* 12, 133-149.

Delcourt, H. R., Delcourt, P. A. and Spiker, E. C. 1983. A 12000-year record of forest history form Cahaba Pond, St. Clair County, Alabama. *Ecology* 64, 874-887.

Delcourt, H. R. and Delcourt, P. A., 1985. Quaternary palynology and vegetational history of the southeastern United States. In: Bryant, V.M.and Holloway, G. (Eds.), Pollen Records of Late-Quaternary North American Sediments, American Association of Stratigraphic Palynologists Foundation, Austin, TX, pp. 1-37.

Delcourt, P. A., 1980. Goshen Springs: Late Quaternary Vegetation Record for Southern Alabama. *Ecology* 61, 371-386.

Denniston, R. F., Gonzalez, L. A., Asmerom, Y., Sharma, R. H. and Reagan, M. K., 2000. Speleothem evidence for changes in Indian summer monsoon precipitation over the last ~2300 Years. *Quaternary Research* 53(2), 196-202.

Diffenbaugh, N. S., Ashfaq, M., Shuman, B., Williams, J. W. and Bartlein, P. J. 2006. Summer aridity in the United States: Response to mid-Holocene changes in insolation and sea surface temperature. *Geophysical Research Letters* 33, L22712.

Dyke, A. S. and Prest, V. K., 1987. The Late Wisconsinan and Holocene history of the Laurentide Ice Sheet. *Géographie physique et Quaternaire*, 41, 237-263.

Edwards, R. L, Chen, H. and Wasserburg, G. J., 1987. $^{238}U–^{234}U–^{230}Th–^{232}Th$ systematics and the precise measurement of time over the past 500,000 years. *Earth and Planetary Science Letters* 81, 175–192.

Goman M. and Leigh, D. S., 2005. Comment on "Holocene aridity and storm phases, Gulf and Atlantic Coasts, USA" by Ervin G. Otvos, 2005. *Quaternary Research* 63, 368-373 Quaternary Research 66,182-184.

Goman, M. and Leigh, D. S., 2004. Wet Early to Middle Holocene Conditions on the Upper Coastal Plain of North Carolina, USA. *Quaternary Research* 61, 256-264.

Grossman, E. L., and Ku, T.-L., 1986. Oxygen and carbon isotope fractionation in biogenic aragonite: temperature effects. *Chemical Geology* 59, 59-74.

Harrison, S. P., Kutzbach, J. E., Liu, Z., Bartlein, P. J., Otto-Bliesner, B., Muhs, D., Prentice, I. C. and Thompson, R. S., 2003. Mid-Holocene climates of the Americas: a dynamical response to changed seasonality. *Climate Dynamics* 20, 663-688.

Hendy, C. H., 1971. The isotopic geochemistry of speleothems, 1. The calculation of the effects of different modes of formation on the isotopic composition of speleothems and their applicability as paleoclimatic indicators. *Geochimica et Cosmochimica Acta* 35, 801-824.

Huang, Y., Shuman, B., Wang, Y., Webb III, T., Grimm, E. C. and Jacobson, J. G. L., 2006. Climatic and environmental controls on the variation of C3 and C4 plant abundances in central Florida for the past 62,000 years. *Palaeogeography, Palaeoclimatology, Palaeoecology* 237, 428-435.

Ivester, A. H., Leigh, D. S. and Godfrey-Smith, D. I., 2001. Chronology of Inland Eolian Dunes on the Coastal Plain of Georgia, USA. *Quaternary Research* 55, 293-302.

Jimenez-Lopez, C. and Romanek, C. S. 2004. Precipitation kinetics and carbon isotope partitioning of inorganic siderite at 25°C and 1 atm. *Geochimica et Cosmochimica Acta* 68, 557-571.

Kutzbach, J. E., 1987. Model simulations of the climatic patterns during the deglaciation of North America. In: Ruddiman, W.F., H. E. Wright, Jr., (Eds.). North America and Adjacent Oceans During the Last Deglaciation. Geological Society of America, Boulder, CO, pp. 425-446.

LaMoreaux, H. K., 1999. Human-Environmental Relationships in the Coastal Plain of Georgia based on High-Resolution Paleoenvironmental Records from Three Peat Deposits. Ph.D. Dissertation, University of Georgia, Athens, GA.

Lauritzen, S.-E., Ford D. C. and Schwarz, H. P., 1986. Humic substances in speleothems matrix-paleoclimate significance. *Proceedings of the 9th International Congress of Speleology* 2,77-79, Barcelona, August, 1986.

Leigh, D. S., 2006. Terminal Pleistocene braided to meandering transition in rivers of the Southeastern USA. *Catena* 66, 155-160.

Leigh, D. S. and Webb, P. A., 2006. Holocene erosion, sedimentation, and stratigraphy at Raven Fork, Southern Blue Ridge Mountains, USA. *Geomorphology* 78, 161-177.

Leigh, D.S., 2008. Late Quaternary climates and river channels of the Atlantic Coastal Plain, Southeastern USA. Geomorphology, doi: 10.1016/j.geomorph.2008.05.024

Leigh, D. S. and Feeney, T. P., 1995. Paleochannels indicating wet climate and lack of response to lower sea level, southeast Georgia. *Geology* 23, 687-690.

Leigh, D. S., Srivastava, P. and Brook, G. A. 2004. Late Pleistocene braided rivers of the Atlantic Coastal Plain. *Quaternary Science Reviews* 23, 65-84.

McDermott, F., 2004. Palaeo-climate reconstruction from stable isotope variations in speleothems: a review. *Quaternary Science Reviews* 23, 901–918.

Moy, C. M., Seltzer, G. O., Rodbell, D. T. and Anderson, D. M., 2002. Variability of El Nino/Southern Oscillation activity at millennial timescales during the Holocene epoch. *Nature* 420, 162-165.

Murray, J. W., 1954. The deposition of calcite and aragonite in caves. *Journal of Geology* 62, 481-492.

O'Neil, J. R., Clayton, R. N. and Mayeda, T., 1969. Oxygen isotope fractionation in divalent metal carbonates. *Journal of Chemical Physics,* 51, 5547-5558.

Otvos, E. G., 2004. Prospects for interregional correlations using Wisconsin and Holocene aridity episodes, northern Gulf of Mexico coastal plain. *Quaternary Research* 61, 105-118.

Otvos, E. G., 2005. Holocene aridity and storm phases, Gulf and Atlantic Coasts, USA. *Quaternary Research* 63, 368–373.

Otvos, E. G., 2006. Reply to letter to the editor from Goman and Leigh re: Quaternary Research 63, 368-373. *Quaternary Research* 66, 185-186.

Otvos, E. G., and Price, D. M., 2001. Late Quaternary inland dunes of southern Louisiana and arid climate phases in the Gulf Coast region. *Quaternary Research* 55,150-158.

Prentice, I. C., Bartlein, P. J. and Iii, T. W. 1991. Vegetation and Climate Change in Eastern North America since the Last Glacial Maximum. *Ecology* 72, 2038-2056.

Quade, J., 2004. Isotopic records from ground-water and cave speleothem calcite in North America. In: Gillespie, A., Porter, S. C., Atwater, B.F. (Eds.), Developments in Quaternary Science, vol. 1. Elsevier Science, New York, pp. 205-219.

Railsback, L. B., Brook, G. A., Chen, J., Kalin, R. and Fleisher, C. J., 1994. Environmental controls on the petrology of a late Holocene speleothem from Botswana with annual layers of aragonite and calcite. *Journal of Sedimentary Research* 64, 147-155.

Ramseyer, K., Miano, T., D'Orazio, V., Wildberger, A., Wagner, T. and Geister, J., 1997. Nature and origin of organic matter in carbonates from speleothems, marine cements and coral skeletons. *Organic Geochemistry* 26, 361–78.

Reams, M.W., 1972. Deposition of Calcite, Aragonite, and clastic sediments in a Missouri cave during four and one-half years. *National Speleological Society Bulletin* 34, 137-141.

Romanek, C. S., Grossman, E. L. and Morse, J. W., 1992. Carbon isotopic fractionation in synthetic aragonite and calcite: effects of temperature and precipitation. *Geochimica et Cosmochimica Acta* 56, 419-430.

Seielstad, C. A., 1994. Holocene environmental history at Chatterton Springs on the southern Coastal Plain of Georgia. M.A. Thesis, Univ. of Georgia, Athens.

Shackleton, N. J., 1987. Oxygen isotopes, ice volume and sea level. *Quaternary Science Reviews,* 6*,* 183-190.

Shen, C.-C., Edwards, R. L., Cheng, H., Dorale, J. A., Thomas, R. B., Moran, S. B., Weinstein, S. and Edmonds, H. N., 2002. Uranium and thorium isotopic and concentration measurements by magnetic sector inductively coupled plasma mass spectrometry. *Chemical Geology* 185, 165–178.

Shopov, Y. Y., Ford, D. C. and Schwarcz, H. P., 1994. Luminescent microbanding in speleothems: high-resolution chronology and paleoclimate. *Geology* 22, 407-410.

Siegel, F. R. and Dort, W. Jr., 1966. Calcite-aragonite speleothems from a hand-dug cave in northeast Kansas. *International Journal of Speleology* 2, 165-169.

Thrailkill, J., 1971. Carbonate deposition in Carlsbad Caverns. *Journal of Geology* 79, 683-695.

van Beynen, P., Bourbonniere, R., Ford, D. C. and Schwarcz, H. P., 2001. Causes of colour and fluorescence in speleothems. *Chemical Geology* 175, 319-341.

Watts, W. A., 1980. Late-Quaternary vegetation history at White Pond on the inner Coastal Plain of South Carolina. *Quaternary Research* 13, 187-199.

Watts, W.A., Grimm, E.C. and Hussey, T.C., 1996. Mid-Holocene forest history of Florida and the Coastal Plain of Georgia and South Carolina. In: Sassaman, K., Anderson, D.G. (Eds.), The Archaeology of the Mid-Holocene Southeast. Univ. Press of Florida, Gainesville. p. 28–38.

Webster, J. W., Brook, G. A., Railsback, L. B., Cheng, H., Edwards, R. L., Alexander, C. and Reeder, P. P., 2007. Stalagmite evidence from Belize indicating significant droughts at the time of Preclassic Abandonment, the Maya Hiatus, and the Classic Maya collapse. *Palaeogeography, Palaeoclimatology, Palaeoecology* 250, 1-17.

Xiao, H. L., Brook, G. A., Rialsback, L. B., Alexander C., Edwards, R. L., Cheng, H., Wang, X. F., Liebig, C. M. and Dennis, W., Asian monsoon activity during the Holocene: Stalagmite evidence from Yangzhipo Cave, Guizhou Province, Southern China. Unpublished manuscript.

Yadava, M. G. and Ramesh, R., 2005. Monsoon reconstruction from radiocarbon dated tropical Indian speleothems. *The Holocene* 15(1): 48-59

CHAPTER 7

COMPARISONS AND CONCLUSIONS

Comparisons of Records

Proxy climate data from speleothems collected in Southwestern China, Northern India, and the Southeastern USA provide high resolution and absolute-dated records of past climate change in these three areas. The records document variations in the Asian and Southeastern USA monsoon during the last ~ 5 ka, and the record for the Southeastern USA extends to the Late Pleistocene.

Data from Shangdong Cave in Southwestern China document a gradual decline in monsoon strength from ~5.1 to 1.5 ka BP in response to decreasing summer solar radiation over the Asian continent (Fig. 3.4; Fig. 7.1). This corresponds with information obtained from stalagmites from Hulu, Sanbao, and Dongge Cave in China (Wang et al., 2001, 2005, 2008, Yuan et al., 2004) that monsoon strength is closely related to changes in summer solar radiation in the Northern Hemisphere back to 224,000 years ago. By contrast, no significant long-term variation in monsoon strength was observed in the records from the Southeastern USA during the mid- to late-Holocene. Instead, this record is characterized by alternating wetter and drier regimes. This

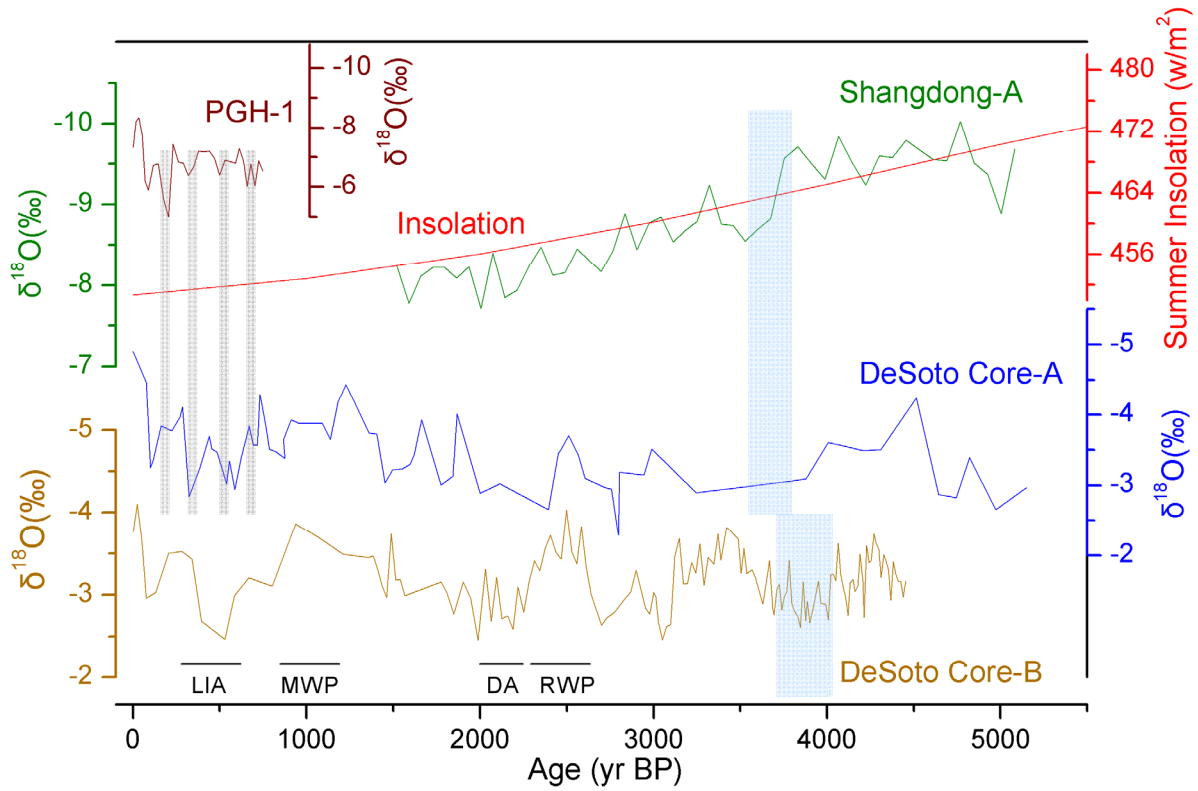

Fig. 7.1. Comparison of the $\delta^{18}O$ records from the PGH-1, Shangdong-A, and DeSoto stalagmites. Gray bars on the diagram from left to right show the Wolf, Spörer, Maunder, and Dalton periods of sunspot minima. "Holocene Event 3" is shown by the blue bar.

apparent lack of agreement may be due to differences in landmass area and physiography between Asia and North America and the less pronounced nature of the Southeastern monsoon system. Monsoonal climates are characterized by a reversal of wind directions between summer and winter due to seasonal changes in air pressure resulting from the temperature gradient between the continent and adjacent oceans. During the warm season, warm air over the continent and cool air over the ocean lead to a marked pressure gradient between the continent and ocean, producing on-shore winds that bring precipitation to the continent. During the cool season, a reverse air pressure gradient over the land and ocean results in off-shore winds and thus significantly drier conditions. As the Euro-Asian continent is much larger in area than North America, the heat gradient, and therefore the resulting pressure gradient, between the Asian continent and adjacent oceans is much more pronounced than it is over North America. The Tibetan Plateau in Central Asia further strengthens the pressure gradient and leads to a stronger monsoon. As a result, the Asian monsoon is more sensitive to variations in insolation over the northern Hemisphere. By contrast, Southeastern USA monsoon variability over the last 5 ka was more influenced by ENSO activity as illustrated by Fig. 5.7, rather than by variations in insolation.

Records from Shangdong Cave and DeSoto Caverns both document the conditions during the "Holocene Event 3" at ~4ka BP when sea surface temperature in the North Atlantic dropped by 1º to 2ºC (Bond, 1997). Significant climate variation during this event is well documented in proxy data from eastern Africa (Thompson et al., 2002), Gulf of Oman (Cullen et al., 2000),

Mesopotamia (deMenocal, 2000), Southwestern China (Wang et al., 2005), Central Plains of China (Wu and Liu, 2004), and Northern Peru (Thompson et al., 2000). This event also was documented by the sharp decrease in monsoon strength (shift from wetter to drier conditions) at 3.5 ka BP in Shangdong record, while it was characterized by drier condition in DeSoto Caverns at ~ 4ka BP.

Millennial-scale climate variations in the Asian and Southeastern USA monsoonal climate during the last 5 ka were punctuated by centennial or even decadal climate fluctuations. These high-frequency climate variations, at least for those in the last 1000 years, probably result from the variation in solar activity, as illustrated in Fig. 4.3 and Fig. 7.1, that periods of sunspot minima are associated with weaker monsoon in Northern India and drier periods in DeSoto Caverns. Speleothem data of higher temporal resolution and better chronology have also shown that decadal variations in Asian summer monsoon strength during the Holocene are closely related to the variation in solar activity (Neff et al., 2001; Wang et al., 2005).

Our records also document changes in paleoclimate in response to variations in monsoon strength during the past 5 ka. As a stronger monsoon brings more intense and higher precipitation to the Asian continent, Southern China was wetter during the period ~ 5 to 3 ka and gradually became drier after 3 ka. However, in the Southeastern USA there was no significant long-term change in paleoclimate over the last 4.4 ka, although the climate was slightly drier before 2 ka than after that time. Instead, the climate of the Southeastern USA during the last 4.4 ka was characterized by alternating ~300-year periods of wetter and drier climate, with wetter periods

during the Roman Warm Period and Medieval Warm Period, and drier phases during the Neoglacial, Dark Age, and Little Ice Age.

The records from Panigarh Cave and DeSoto Caverns document paleoenvironmental conditions during the last 750 years. Monsoon strength in Northern India was more or less stable during from AD 1250 to 1770 years B.P. and decreased abruptly at AD 1800. After that, the Southwest monsoon strengthened gradually peaking in AD 1970. As a result, the Little Ice Age was wetter in Northern India. By contrast, the climate of the Southeastern USA fluctuated significantly during this period with a general wetter Medieval Warm Period and a drier Little Ice Age. Records from Northern India and Southeastern USA all document a gradual shift to wetter conditions during the last ~300 years; although this trend is punctuated by a short drier spells at around ~220 years BP.

Conclusions

Supporting other stalagmite studies in the Asian monsoon area, variations in $\delta^{18}O$ along the central growth axis of the Shangdong-A stalagmite document a gradual weakening of the Asian summer monsoon from the mid-Holocene in response to declining summer solar radiation over the Northern Hemisphere. A stronger summer monsoon around 5 ka B.P. brought intense rains and more precipitation to the Yangtze River Valley of China and Northern China, as the monsoon front penetrated further north. By contrast, as the monsoon weakened around 4 ka B.P., the monsoon front remained longer in the Southern China and so brought less rainfall to Northern

China. Southern China experienced intense rainfall. As a result, instead of homogeneous changes in precipitation across China, there was significant spatial variation in precipitation in response to variations in monsoon strength and in the location of the monsoon front.

The stalagmite record from northern India documents a wetter Little Ice Age suggested by deposition of calcite during the period from AD 1480-1900, while aragonite deposited prior to and after this interval suggests drier conditions. This shows that petrographic evidence can provide useful information on past climate change. This northern India record also indicates that climate was relatively constant from AD 1250-1800, but fluctuated much more during the last 200 years. Variations in luminescence and gray color along the central growth axis of the Panigarh stalagmite agree very well with the reconstructed temperature of the Northern Hemisphere over the past 750 years, suggesting that color and luminescence are probably solar activity.

Paleoclimate proxy information obtained from vertical cores drilled from two active stalagmites in DeSoto Caverns, Alabama; clearly show the value of this approach to stalagmite studies. If used in the future, this approach could be used to access information in very large stalagmites around the world that cannot be accessed in any other way. What is more, this approach does not significantly damage either the stalagmite being drilled or the cave, thus preserving valuable cave environments around the world.

Records derived from the two DeSoto Cavern stalagmite cores document alternating wetter and drier climate regimes during the past 4400 years. In particular, they suggest a wetter

Medieval Warm Period and a drier Little Ice Age in the Southeastern USA. The data also suggest a link between the climate of the Southeastern USA and conditions in the North Atlantic.

The study of a DeSoto Caverns column has shown that columns as well as stalagmites can provide proxy paleoclimate information, although stable isotope variations are not as useful due to marked kinetic fractionation before and during deposition of the speleothem carbonate. This study also showed that valuable paleoclimate information can be extracted from dirty speleothems although chronological data for such deposits may not be as reliable as is the case with clean deposits. The DeSoto column record shows that that the early Holocene in Alabama was wetter than the late Holocene, as indicated by a change from calcite deposition from ~13-6 ka to aragonite deposition after 6 ka.

The DeSoto column also provided evidence that wetter conditions in the late-Pleistocene and early Holocene were punctuated by several brief drier phases. These phases are documented by aragonite layers or clear calcite layers indicating drier conditions with less intense rainfall. In fact, an aragonite layer deposited during the 8200-year cold event indicates that Southeastern USA was much drier than today at this time.

Although the speleothem records presented in this dissertation are not perfect for examining the possible driving mechanisms of climate change in the three areas examined, they do show that millennial, centennial, and decadal variations in solar insolation have greatly influenced the past monsoon climates of Southern China, Northern India, and the Southeastern USA. Variations in $\delta^{18}O$ of the Shangdong Cave stalagmite parallel millennial-scale variations in Northern

Hemisphere summer insolation. In northern India, where the record is short, variations in luminescence and gray color of the Panigarh Cave stalagmite parallel reconstructed Northern Hemisphere temperature and show a strong correlation with periods of low sunspot activity. In the Southeastern USA, the stalagmite $\delta^{18}O$ record from DeSoto Caverns parallels reconstructed Bermuda Rise ocean temperatures over the past 3500 years. All of these evidences suggest that variations in the thermal contrast between the Asian and North American landmasses and adjacent oceans, most likely due to long-term and short-term changes is solar insolation, were the main controls on climate changes during the Holocene.

The research outlined here cannot provide evidence on whether the monsoonal climates of Asia and the Southeastern USA changed synchronously during the Holocene as the records cover only the middle to late Holocene. However, the records from Southern China and the Southeastern USA do suggest that there was a major shift in climate in both areas at 5-4 ka and this period appears to have been a time of change worldwide.

Overall, the research outlined in this dissertation demonstrates that speleothems have the potential to provide valuable information on past monsoonal climate in many areas of the world. If the drilling technique used to obtain cores from DeSoto Caverns stalagmites is used on very large (>5 m high) stalagmites in other caves around the world, very long records of climate change are possible. Furthermore, proxy variables such as color, luminescence and , δ^{13C}, in addition to $\delta^{18}O$, can provide important new information on paleoenvironmental variations in a

specific area due to changes in monsoon characteristics. They can also provide information on the potential external factors that have induced the observed changes in climate.

Summary of Major Findings

1). High-resolution records of climate change can be obtained from large stalagmites by extracting vertical, axial cores. This now allows long cores to be obtained from large stalagmites around the world allowing records to the limit of U-series dating (ca. 500 ka) to be obtained and possibly even longer records (millions of years) dated by U-Pb methods.

2). Speleothems other than stalagmites (e.g. columns), and dirty speleothems, can provide important paleoclimatic information and should not be ignored by researchers.

3). Weakening of the Asian monsoon in the last ca. 5 ka parallels the decline in summer solar radiation in the northern hemisphere suggesting that this is a major control on monsoon strength as it affects the temperature and pressure gradients between large landmasses and nearby oceans.

4). There was a significant change in the climates of Southwestern China and the Southeastern USA around 5-4 ka. In China, the Asian monsoon strength diminished substantially in a short period of time and in the Southeastern USA more marked ENSO events led to a generally drier and more variable climate. This seems to have been a global climate event recorded at many sites around the world. Its exact cause is not known at this time.

5). Contrary to expectations, the climate of the Little Ice Age in northern India seems to have been wetter than today and the Medieval Warm Period drier. This contrasts with the situation in Alabama where these periods were drier and wetter respectively. These findings emphasize that particular climatic periods can show one change in one area of the world and a very different change in another area.

6). Evidence from Southern China and Northern India shows very clearly the strong relationship between climate change in these areas and variations in solar radiation. In China Asian monsoon strength is clearly related directly with northern hemisphere summer solar radiation while in Northern India Southwest monsoon strength correlates strongly with variations in sunspot activity.

7). The previous suggestions made by others that the Southeastern USA was wetter during the early Holocene and drier during the late Holocene are supported by totally independent evidence from DeSoto Caverns speleothems.

References

Bond, G., Showers, W., Cheseby, M., Lotti, R., Almasi, P., deMenocal, P., Priore, P., Cullen, H., Hajdas, I. and Bonani, G. 1997. A Pervasive Millennial-Scale Cycle in North Atlantic Holocene and Glacial Climates. *Science* 278, 1257-1266.

Cullen, H. M., deMenocal, P. B., Hemming, S., Hemming, G., Brown, F. H., Guilderson, T. and Sirocko, F. 2000. Climate change and the collapse of the Akkadian empire: Evidence from the deep sea. *Geology* 28, 379-382.

deMenocal, P., Ortiz, J., Guilderson, T. and Sarnthein, M., 2000. Coherent high- and low-latitude climate variability during the Holocene warm period. *Science* 288, 2198-2202.

Neff, U., Burns, S. J., Mangini, A., Mudelsee, M., Fleitmann, D. and Matter, A., 2001. Strong coherence between solar variability and the monsoon in Oman between 9 and 6 kyr ago. *Nature* 411, 290-293.

Thompson, L. G., Mosley-Thompson, E. and Henderson, K. A. 2000. Ice-core palaeoclimate records in tropical South America since the Last Glacial Maximum. *Journal of Quaternary Science* 15, 377-394.

Thompson, L. G., Mosley-Thompson, E., Davis, M. E., Henderson, K. A., Brecher, H. H., Zagorodnov, V. S., Mashiotta, T. A., Lin, P.-N., Mikhalenko, V. N., Hardy, D. R. and Beer, J. 2002. Kilimanjaro Ice Core Records: Evidence of Holocene Climate Change in Tropical Africa. *Science* 298, 589-593.

Wang, Y. J., Cheng, H., Edwards, R. L., An, Z. S., Wu, J. Y., Shen, C. C. and Dorale, J. A., 2001. A high-resolution absolute-dated late Pleistocene monsoon record from Hulu Cave, China. *Science* 294, 2345-2348.

Wang, Y. J., Cheng, H., Edwards, R. L., He, Y. Q., Kong, X.G., An, Z. S., Wu, J. Y., Kelly, M. J., Dykoski, C. A. and Li, X. D., 2005. The Holocene Asian Monsoon: links to solar changes and North Atlantic climate. *Science* 308, 854-857.

Wang, Y., Cheng, H., Edwards, R. L., Kong, X., Shao, X., Chen, S., Wu, J., Jiang, X., Wang, X. and An, Z., 2008. Millennial- and orbital-scale changes in the East Asian monsoon over the past 224,000 years. *Nature* 451, 1090-1093.

Yuan, D. X., Cheng, H., Edwards, R. L., Dykoski, C. A., Kelly, M. J., Zhang, M .L., Qin, J. M., Lin, Y. S., Wang, Y. J., Wu, J. Y., Dorale, J. A., An, Z. S. and Cai, Y. J., 2004. Timing, duration, and transitions of the last interglacial Asian monsoon. *Science* 304, 575-578.